AD_____

Award Number: W81XWH-04-1-0483

TITLE: Combined Biology and Bioinformatics Approaches to Breast Cancer

PRINCIPAL INVESTIGATOR: Zhongxian Lu, Ph.D.

CONTRACTING ORGANIZATION: University of California, Irvine
Irvine, CA 92697-1875

REPORT DATE: April 2006

TYPE OF REPORT: Annual

PREPARED FOR: U.S. Army Medical Research and Materiel Command
Fort Detrick, Maryland 21702-5012

REPORT DOCUMENTATION PAGE

Form Approved
OMB No. 0704-0188

1. REPORT DATE	2. REPORT TYPE	3. DATES COVERED
01-04-2006	Annual	1 Apr 2005 – 31 Mar 2006

4. TITLE AND SUBTITLE

Combined Biology and Bioinformatics Approaches to Breast Cancer

5a. CONTRACT NUMBER

5b. GRANT NUMBER
W81XWH-04-1-0483

5c. PROGRAM ELEMENT NUMBER

6. AUTHOR(S)

Zhongxian Lu, Ph.D.

5d. PROJECT NUMBER

5e. TASK NUMBER

5f. WORK UNIT NUMBER

7. PERFORMING ORGANIZATION NAME(S) AND ADDRESS(ES)

University of California, Irvine
Irvine, CA 92697-1875

8. PERFORMING ORGANIZATION REPORT NUMBER

9. SPONSORING / MONITORING AGENCY NAME(S) AND ADDRESS(ES)
U.S. Army Medical Research and Materiel Command
Fort Detrick, Maryland 21702-5012

10. SPONSOR/MONITOR'S ACRONYM(S)

11. SPONSOR/MONITOR'S REPORT NUMBER(S)

12. DISTRIBUTION / AVAILABILITY STATEMENT
Approved for Public Release; Distribution Unlimited

13. SUPPLEMENTARY NOTES
Original contains colored plates: ALL DTIC reproductions will be in black and white.

14. ABSTRACT – SEE ATTACHED PAGE

15. SUBJECT TERMS
LMO4, Breast cancer cell line, cellular proliferation, cellular migration, cellular apoptosis, BMP-7, ChIP assay, HADC2, gene microarray

16. SECURITY CLASSIFICATION OF:				18. NUMBER OF PAGES	19a. NAME OF RESPONSIBLE PERSON
a. REPORT	b. ABSTRACT	c. THIS PAGE			USAMRMC
U	U	U	UU	73	19b. TELEPHONE NUMBER *(include area code)*

Standard Form 298 (Rev. 8-98)
Prescribed by ANSI Std. Z39.18

ABSTRACT

LMO4 is highly expressed in breast epithelial cells and is related to cell proliferation and/or invasion in vivo. Because these cellular features are associated with breast carcinogenesis and because LMO4 is overexpressed in more than 50% of breast cancer cases, we hypothesize that LMO4 may play roles in oncogenesis of breast epithelial cells by regulating proliferation, invasion and/or other cellular features. Last year (first year), I demonstrated that LMO4 can modulate the proliferative response of epithelial cells to TGFβ signaling and linked LMO4 to a conserved signaling pathway that plays important roles in epithelial homeostasis. This year, I continued to be trained in bioinformatics; I took classes in statistical methods, and received practical training in evaluating large microarray datasets. In addition, I evaluate the regulation by LMO4 of cellular feature of normal breast epithelial cells and cancer cell lines. Both overexpression and knockdown of the LMO4 protein did not have major effects on cell proliferation, migration, invasion and colony formation of primary mammary gland epithelial cell and cancer cell lines (MCF-7, MDA-MB-231 or T47D). However, changes in LMO4 protein level markedly increased apoptosis of mammary normal or cancer cells. Using cDNA microarrays, we screened several LMO4-responsive genes. BMP7 was identified as a key down-stream gene by ChIP assays and promoter reporter assays. Both increase and decrease in LMO4 level can increase BMP7 transcription. BMP7 signaling inhibitor blocked the LMO4 induced apoptosis of MCF-7 cells, indicating that BMP7 mediates LMO4 effects on apoptosis in MCF-7 breast cancer cells. In addition, we found a significant correlation between LMO4 and BMP7 transcript levels in a large dataset of human breast cancers, providing additional support that BMP7 is a bona fide target gene of LMO4. We further demonstrated that LMO4 binds to HDAC2 and that they are recruited together to the BMP7 promoter. Our studies suggest a novel mechanism for LMOs; LMO4, Clim2 and HDAC2 are part of a transcriptional complex, and alterations in LMO4 levels can disrupt the complex, leading to decreased HDAC2 recruitment and increased promoter activity. These results strengthen the hypothesis that LMO4 may contribute to the oncogenesis of breast tissue and indicates that our work will play a role in solving the breast cancer problem with the support of the Army Breast Cancer Research Program.

Table of Contents

Zhongxian Lu, Kaye Starr Lam, Ning Wang, Xiaoman Xu, Manuel Cortes, and Bogi Andersen. A Novel Smad-associating Protein, LIM-only protein 4 (LMO4), modulates TGFβ Signaling in Mammary Gland Epithelial Cells. The 2005 Conference of Chao Family Comprehensive Cancer Center, Palm Spring, California, Novermber

C. Manuscripts:

1. **Zhongxian Lu**, Kaye Starr Lam, Ning Wang, Xiaoman Xu, Manuel Cortes, and Bogi Andersen. LMO4 can interact with Smad proteins and modulate transforming growth factor-beta signaling in epithelial cells. Oncogene, 2006, in press.
2. Ning Wang, **Zhongxian Lu**, Kervin Lin, Kaye Starr Lam, Xiaoman Xu, Gordon N. Grill, Bogi Andersen. The LIM only factor LMO4 regulates expression of the BMP7 gene through an HDAC2-dependent mechanism, and controls cell proliferation and apoptosis of mammary epithelial cells. Submitted to *Molecular and Cellular Biology*.

INTRODUCTION

My training program contains two distinct components: molecular research in breast cancer and computational biology and bioinformatics. The two components will be integrated because analyses of data obtained from my laboratory research will be one of my entry points into computational biology. In addition, results from the computational part of my project will spurn biological experiments. **A**. My training in computational biology will involve formal course work from the UCI Bioinformatics Training Program. These courses include *Basic Statistics (Math 7, 4u), Introduction to Computer Science (ICS 21, 6u), Representations and Algorithms for Molecular Biology (ICS 277A, 4u)* and *Probabilistic Modeling of Biological Data (ICS 277B, 4u)***. B.** My molecular laboratory research training focuses on the LIM-only factor (LMO) 4 genes. LMO4 belongs to a family of four mammalian LMO proteins, which are only composed of two LIM domains (1). LMOs are thought to act as adapter molecules in transcriptional complexes, tethering the co-activators CLIM (Nli/Ldb) to various DNA-binding proteins (2). LMOs family proteins show a crucial role not only during development, but also in tumorigenesis. LMO1 and LMO2 act as oncogenes in acute lymphoblastic leukemia (3). LMO4 is also referred to as Human Breast Tumor Autoantigen based on that LMO4 was also first isolated from breast cancer tissue and overexpressed in more than 50% of breast cancer cases (4, 5). Furthermore, LMO4 interacts with BRCA1 and inhibits the activation of BRCA1 (6). In study comparing expression profiles in estrogen positive and negative breast cancer, LMO4 was found in a panel of genes that strongly predicted estrogen negative status of breast cancer. My hypothesis is that, analogous to the role of LMO2 in leukemia, LMO4 overexpression promotes oncogenesis of breast epithelial cells by deregulating one or more of the following cellular features: differentiation, proliferation, apoptosis or invasion. In addition, we hypothesize that LMO4 acts, at least in part, by interacting with BRCA1, thereby interfering with the regulation of BRCA1 target genes.

Our specific aims were: #1. To test the effects of LMO4 overexpression or LMO4 interference in breast cancer by conditional expression systems and an interfering RNA plasmid system to increase and decrease, respectively, LMO4 protein levels in breast cancer cell lines. #2. To use gene expression profiling in MCF-7 breast cancer cells to elucidate the mechanisms of action for LMO4 overexpression. To gain insights into how LMO4 acts at a molecular level, we will use Affymetrix microarrays to define the profile of genes altered by LMO4 in breast cancer cells. I will also use the same approach to compare the target genes of LMO4 and BRCA1.

BODY

Task 1. Test the phenotypic effects of conditional LMO4 overexpression and LMO4 interference in human breast cancer cells.

Last year, we finished the following work:

1. Created a retroviral gene transduction system and overexpressed LMO4 in breast cancer cell lines.
2. Established breast cancer cell lines that express LMO4-RNAi.

3. Found that LMO4 modulates TGFβ signaling as a part of Smads-DNA complex and that LMO4 enhances TGFβ inhibition of cell proliferation in mammary gland epithelial cell.

This year, we continued to evaluate the roles of LMO4 in the regulating the cellular feature of normal breast epithelial cells and cancer cell lines.

In our experiments, we first assessed the effect of overexpression or deletion of LMO4 on cell proliferation, migration, invasive, colony formation and apoptosis using the retrovirus infect system and stable expression cell line systems built last year.

For cell proliferation, breast cancer cells MDA-MB-231, MCF-7 and T47D that overexpress LMO4 or a control gene were grown for one week, and their growth curves were assess by MTT assay (Method, see First year annual report). Compared to the control cells, LMO4-overexpressed MDA-MB-231 cells have a similar growth curve (Fig. 1A). LMO4 overexpression has no influence on the proliferation of MCF-7 and T47D cells. For overexpressing LMO4, we also took advantage of the Tet-off system [7], and established several distinct MCF-7 cell clones, referred to as MCF7-LMO4-TetOff cells, in which removal of doxycycline resulted in the increased expression of LMO4 (Fig. 1B,upper panel). In contrast to the *in vivo* mouse results, we did not observe striking LMO4 effects on proliferation in the MCF-7 cells (Fig. 1B, bottom panel). Using the above cells, we also evaluated the functions of LMO4 overexpression on cell migration and invasion, respectively. However, no clear effects of LMO4 on these functions were observed (data not show).

Using small RNA interference, we successfully reduced the LMO4 protein level in the MDA-MB-231 breast cancer cell line (see First year annual report). The proliferation, migration and invasion of these cell lines were not clearly different than control cells (Fig. 1C). In contrast, T47D cells stably expressing LMO4 siRNA were plated in 100mm dishes (1000 cell/dish), and then grown in an incubator for 15 days. Cells were stained with 0.2% violet solution and counted. LMO4 siRNA reduced the colony formation in T47D cells (Fig. 1D). This result indicates that LMO4 may regulate breast cancer cell survival, and that its regulation is context dependent and only observed in some breast cancer cell lines.

We also employed an Engailed-LMO4 fusion protein to block LMO4 regulation. The fusion of the engrailed repression domain to LMO4 creates a strong dominant-negative molecule predicted to actively repress LMO4 target genes [8]. We expressed Engrailed-LMO4 fusion protein in normal human mammary epithelial cells (HMEC) with the retrovirus expressing system, and analyzed its effects on proliferation and apoptosis (Method, see First year annual report). The Engrailed-LMO4 fusion protein clearly inhibited cell growth (Fig. 2 A and B). To test whether the effect of Engrailed-LMO4 was due to inhibition of proliferation or increased apoptosis, we used a FACS-based CSFE assay (Method, see First year annual report, [9]) (Fig. 2D). In vector-infected (TAPc) cells, two peaks were observed with the left peak representing cells having undergone one cell division (Fig. 2D, black). In LMO4-infected cells, the left peak is higher, indicating somewhat increased rate of proliferation (Fig. 2D, green). In Engrailed-

infected cells, only the right peak is observed (Fig. 2D, red), indicating a striking decrease in proliferation. In the Engrailed-LMO4-infected cells, the overall number of cells is decreased probably due to increased cell death (see later). To test whether there was increased cell death, we used a FACS-based Annexin V assay (Method, see First year annual report, [9]). Whereas LMO4 had small effect on apoptosis, Engrailed-LMO4 nearly doubled live Annexin V staining cells, and caused increased number of dead cells (Fig. 3E). In summary, expression of a dominant negative LMO4 leads to a decrease in proliferation and an increase in apoptosis in normal mammary epithelial cells. Same experiments have been done in breast cancer cells MDA-MB231 and T47D. Increased apoptosis was clearly observed in MDA-MB231 and T47D cells expressing the Engrailed-LMO4. In these experiments we used either FACS-based Annexin V assay or Cell Death Detection ELISA^{PLUS} assay, which is based on quantitative detection of histone-associated DNA fragments in mono- and oligo-nucleosomes (Fig. 3A and B).

Unlike the effects of LMO4 deletion, effects of LMO4 overexpression on apoptosis are not consistent in different types of breast cancer cells. Overexpressed LMO4 did not induce cell death in T47D cells (Fig 3B), but increased apoptosis in MDA-MB-231. We also measured apoptosis in MCF7-LMO4-TetOff cells with cell death detection ELISA assay. Removal of doxycycline to overexpress LMO4 significantly increased apoptosis in the MCF7-LMO4-TetOff cell, whereas no effect was observed in vector-transfected cells (Fig. 4A); LMO4 increased apoptosis in a time-dependent manner (Fig. 4B). Consistent with results from the cell death detection ELISA assay, FACS analysis detected a moderate increase in annexin V staining, as well as more annexin V positive dead cells, in the absence of doxycycline (increased LMO4) than in the presence of doxycycline (low LMO4) (data not show). In addition, elevated expression of LMO4 clearly increased the amount of cleaved caspase 7 as detected by western blotting with antibodies against both uncleaved and cleaved caspase 7 (Fig. 4C). When MCF7-LMO4-TetOff cells were treated with the general caspase inhibitor Z-VAD-FMZ, LMO4 was incapable of inducing apoptosis, indicating that the process was caspase dependent (Fig. 4D).

In summary, our results in the last year and this year clearly showed that LMO4 regulates cellular features (such as proliferation and apoptosis) of normal mammary gland epithelial cells and breast cancer cells. Stable LMO4 protein level is important for cell survival and proliferation. The effects of LMO4 in mammary epithelial cells or breast cancer cells may be context dependent and dose dependent. Increased or decreased LMO4 levels disrupt homeostasis leading to cell dysfunction or death in the mammary gland [9]. These discoveries from the Task #1 strongly suggest that LMO4 plays important roles during mammary gland development and in breast cancer progression, and supports the hypothesis in my proposal.

Task 2. **To use gene expression profiling in MCF-7 breast cancer cells to elucidate the mechanisms of action for LMO4 overexpression.**

Experimental series 1 – the effect of LMO4 overexpression.

To identify LMO4-responsive genes, we profiled gene expression in three distinct MCF7-LMO4-TetOff cell clones, L1-3, in the presence (low LMO4) and absence (increased LMO4) of doxycycline (Fig. 1B). After labeling and hybridization to Affymetrix HG-U133 A and B gene arrays [10], we used the Cyber-T program to identify statistically significant differentially expressed genes [10]. Using a cutoff *P*-value of <0.01, we found that out of nearly 18,000 expressed probe sets only 111 and 98 were up-regulated and down-regulated, respectively. We used Quantitative real-time PCR to validate the microarray results for several LMO4-responsive genes (data not show). We then used DAVID 2.1 to determine which biological processes were over represented in the significantly differentially expressed genes [10]. Of all Gene Ontology biological processes, only apoptosis was significantly (*P*=0.006) enriched (data not show), which is consistent with and supports the biological data presented in Fig. 4.

To evaluate the possible roles of LMO4 in breast cancer, we investigated the correlation between LMO4 and its target gene in breast tumor using human primary breast tumor gene profiling databases. We found there was a good correlation between LMO4 and BMP7 levels in 49 primary breast cancers that also used Affymetrix microarrays to profile expression [11]. Consistent with a previous report, showing association between high LMO4 expression and ER-negative status of tumors [58], the average LMO4 expression level is significantly higher (2.21 fold; *P*<0.0001) in basal than luminal tumor samples (Fig. 5A). In addition, there is a strong correlation (r=0.69) between LMO4 and BMP7 expression levels in all subtypes of tumors (Fig. 5B). When we examined the distribution of correlation coefficients between the expression of LMO4 and each probe set on the Affymetrix U133A array across all breast tumors, we found that BMP7 has one of the highest correlation coefficients and is significantly (*P*<0.0001) correlated (Fig. 5C). As expected, the top correlation coefficient is another probe set for LMO4 (Fig. 5C).

We cloned 1.9kb of the proximal 5' flanking region of the *BMP7* gene [63, 64] upstream of the luciferase reporter gene in the pGL3 vector (pGL3-1.9BMP7) and transfected into HEK293T cells, LMO4 was able to up-regulate luciferase activity by as much as 8-fold (Fig. 6A), indicating LMO4 directly regulates the *BMP7* gene. Under conditions where MCF7-LMO4-TetOff cells were maintained without doxycycline, the BMP inhibitor follistatin decreased apoptosis by approximately 50% as monitored by Cell Death Detection ELISA assay (Fig. 6B), indicating that LMO4-stimulated apoptosis is at least in part mediated by BMPs. Estradiol has been shown to downregulate BMP7 and estradiol inhibits apoptosis in epithelial cells of the endometrium by suppressing BMP7 signaling [59, 62]. Interestingly, estradiol completely inhibited LMO4-mediated apoptosis in MCF7 cells (Fig. 6B). These results suggest that BMP7 contributes to LMO4-induced apoptosis.

We performed chromatin immunoprecipitation assays in MCF7-LMO4-TetOff cells in the presence and absence of doxycycline. A Myc antibody precipitated the BMP7 promoter in the absence of doxycycline (high LMO4) (Fig. 6C-a), indicating that LMO4 associates with the BMP7 promoter. These results are specific because the BMP7 promoter was not precipitated by normal serum IgG (Fig. 6C-a), and the Myc antibody did not precipitate the U6 promoter, which is not regulated by LMO4 (Fig. 6C-a, lanes 3-

6). Since LMO4 proteins lack DNA-binding domains, and are thought to regulate gene expression by forming the protein complex with other protein. Clim2 is a partner protein of LMO4. We performed similar experiments in the MCF7-DN-Clim-TetOff cells. Also in these cells, Myc antibody specifically precipitated the BMP7 promoter under conditions of high DN-Clim expression (Fig. 6C-b), indicating that the DN-Clim associates with the BMP7 promoter. Together, these studies suggest that Clim and LMO4 can form a complex on the BMP7 promoter. To test this idea, we performed double chromatin immunoprecipitation assays in the MCF7-LMO4-TetOff cells, first precipitating LMO4 with a Myc antibody and then with a Clim2 antibody against the endogenous Clim2 protein. Under conditions of high LMO4 expression, Clim antibody could precipitate the LMO4 complex on the BMP7 promoter (Fig. 6C-c), indicating that both LMO4 and Clim2 bind to the BMP7 promoter, most likely in a complex given the high-affinity interaction between these proteins.

To understand the mechanisms whereby modulation of LMO4 levels can regulate transcription of the *BMP7* gene, we investigated the recruitment of histone deacetylases to the BMP7 promoter. First, we performed *BMP7* chromatin immunoprecipitation assays in the MCF7-LMO4-TetOff cells, using specific antibodies against HDAC1, HDAC2, HDAC3 and HDAC4. Under condition of low LMO4 expression, we could clearly detect HDAC2 and HDAC3 association with the BMP7 promoter (Fig. 7A; upper panel, lanes 2 and 3). While HADC3 binding was unchanged, HDAC2 binding to BMP7 promoter was moderately decreased under conditions of high LMO4 expression, (Fig. 7A; upper panel, lanes 6 and 7). Since HDAC2 is a well-known inhibitor of transcription [65, 66], these findings suggested that LMO4 might up-regulate the BMP7 gene by decreasing recruitment of HDAC2 to the promoter. To test this hypothesis, we performed double chromatin immunoprecipitation studies, first precipitating LMO4 and then HDAC2 in the MCF7-LMO4-TetOff cells (Fig. 7A, bottom panel). Consistent with the model of LMO4 regulation of HDAC2 recruitment, we found that HDAC2 was primarily recruited to the BMP7 promoter under low LMO4 levels (Fig. 7A, bottom panel, lanes 3 and 6). As expected, high LMO4 levels increased the recruitment of Clim2 to the promoter (Fig. 7A, bottom panel; lanes 2 and 5). Further support for LMO4 involvement in HDAC2 regulation are from immunoprecipitation experiments where HDAC2 antibody could pull down LMO4 (Fig. 7B), consistent with a recent report also showing that LMO4 can interact with HDAC2 [18]. In transfection assays, an HDAC2siRNA and HDAC2 expression vector increased and decreased, respectively, expression of the BMP7 promoter indicating that HDAC2 suppresses the promoter under basal conditions. When the HDAC2 expression vector was co-transfected with LMO4, it blocked the LMO4-mediated stimulation of the BMP7 promoter (Fig. 7C), consistent with the idea that decreased recruitment of HDAC2 could account for LMO4-regulation of the promoter.

Our findings suggest a novel mechanism for LMO-mediated stimulation of gene expression. According to this model, a transcription complex containing LMO4, Clim2 and HDAC2 is sensitive to stoichiometry of components such that either overexpression or lowering of LMO4 leads to decreased recruitment of HDAC2 and increased promoter activity.

Experimental series 2 – the effect of lowering BRCA1 expression. (working on)

Experimental series 3 – validation of selected targets from the microarray data. (working on)

Experimental series 4 – validation of functional LMO4/BRCA1 interaction. (working on)

Task 3. **Formal training in bioinformatics.**

Last year, I took *Basic Statistic* and *Representations and Algorithms for Molecular Biology* courses. This year, I studied *Introduction to Computer Science (ICS 21, 6u).* This course introduces a high-level programming language, Java. Based Java language, fundamental concepts related to computer software design and construction were learned, and skills of design program were developed. This course greatly improves my ability in working on computational experiments (such as understanding and designing program to analyze gene profiling in microarray database, which is the major experiment in specific aim #2.). In addition, I obtained significant practical experience in bioinformatics as my progress report indicates. I statistically evaluated a large microarray dataset and used this analysis to discover LMO4 target genes. In addition, I used computational methods to study the correlation between LMO4 transcript levels and expression of other genes in a large breast cancer dataset. Using this approach, I demonstrated the validity of BMP7 as an LMO4 target gene.

KEY RESEARCH ACCOMPLISHMENT

1. Demonstrated that LMO4 plays a crucial role in cell survival of mammary gland cells or breast cancer cells by regulating cell apoptosis.
2. Defined BMP-7 as a key LMO4 target gene that can mediate some of the effects of LMO4 on breast cancer cells.
3. Discovered novel regulatory mechanisms for LMO4 gene regulation, involving histone deacetylases, in mammary gland development and breast cancer progression.

REPORTABLE OUTCOMES TO DATE

1. A dominant-negative LMO4 construct: Engrail fused to LMO4.
2. The retrovirus infection system of Engrail-LMO4 to control genes.
3. Published paper: **Zhongxian Lu**, Kaye Starr Lam, Ning Wang, Xiaoman Xu, Manuel Cortes, and Bogi Andersen. LMO4 can interact with Smad proteins and modulate transforming growth factor-beta signaling in epithelial cells. Oncogene, 2006, in press.
4. Manuscript: Ning Wang, **Zhongxian Lu**, Kervin Lin, Kaye Starr Lam, Xiaoman Xu, Gordon N. Grill, Bogi Andersen. The LIM only factor LMO4 regulates expression of the BMP7 gene through an HDAC2-dependent mechanism, and controls cell proliferation and apoptosis of mammary epithelial cells. Submitted to *Molecular and Cellular Biology*.

5. Abstract: **Zhongxian Lu**, Kaye Starr Lam, Ning Wang, Xiaoman Xu, Manuel Cortes, and Bogi Andersen. A Novel Smad-associating Protein, LIM-only protein 4 (LMO4), modulates TGFβ Signaling in Mammary Gland Epithelial Cells. The 2005 Conference of Chao Family Comprehensive Cancer Center, Palm Spring, California, November

CONCLUSION

In summary, with the support of the Army Fellowship Award, I continue to obtain excellent training in both molecular research in breast cancer and computational biology; I am acquiring expertise in working on the breast cancer problem at a high level. This year, I made significant progress on specific aims of my proposal, and my training in breast cancer has been greatly enhanced. I have published one first-author paper and an abstract, and submitted a manuscript, which describes my recent finding with LMO4 in breast cancer. My major achievements are described as following: (1) I have demonstrated that LMO4 regulates cell proliferation dependent on the type of breast cancer cells. (2) I have found LMO4 play crucial roles on cell apoptosis of mammary gland normal epithelial cell and breast cancer cell lines, and its regulation is sensitive to its protein level. Both overexpression and deletion LMO4 protein can cause cell apoptosis. (3) I have completed the screen for LMO4-regulated genes, using microarray technology in MCF-7 cells overexpressing LMO4. (4) I have defined that BMP7 is a key down-stream gene of LMO4, and contributes to LMO4-induced apoptosis. (5) I have discovered that LMO4 modulates the recruitment of HDAC2 to the BMP7 promoter, suggesting a novel mechanism for LMO-mediated stimulation of gene expression. LMO4 is a part of a transcription complex containing LMO4, Clim2 and HDAC2, which is sensitive to stoichiometry of components such that either overexpressing or lowering of LMO4 leads to decreased recruitment of HDAC2 and increased promoter activity.

In conclusion, we demonstrated a crucial role for LMO4 in cell proliferation and apoptosis, and defined a key target gene of LMO4 and a regulatory mechanism for LMO4 at a transcriptional level. These results strengthen the hypothesis that LMO4 may contribute to the oncogenesis of breast tissue. I also finished one computational science course, which greatly enhances my ability to analyze data. Together, these results signify outstanding progress and provide a strong support for the completion of the whole project. These results also indicate that this work will play a role in solving the breast cancer problem with the support of the Army.

REFERENCE

1. Bach, I., *The LIM domain: regulation by association.* Mech Dev, 2000. **91**(1-2): p. 5-17.
2. Dawid, I.B., J.J. Breen, and R. Toyama, *LIM domains: multiple roles as adapters and functional modifiers in protein interactions.* Trends Genet, 1998. **14**(4): p. 156-62.

3. Rabbitts, T.H., *LMO T-cell translocation oncogenes typify genes activated by chromosomal translocations that alter transcription and developmental processes.* Genes Dev, 1998. **12**(17): p. 2651-7.
4. Racevskis, J., et al., *Molecular cloning of LMO41, a new human LIM domain gene.* Biochim Biophys Acta, 1999. **1445**(1): p. 148-53.
5. Visvader, J.E., et al., *The LIM domain gene LMO4 inhibits differentiation of mammary epithelial cells in vitro and is overexpressed in breast cancer.* Proc Natl Acad Sci U S A, 2001. **98**(25): p. 14452-7.
6. Sum, E.Y., et al., *The LIM domain protein LMO4 interacts with the cofactor CtIP and the tumor suppressor BRCA1 and inhibits BRCA1 activity.* J Biol Chem, 2002. **277**(10): p. 7849-56.
7. Gossen, M. and H. Bujard, *Tight control of gene expression in mammalian cells by tetracycline-responsive promoters.* Proc Natl Acad Sci U S A, 1992. **89**(12): p. 5547-51.
8. Wang, N., et al., Expression of an engrailed-LMO4 fusion protein in mammary epithelial cells inhibits mammary gland development in mice. Oncogene, 2004. **23**(8): p. 1507-13.
9. Lu, Z., et al., *LMO4 can interact with Smad proteins and modulate transforming growth factor-beta signaling in epithelial cells.* Oncogene, 2006.
10. Lin, K.K., et al., *Identification of hair cycle-associated genes from time-course gene expression profile data by using replicate variance.* Proc Natl Acad Sci U S A, 2004. **101**(45): p. 15955-60.
11. Farmer, P., et al., *Identification of molecular apocrine breast tumours by microarray analysis.* Oncogene, 2005. **24**(29): p. 4660-71.

Fig. 1

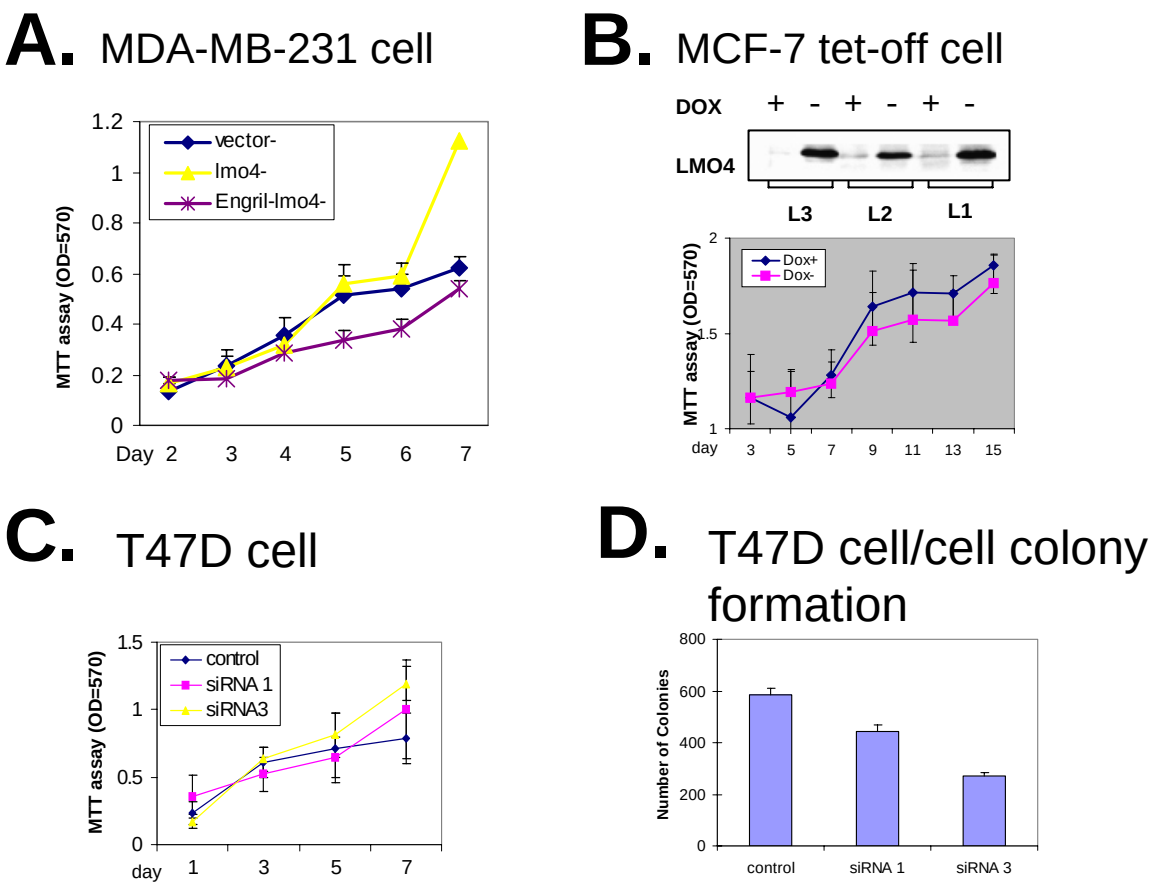

Fig.1 The effects of LMO4 on cellular process of breast cancer cell lines. (**A**) MDA-MB-231 cells were infected with retrovirus encoding the indicated proteins. After infection, cells were plated.The growth curves was evaluated using MTT assay (Celltiter 96 Aqueous Non-radioactive cell proliferation assay kit, Promega). **(B)** The upper panel show LMO4 expression in three distinct MCF7-LMO4-TetOff cell clones, L1-3 by western blotting. Equal amount of protein extracts from cells treated with (+) and without (-) doxycycline were fractionated by SDS-PAGE and probed with a antibody to detect the Myc-tagged LMO4. The bottom figure represents the growth curve of MCF7-LMO4-TetOff cells with and without doxycycline for 15 days measured with MTT assay. (**C**) The cell growth curve of T47D cells stable expressed LMO4 siRNA or control siRNA (MTT assay). (**D**) The cell colony formation of T47D cells stable expressed LMO4 siRNA or control siRNA.

Fig. 2

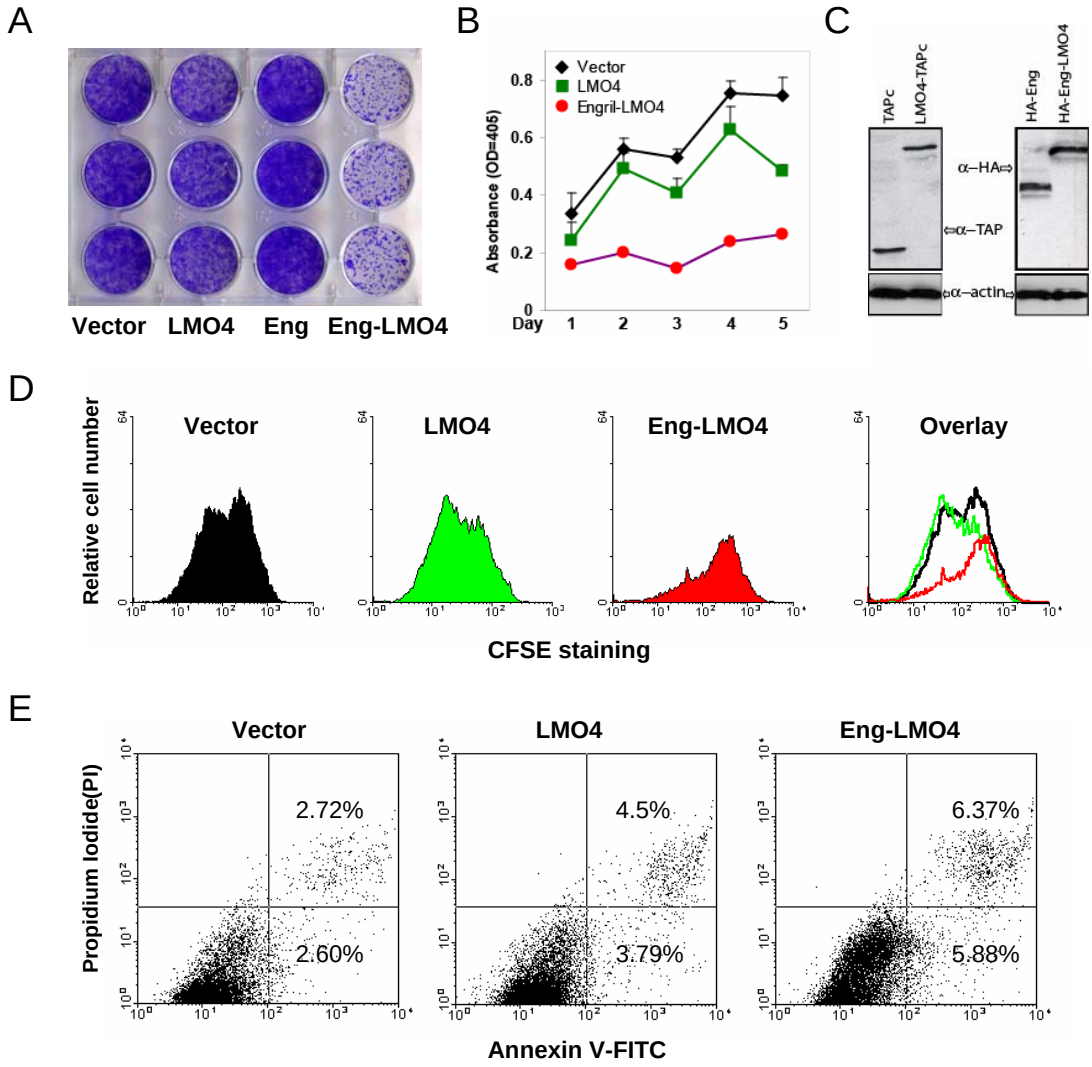

FIG. 2. Engrailed- LMO4 inhibits normal human mammary epithelial cell growth. (**A**) HMEC were infected with pLNCX2 retroviral vectors encoding the indicated proteins. After infection, cells were plated and cell number was estimated after 7 days using crystal violet staining. (**B**) Growth curves of HMEC after retroviral infection with the indicated vectors using Celltiter 96 Aqueous Non-radioactive cell proliferation assay (Promega). (**C**) Western blots showing the expression of the indicated proteins from the viral vectors in the experiment described in A and B. (**D**) HMEC were infected with the retroviruses encoding the indicated proteins and then labeled with CFSE. CFSE intensity was measured by FACS after 4 days. (**E**) HMEC infected with retroviruses encoding the indicated proteins was stained with PI and annexin V-FITC, and then analyzed by FACS.

Fig. 3

A. MDA-MB-231/Apoptosis assay with Annexin V staining

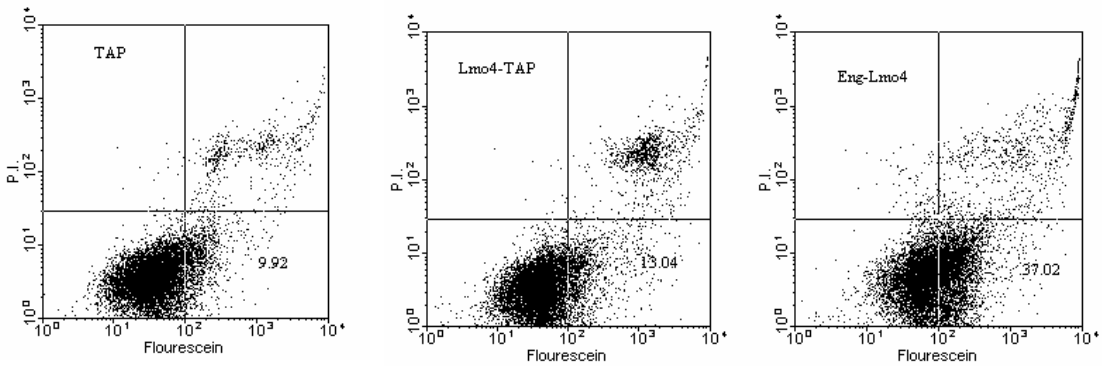

B. Cell death assay

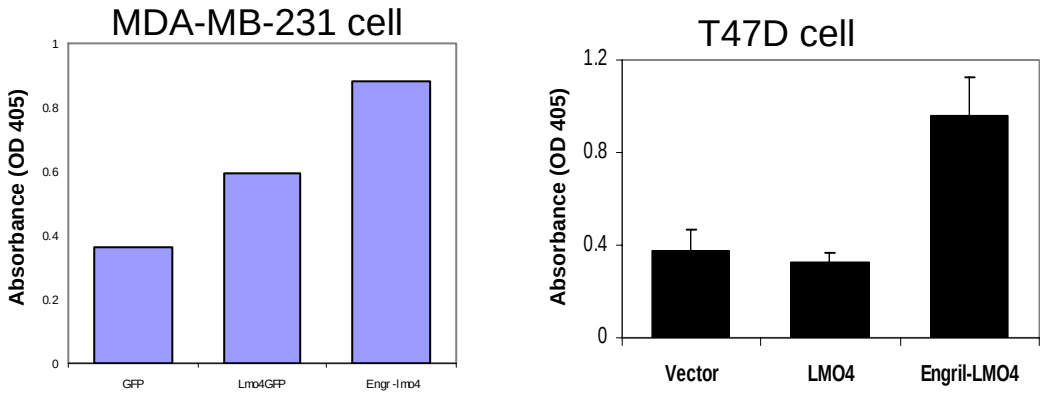

FIG.3 Engrailed- LMO4 induced breast cancer cells apoptosis. Breast cancer cells MDA-MB-231 or T47D were infected with pLNCX2 retroviral vectors encoding the indicated proteins. After infection, cells were plated, and then apoptosis was assessed with annexin V-FITC staining by FACS (**A**) or with Cell Death Detection ELISAPLUS kit (**B**).

Fig. 4

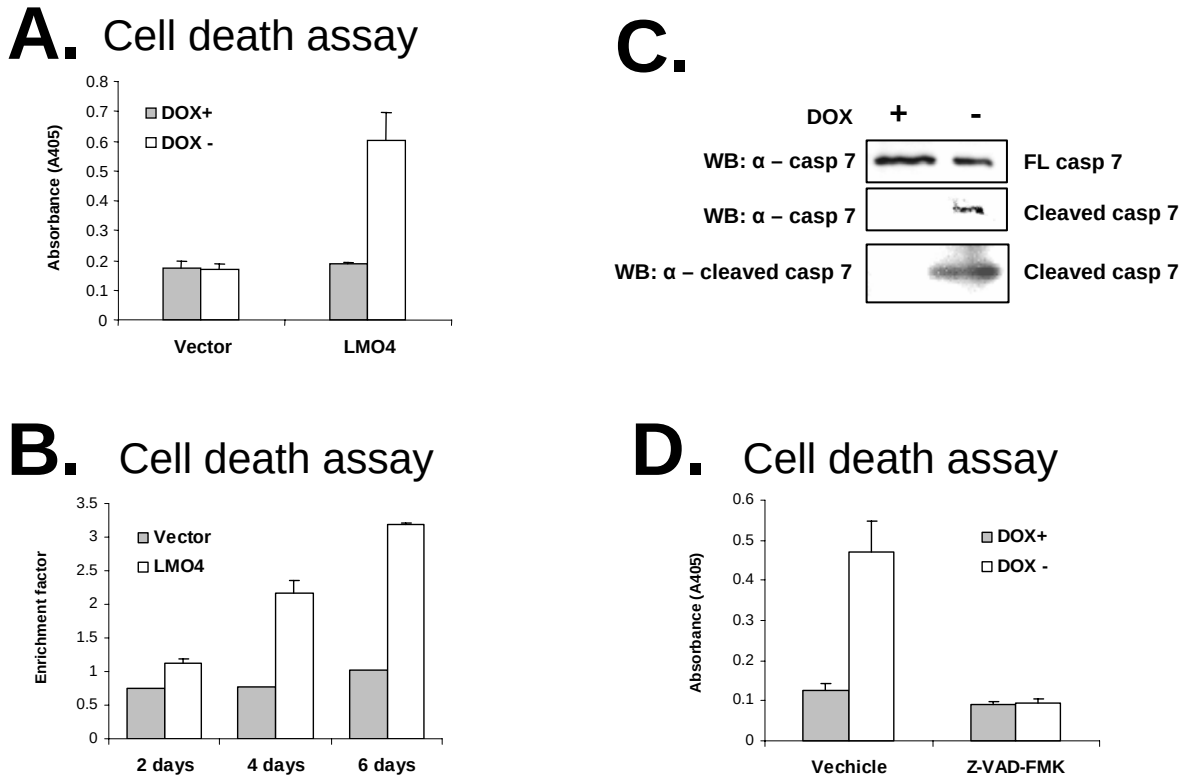

FIG. 4. LMO4 expression increases apoptosis in MCF-7 cells. (**A**) MCF7-LMO4-TetOff cells and control cells were treated with and without doxycycline for 6 days. Apoptosis was evaluated with Cell Death Detection ELISAPLUS kit. (**B**) MCF7-LMO4-TetOff cells and MCF-7 cells transfected with an empty vector were treated with doxycycline for the indicated times. Apoptosis was measured with Cell Death Detection ELISAPLUS kit as described in panel B. The enrichment factor is the ratio of apoptosis in cells grown in the absence of DOX to apoptosis in the corresponding control cells grown in the presence of DOX.(**C**) MCF7-LMO4-TetOff cells were treated with (+) and without (-) doxycycline for 6 days. Cell lysates were fractionated and analyzed by caspase 7 and cleaved caspase 7 antibodies. (**F**) MCF7-LMO4-TetOff cells were treated with (+) and without (-) doxycycline for 4 days in the presence of vehicle or the caspase inhibitor Z-VAD-FMK. Apoptosis was assessed with the Cell Death Detection ELISAPLUS kit. The data in A, B and D represents mean and SEM from at least three different experiments.

Fig. 5

A. LMO4 transcriptional level in primary breast tumor

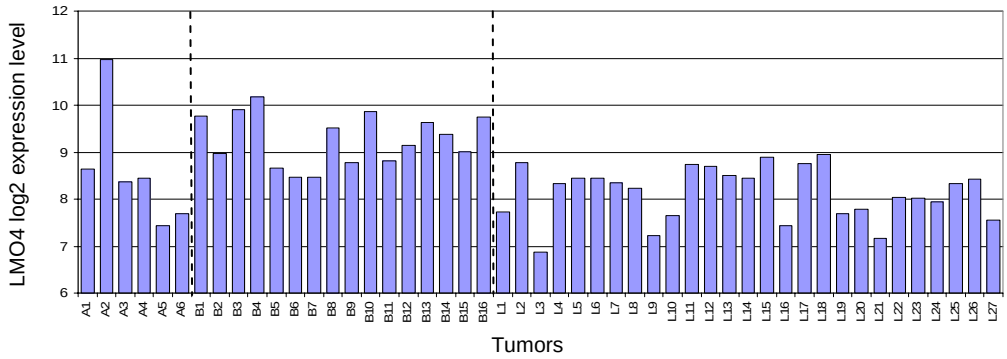

B. Correlation between LMO4 and BMP7 expression levels

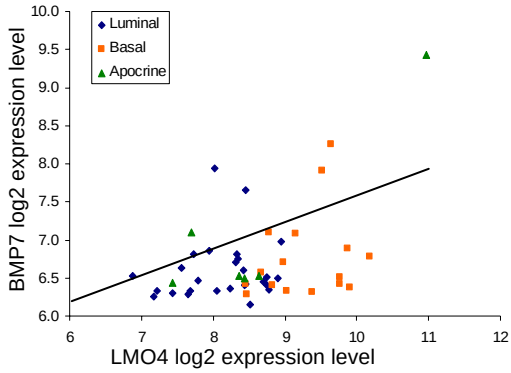

C. Distribution of correlation coefficients between the expression of LMO4 and each probe set

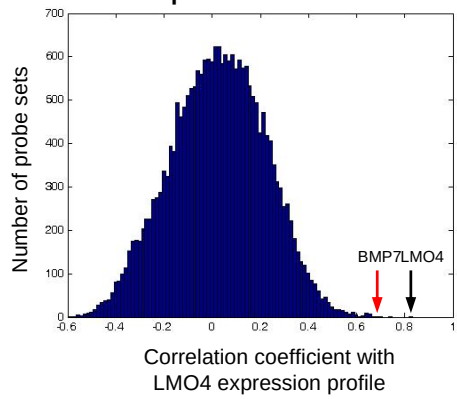

FIG. 5. Identification of LMO4 target genes. (**A**) LMO4 transcript levels, shown as log base 2 transformed RMA (Robust Multichip Average) normalized expression levels, in a previous microarray study of 49 individual breast cancer samples. Broken vertical lines separate the three tumor subtypes defined in this study: apocrine, A; basal, B; and luminal, L. (**B**) Correlation between LMO4 and BMP7 expression levels in breast tumors. Pearson product moment correlation coefficient, r, for the unlogged RMA values is 0.69. (**C**) Distribution of correlation coefficients between the expression of LMO4 and each probe set on the Affymetrix HG-U133A array across all breast tumors. Red arrow, probe set for BMP7. Black arrow, another probe set for LMO4.

Fig. 6

A. BMP-7 promoter reporter assay

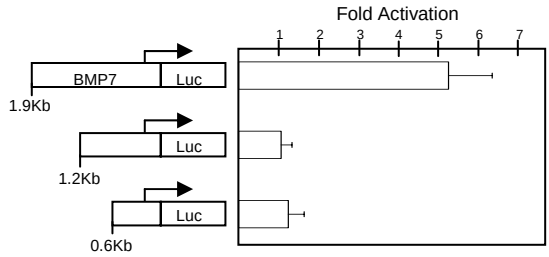

B. BMP-7 signaling inhibitor block the LMO4 induced apoptosis

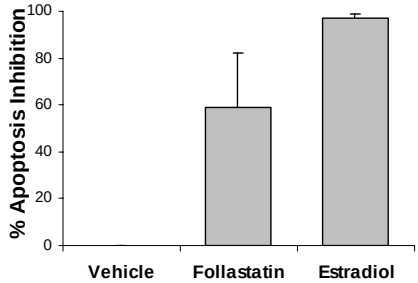

C. Ch IP assay

a. LMO4 complex binds to BMP DNA

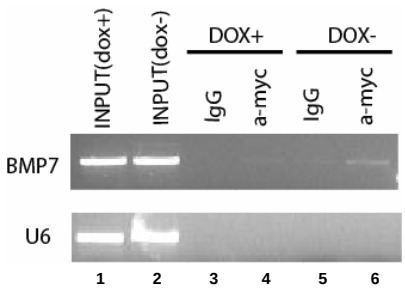

b. Clim2 complex binds to BMP DNA

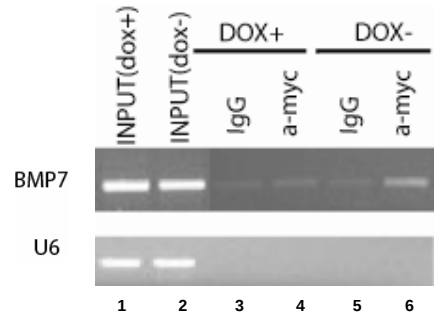

c. LMO4 and Clim2 together binds to BMP DNA

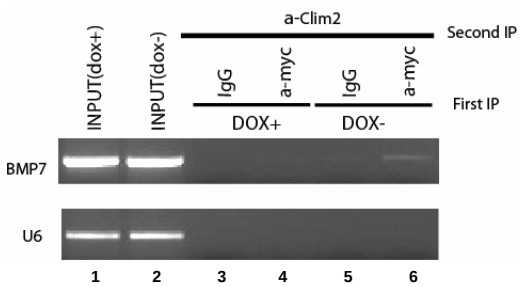

FIG. 6. LMO4 and Clim2 associate with and regulate the BMP7 promoter.(**A**) The indicated deletion constructs of pGL3-1.9BMP7 were cotransfected with an LMO4 expression plasmid into HEK293T cells. The luciferase activity represents the mean and SEM from at least 3 independent experiments. (**B**) Inhibition of apoptosis in MCF7-LMO4-TetOff cells by follistatin and estradiol. Doxycycline was removed from MCF7-LMO4-TetOff cell cultures and 3 days later follistatin (250ng/ml) or estradiol (20nM) was added for 3 days. Apoptosis was assessed with the Cell Death Detection ELISAPLUS kit. Results represent the mean and SEM from 3 independent experiments. (**C**) Chromatin immunoprecipitation assays in MCF7-TetOff cells in the presence (DOX+) and absence (DOX-) of doxycycline. **a**. Antibodies were against Myc to precipitate the Myc-tagged LMO4 and non-specific IgG as a negative control. Primers were located at 1733-2008 (AF289090) and 141158-141488 (AC022254) on the BMP7 and U6 promoter regions, respectively. **b.** Antibodies were against Myc to precipitate the Myc-tagged DN-Clim and non-specific IgG as a negative control. **c.** Double chromatin immunoprecipitation assays in the MCF7-LMO4-TetOff cells under the indicated conditions. The first antibody was against Myc to precipitate the Myc-tagged LMO4.The second antibody recognized the endogenous Clim2 protein.

Fig. 7

A. Ch IP assay

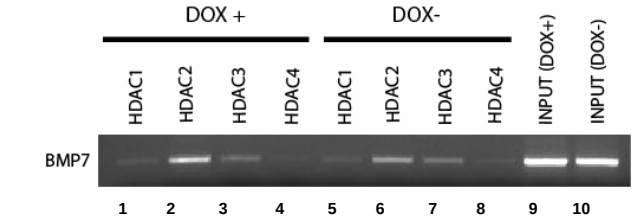

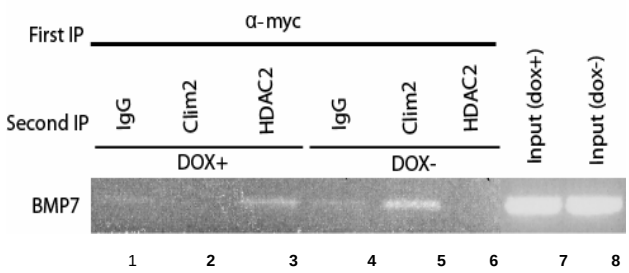

B. LMO4 and HDAC2 interaction

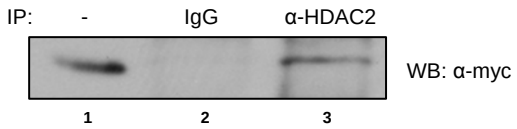

C. BMP promoter reporter assay

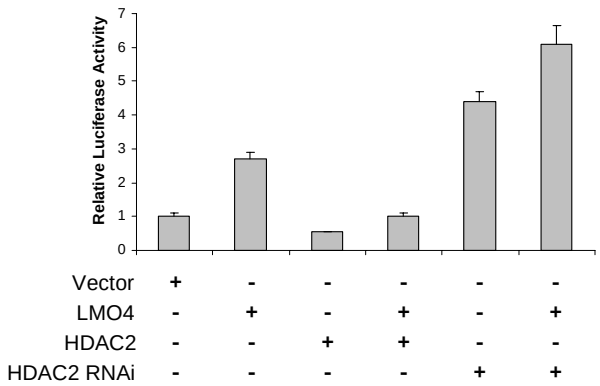

FIG. 7. Interactions between LMO4 and HDAC2 on the BMP7 promoter.(**A**) Chromatin immunoprecipitation assays in MCF7-LMO4-TetOff cells in the presence (DOX+) and absence (DOX-) of doxycycline. Antibodies were against HDAC1, HDAC2, HDAC3 and HDAC4, and primers were the same as in FIG. 6C. The bottom figure show the double chromatin immunoprecipitation assays in MCF7-LMO4-TetOff cells under the indicated conditions. The first antibody was against Myc to precipitate the Myc-tagged LMO4. The second antibody recognized HDAC2 and Clim2, respectively, Ig G as a negative control. (**B**) Immunoprecipitation of MCF7-LMO4-TetOff cell lysates with IgG and HDAC2 antibodies. The western blot was probed with antibody against Myc to detect the Myc-tagged LMO4. (**C**) The PGL3-1.9 BMP7 reporter plasmid was co-transfected with the indicated expression plasmids into HEK293T cells. Luciferase activity represents the mean and SEM from at least 3 independent experiments.

CHAO FAMILY COMPREHENSIVE CANCER CENTER CONFERENCE
NOVEMBER 11-13, 2005
HYATT REGENCY SUITES
PALM SPRINGS, CA

ABSTRACT FORM

Zhongxian Lu, Kaye Starr Lam, Ning Wang, Xiaoman Xu, Manuel Cortes, and Bogi Andersen

Departments of Medicine and Biological Chemistry, Division of Endocrinology, University of California, Irvine, California 92697-4075

TGFβ signals have multiple and complex biological effects in mammary gland development and tumor progression. By modulating the binding and activity of Smad proteins on target genes, Smad-associating proteins are thought to play key roles in TGFβ signal transduction by affecting the specificity and magnitude of TGFβ signal in response to environmental effects. Here, we identified a new Smad-associating protein, LIM-only protein 4 (LMO4), which plays critical roles in mammalian development, and has been proposed to play roles in epithelial oncogenesis, including breast cancer. Using co-immunoprecipitation, we found the interaction between endogenous and transiently overexpressed LMO4, and receptor-mediated Smad proteins (R-Smads). GST pull-down assays confirmed this interaction, and showed that LMO4 can interact with the MH1 and linker domains of R-Smad proteins. Furthermore, LMO4 associated with the endogenous TGFβ-responsive Plasminogen Activator Inhibitor-1 gene promoter in a TGFβ-dependent manner, suggesting that LMO4 may modulate TGFβ signaling as a Smad-associating protein in a biologically relevant manner. To test this hypothesis, we assessed the effect of LMO4 on TGFβ signaling, using a TGFβ-responsive reporter gene. The results show that the transcriptional response to TGFβ in epithelial cells is sensitive to LMO4 levels; both up- and down-regulation of LMO4 can enhance TGFβ signaling. When introduced into mammary epithelial cells, LMO4 leads to enhanced stimulation of p21 and p27, as well as potentiation of the growth-inhibitory effects of TGFβ in those cells. These results define a new function for LMO4 as a coactivator in TGFβ signaling, and provide a novel mechanism for LMO4-mediated regulation in development and oncogenesis. Because LMO4 is expressed at highly different levels during mammary gland development and tumor progression, our results provide insights into how TGFβ signaling may be modified in response to specific environmental effects both in development and during cancer progression in the mammary gland.

Abstract Title:	**A Novel Smad-associating Protein, LIM-only protein 4 (LMO4), Modulates TGFβ Signaling in Mammary Gland Epithelial Cells**
Presenter's Name:	ZHONGXIAN LU
Department:	Medicine and Biology Chemistry
Mailing Address:	Spraque Hall 250
Telephone Number:	949-824-9372
Fax Number:	949-824-3300
E-mail Address:	zhongxil@uci.edu

Oncogene (2006), 1–11

www.nature.com/onc

ORIGINAL ARTICLE

LMO4 can interact with Smad proteins and modulate transforming growth factor-β signaling in epithelial cells

Z Lu[1,2], KS Lam[1,2], N Wang[1,2], X Xu[1,2], M Cortes[1,2] and B Andersen[1,2]

[1]*Division of Endocrinology, Department of Medicine, University of California, Irvine, CA, USA and* [2]*Department of Biological Chemistry, University of California, Irvine, CA, USA*

LIM-only protein 4 (LMO4) plays critical roles in mammalian development, and has been proposed to play roles in epithelial oncogenesis, including breast cancer. As LMO4 is highly expressed in the epithelial compartments at locations of active mesenchymal–epithelial interactions, we reasoned that LMO4 might act by modulating signaling pathways involved in mesenchymal–epithelial signaling. One such candidate signal is the transforming growth factor-β (TGFβ) cytokine pathway, which plays important roles both in development and cancer. We show here that the transcriptional response to TGFβ in epithelial cells is sensitive to LMO4 levels; both up- and downregulation of LMO4 can enhance TGFβ signaling as assessed by a TGFβ-responsive reporter gene. Furthermore, LMO4 can interact with the MH1 and linker domains of receptor-mediated Smad proteins, and associate with the endogenous TGFβ-responsive Plasminogen Activator Inhibitor-1 gene promoter in a TGFβ-dependent manner, suggesting that such interactions may mediate the effects of LMO4 on TGFβ signaling. When introduced into mammary epithelial cells, LMO4 potentiated the growth-inhibitory effects of TGFβ in those cells. These results define a new function for LMO4 as a coactivator in TGFβ signaling, and provide a potential novel mechanism for LMO4-mediated regulation in development and oncogenesis.

Oncogene advance online publication, 9 January 2006; doi:10.1038/sj.onc.1209318

Keywords: LMO4; transforming growth factor-β; Smads; mammary gland epithelial cells; cellular proliferation

Introduction

LIM-only factor (LMO) 4 belongs to a family of four mammalian LMO proteins (Grutz *et al*., 1998; Kenny *et al*., 1998; Sugihara *et al*., 1998; Racevskis *et al*., 1999); all family members are short transcriptional regulators composed almost entirely of two LIM domains (Bach, 2000). The four LMOs play roles in mammalian development (Yamada *et al*., 1998; Hahm *et al*., 2004; Tse *et al*., 2004; Lee *et al*., 2005). In addition, LMO1 and LMO2 act as oncogenes in acute lymphoblastic leukemia (Rabbitts, 1998), and recent studies have defined LMO3 as an oncogene in neuroblastoma (Aoyama *et al*., 2005) and LMO4 as a protumorigenic factor in breast cancer (Visvader *et al*., 2001; Sum *et al*., 2005b). LMOs interact strongly with transcriptional coregulators referred to as Co-factors of LIM domains (Clims)/LIM domain-binding proteins (Ldb)/nuclear LIM interactors (Nli) (Agulnick *et al*., 1996; Jurata *et al*., 1996; Bach *et al*., 1997, 1999; Visvader *et al*., 1997; Matthews and Visvader, 2003). The Clims also interact with the LIM domains of LIM homeodomain proteins as well as with some transcription factors that lack LIM domains (Torigoi *et al*., 2000; Matthews and Visvader, 2003). Clims, which interact with transcription factors via the C-terminus, are thought to coordinate the assembly of large multiprotein transcriptional complexes through their N-terminally located dimerization domains (Matthews and Visvader, 2003).

LMOs are thought to regulate transcription by several distinct mechanisms. First, by sequestering Clim coregulators participating in gene activation, upregulation of LMOs may repress transcription of genes that are activated by the association of Clims with LIM homeodomain factors (Milan *et al*., 1998; Zeng *et al*., 1998; Milan and Cohen, 2000). Second, LMOs interact with several DNA-binding proteins that lack LIM domains; the best characterized are certain Helix–Loop–Helix and GATA transcription factors (Wadman *et al*., 1994, 1997; de la Calle-Mustienes *et al*., 2003). LMOs are thought to recruit Clim cofactors to such complexes, thereby activating transcription of target genes. Third, because LMOs participate in multiprotein transcription complexes, the stoichiometry of these complexes is critical for transcriptional regulation (Ramain *et al*., 2000; Thaler *et al*., 2002; Lee and Pfaff, 2003). Coordinated upregulation of LMOs, Clims, and associated DNA-binding proteins may lead to activation, whereas both upregulation and downregulation of individual components may disrupt such complexes. While the levels of LMO4 and Clims are often coordinately regulated during development, in breast

Correspondence: Dr B Andersen, Division of Endocrinology, Departments of Medicine and Biological Chemistry, Sprague Hall, Room 206, University of California, Irvine, CA 92697-4030, USA.
E-mail: bogi@uci.edu
Received 8 October 2005; revised 9 November 2005; accepted 10 November 2005

cancer cells, where LMO4 has been proposed to act in a pro-oncogenic fashion (Sum *et al*., 2005b), LMO4 is often upregulated disproportionately to Clims (Visvader *et al*., 2001; Wang *et al*., 2004).

In addition to neurons, LMO4 is highly expressed in epithelial cells, often at locations of active mesenchymal–epithelial interactions, such as in hair follicles, teeth, epidermis, mammary gland, kidney, and lungs (Sugihara *et al*., 1998; Hermanson *et al*., 1999; Wang *et al*., 2004; Sum *et al*., 2005a). We and others have found that LMO4 can interact with distinct DNA-binding proteins expressed at these locations (Sugihara *et al*., 1998; Sum *et al*., 2002; Kudryavtseva *et al*., 2003; Manetopoulos *et al*., 2003). As LMO4 is highly expressed at multiple sites of mesenchymal–epithelial interactions, it is attractive to propose that LMO4 interacts with and modulates the function of DNA-binding proteins in conserved signaling pathways involved in mesenchymal–epithelial signaling.

The Smad proteins, key mediators of the transforming growth factor-β (TGFβ)/bone morphogenic protein (BMP) superfamily of ligands, provide an example of DNA-binding proteins that play roles in mesenchymal–epithelial interactions in development and cancer (Massague and Wotton, 2000). Smads respond to phosphorylating signals by translocating into the nucleus and associating with target genes as a complex of receptor-activated Smads (R-Smads) and common mediator Smads (Co-Smad; Smad4). Previous work has shown that the Smad transcription complex interacts with several transcription factors, which can positively or negatively modulate TGFβ signal (Derynck and Zhang, 2003). By modulating the binding and activity of Smad proteins on target genes, these Smad-associating proteins are thought to play key roles in TGFβ/BMP signal transduction by affecting the specificity and magnitude of the TGFβ signal in response to environmental effects (Massague and Wotton, 2000).

In this paper, we demonstrate that LMO4 can modulate the proliferative response of epithelial cells to TGFβ signaling. Furthermore, we show that LMO4 interacts with R-Smads and is recruited to genomic Smad-binding sites, suggesting a mechanism for the ability of LMO4 to modulate TGFβ signaling. Our findings link LMO4 to a conserved signaling pathway that plays important roles in epithelial homeostasis.

Results

*LMO4 enhances TGF*β*-mediated transcriptional signal*

LMO4 is upregulated in epithelial cells during the proliferative phase of mammary gland development and in about half of invasive breast cancer cases (Visvader *et al*., 2001; Wang *et al*., 2004). To determine whether LMO4 upregulation could modulate TGFβ signaling, we tested the ability of LMO4 to affect the expression of a well-characterized TGFβ-responsive reporter gene, 9xGAGA-Luciferase (Wieser *et al*., 1995; Dennler *et al*., 1998), which is derived from the regulatory region of the Plasminogen Activator Inhibitor 1 (PAI-1) gene. When the 9xGAGA-Luciferase plasmid was cotransfected with a constitutively active TGFβ receptor 1 (TβR1-AAD) into the kidney epithelial cell line HEK293T, luciferase expression was increased nine-fold (Figure 1a), consistent with previously published data (Dennler *et al*., 1998). Cotransfection of an expression plasmid encoding LMO4 resulted in a dose-dependent expression of LMO4 (Figure 1b) and markedly increased the TβR1-AAD-stimulated luciferase activity, also in a dose-dependent manner (Figure 1a). Moreover, we observed similar enhancing effects of LMO4 on TGFβ1-stimulated 9xGAGA-Luciferase expression in normal human mammary epithelial cells (HMEC) (Figure 1c), and the mouse mammary epithelial cell line NMuMG (Figure 1d). These results indicate that LMO4 can enhance TGFβ-mediated signaling as monitored by the PAI-1 promoter in HEK293T and mammary epithelial cells.

To test whether LMO4 could also modulate the expression of the endogenous PAI-1 gene, we used retroviral transduction to introduce the LMO4 protein into NMuMG cells, and measured PAI-1 mRNA levels with quantitative real-time PCR. Consistent with previous results (Dong-Le Bourhis *et al*., 1998), TGFβ1 increased PAI-1 mRNA expression several fold ($\Delta\Delta C_t = 3$). LMO4 increased PAI-1 mRNA several fold under both basal ($\Delta\Delta C_t = 2.3$) and TGFβ1-stimulated ($\Delta\Delta C_t = 5.7$) conditions (Figure 1e). Taken together, these results suggest that LMO4 upregulation is capable of enhancing TGFβ-stimulated transcription of the PAI-1 gene.

*LMO4 regulates the transcriptional response to TGF*β *in a biphasic manner*

LMO4 regulates transcription by participating in multiprotein complexes that often involve both DNA-binding proteins and other transcriptional coregulators, such as Clims. The stoichiometry of these complexes is critical for their activity and LMO4 upregulation may therefore modulate transcription by disrupting such complexes (Ramain *et al*., 2000; Thaler *et al*., 2002; Lee and Pfaff, 2003). If this is true, then lowering of LMO4 levels might also lead to changes in gene expression that are similar to those found with LMO4 upregulation; both perturbations, up- and downregulation, would alter the stoichiometry of LMO4-containing transcription complexes. For example, both up- and downregulation of the *Drosophila* Clim homologue, Chip, lead to similar phenotypes in proneural (Ramain *et al*., 2000) and wing (Milan and Cohen, 1999; van Meyel *et al*., 1999) patterning.

To test this idea, we designed three siRNAs against human LMO4 and tested their ability to lower LMO4 levels in T47D breast cancer cells, which express LMO4 at a relatively high level, facilitating the monitoring of endogenous LMO4 protein levels. Of the three LMO4 siRNAs, LMO4 siRNA #1 and #3 effectively decreased endogenous LMO4 levels (Figure 2a; lanes 1 and 3) compared to a negative control siRNA. To test the

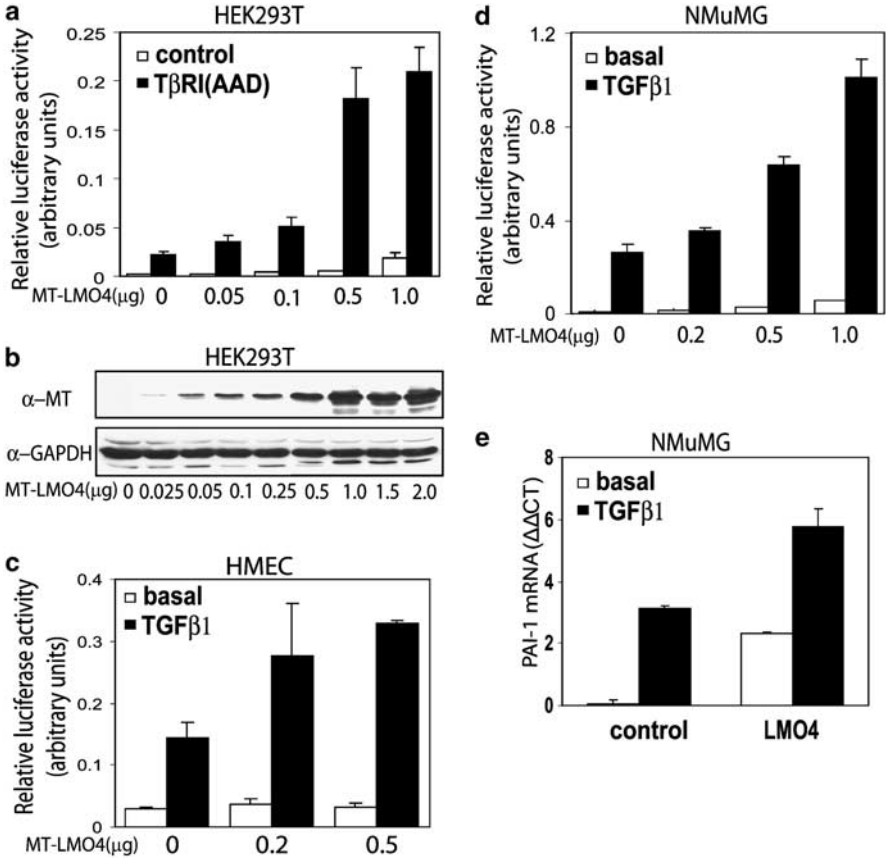

Figure 1 LMO4 potentiates TGFβ-mediated transcriptional activity in epithelial cells. (**a**) The 9xCAGA-Luciferase reporter plasmid (0.5 μg) was transiently cotransfected into HEK-293T cells with either an empty expression plasmid (control) or a plasmid encoding a constitutively activated receptor I of TGFβ (TβRI-AAD; 0.1 μg), which activates TGFβ signaling. An expression plasmid encoding MT-LMO4 was cotransfected in the indicated amounts, ranging from 0 to 1.0 μg; equal amount of DNA was included in all transfections by adjusting the amount of empty expression vector. We determined relative luciferase activity 40 h after the transfection. (**b**) The MT-LMO4 expression plasmid was transfected into HEK293T cells in the indicated concentrations. We isolated whole-cell lysates 40 h later and determined the expression of MT-LMO4 protein by Western blotting with an MT antibody (top panel). As a control for protein concentration and loading, the same blot was also bound to a GAPDH antibody (bottom panel). (**c**) Normal human mammary epithelial (HME) cells were cotransfected with the 9xCAGA-Luciferase reporter plasmid (0.5 μg) and an expression plasmid encoding MT-LMO4 in the indicated amounts. After 24 h, the cells were treated either with vehicle (basal) or TGFβ1 (1 ng/ml) for 20 h before relative luciferase activity was determined. (**d**) Mouse mammary gland (NMuMG) cells were cotransfected with the 9xCAGA-Luciferase reporter plasmid (0.5 μg) and an expression plasmid encoding MT-LMO4 in the indicated amounts. After 24 h, the cells were treated either with vehicle (basal) or TGFβ1 (1 ng/ml) for 20 h before relative luciferase activity was determined. (**e**) NMuMG cells were infected with a retroviruses expressing GFP (control) or LMO4-GFP fusion protein (LMO4). When approximately 80% of the cell monolayers were expressing the target proteins as judged by fluorescent microscopy, the cells were treated either with vehicle alone (basal) or TGFβ1 (1 ng/ml) for 6 h. Total RNA was extracted and endogenous PAI-1 mRNA relative to 18S mRNA levels were determined by real-time PCR. All experiments were carried out in triplicate, and luciferase activity and mRNA levels are expressed as the mean$\pm$s.d. Similar results were obtained in three different experiments, each one performed in triplicate.

effect of LMO4 siRNA on TGFβ signaling, we transfected into HEK293T cells an expression vector encoding LMO4 shRNA#1 with 9xGAGA-Luciferase reporter plasmid, with and without a TGFβ activator. While the control shRNA had little effect on TGFβ stimulation of reporter activity, the LMO4 shRNA markedly enhanced TGFβ stimulation (Figure 2b). The effect of the LMO4 shRNA was specific because the expression vector that encodes mouse LMO4, which is not targeted by the shRNA, could partially reverse the stimulatory effect of LMO4 shRNA (Figure 2c). As predicted from the experiments described previously (Figure 1), higher amounts of transfected LMO4 ultimately resulted in stimulation of gene expression, creating a U-shaped dose–response curve for the effect of LMO4 on TGFβ-stimulated gene expression (Figure 2c).

Together, these experiments show that in this system, TGFβ signaling is sensitive to LMO4 levels. Very high or low concentration of LMO4 can enhance TGFβ-dependent transcription of the PAI-1 gene reporter. These findings are consistent with results from other systems, showing that the stoichiometry of the components of transcription complexes involving LIM domain transcription factors is critical for regulation of gene activation (Milan and Cohen, 1999; van Meyel *et al*.,

1999; Ramain *et al*., 2000; Thaler *et al*., 2002; Lee and Pfaff, 2003; Matthews and Visvader, 2003).

LMO4 interacts with several R-Smads

TGFβ regulates transcription of the PAI-1 gene by facilitating the nuclear translocation and DNA binding of a complex composed of R-Smads (Smad2 and/or Smad3) and the co-Smad, Smad4 (Massague and Wotton, 2000; Derynck and Zhang, 2003). To investigate the mechanisms of action for the effect of LMO4 on TGFβ-mediated transcription, we tested whether LMO4 could interact with these key mediators of TGFβ-regulated transcription. An expression vector encoding myc-tagged LMO4 was transfected into HEK293T cells with or without HA-tagged Smad1, Smad2, Smad4, and Smad5. Whole-cell extracts were isolated and immunoprecipitated with an myc-tagged antibody followed by SDS gel electrophoresis and immunoblotting with an HA antibody. Smad1, Smad2 and Smad5 were all clearly co-immunoprecipitated with LMO4 (Figure 3a; top panel), suggesting that LMO4 is capable of interacting with several Smad proteins. A weak interaction was also detected between LMO4 and the co-Smad, Smad4 (Figure 3a; lane 5). LMO4 was also co-immunoprecipitated with a Smad2 antibody in non-transfected HEK293T cells (Figure 3b), indicating interaction of endogenous LMO4 and Smad2 proteins.

To validate the co-immunoprecipitation results, and to test whether the LMO4–Smad interactions are direct, we performed GST pull-down assays. We found that LMO4 clearly interacts with Smad2, Smad3, Smad5, and Smad8, with the strongest LMO4 interactions detected with Smad8 (Figure 4a). Consistent with the co-immunoprecipitation results, a weak LMO4 interaction was also detected with Smad4. To map the Smad domains that are responsible for interactions with LMO4, we tested the interactions of LMO4 with subregions of the Smad3 protein. Smad proteins are composed of an N-terminal Mad homology (MH) domain 1, which is responsible for nuclear import and DNA binding, except in the case of the major splice form of Smad2, which contains an insertion in these regions and does not directly bind DNA. A C-terminal MH2 domain, which mediates Smad oligomerization, is linked to the MH1 domain with a less-conserved linker domain (Massague and Wotton, 2000; Derynck and Zhang, 2003). All three domains have been shown to interact with several transcription factors as well as cytoplasmic adaptors (Massague and Wotton, 2000; Derynck and Zhang, 2003). In these experiments, LMO4 interacted with the MH1 and linker domains of Smad3; no interaction was found with the MH2 domain (Figure 4b).

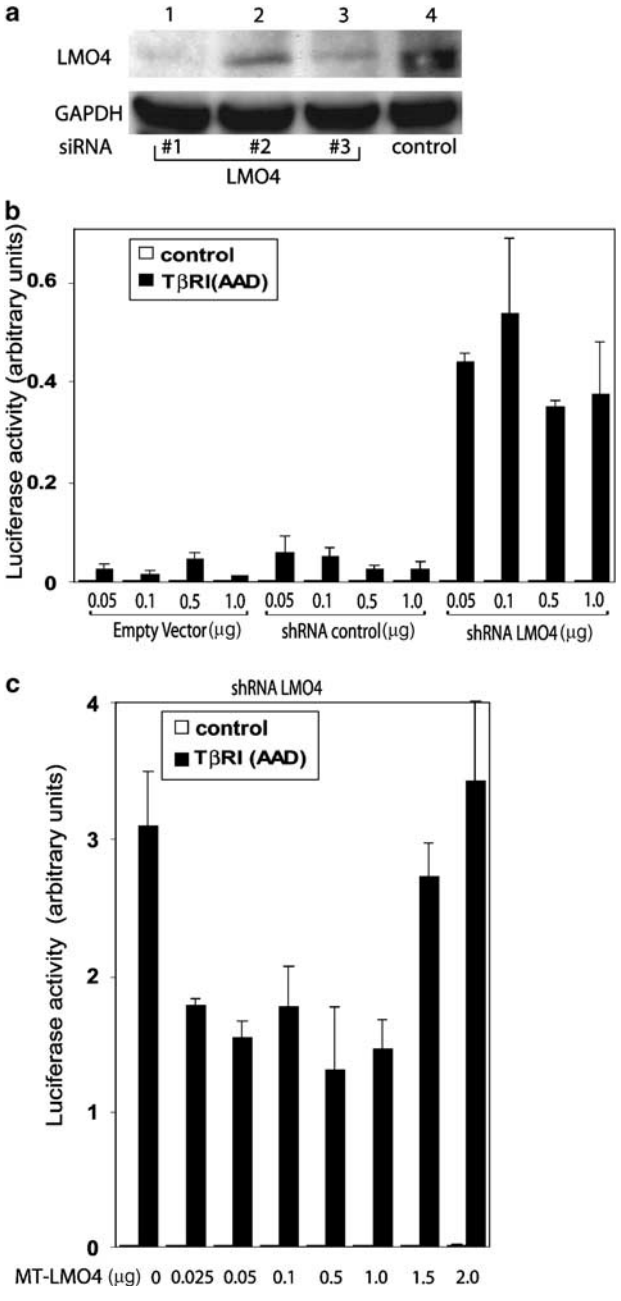

Figure 2 Biphasic regulation of PAI-1 reporter activity by LMO4. (**a**) Three distinct siRNAs targeting human LMO4 and a control siRNA were transfected into T47D breast cancer cells, using RNAiFect transfection reagent (Qiagen). After 40 h, LMO4 protein levels were determined by Western blotting of whole-cell lysates with LMO4 antibody (top panel). As a control, the same blot was bound to GAPDH antibody (bottom panel). (**b**) HEK293T cells were cotransfected with the 9xCAGA-Luciferase construct (0.5 μg) and either an empty expression plasmid (control) or a plasmid encoding a TGFβ activator (TβRI-AAD; 0.1 μg). To test the effect of lowering LMO4, we also transfected the indicated amounts of empty shRNA expression vector, control shRNA expression vector, and LMO4 shRNA expression vector. (**c**) HEK293T cells were cotransfected with the 9xCAGA-Luciferase construct (0.5 μg) and either an empty expression plasmid (control) or a plasmid encoding a TGFβ activator (TβRI-AAD; 0.1 μg). In addition, the vector expressing human LMO4 shRNA#1 (0.5 μg) was included under all conditions. An expression vector that encodes mouse MT-LMO4 in the indicated concentrations was cotransfected. At 40 h after transfection, luciferase activity was determined; relative luciferase activity is expressed as the mean $\pm$ s.d. from triplicate transfection. Similar results were obtained in three independent experiments.

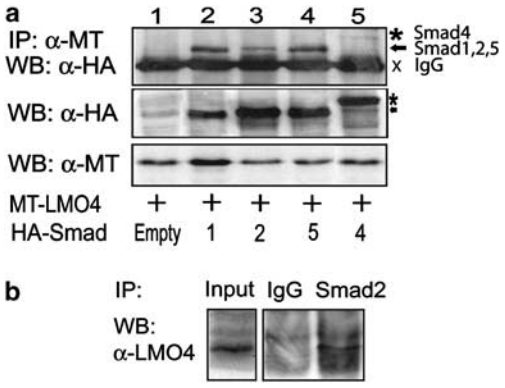

Figure 3 LMO4 interacts with several Smad proteins. (**a**) MT-tagged LMO4 and HA-tagged Smad1 (lane 2), Smad2 (lane 3), Smad4 (lane 5), and Smad5 (lane 4) were cotransfected into HEK293T cell. At 2 days after transfection, whole-cell lysates were isolated. Cell lysates were immunoprecipitated with anti-MT and the Smad proteins in the complex identified with immunoblotting with anti-HA (top panel). Smad and LMO4 protein expression was demonstrated with direct immunoblotting of cell lysates with HA antibody (middle panel) and MT antibody (bottom panel), respectively. The asterisk indicates the location of Smad4, the arrow the location of Smad2, -3 and -5, and the X the location of IgG. (**b**) Lysates from HEK293T cells were immunoprecipitated with either IgG or Smad2 antibody, and immunoblotted with an LMO4 antibody.

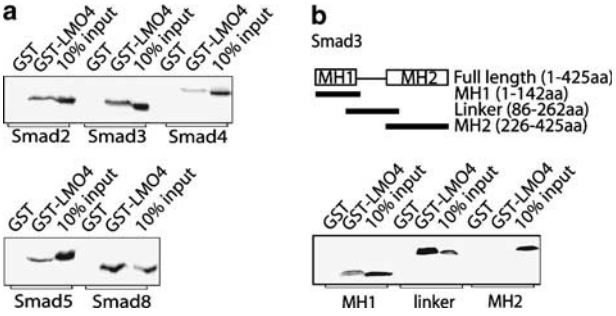

Figure 4 LMO4 interacts with the MH1 and linker regions of Smad proteins. (**a**) Full-length, ^{35}S-labeled Smad2, Smad3, Smad4, Smad5, and Smad8 were incubated with either GST alone or GST-LMO4. LMO4–Smad interactions were determined with GST pull-down assays and compared to 10% of the Smad protein input as visualized by SDS–PAGE and autoradiography. (**b**) GST pull-down assays were used to determine interactions between GST-LMO4 and the indicated ^{35}S-labeled subdomains of Smad3.

These data suggest that LMO4 may modulate the transcriptional response to TGFβ by interacting with Smad proteins, and that both the MH1 and linker domains of Smad3 participate in the interaction.

LMO4 can associate with the PAI-1 endogenous promoter in vivo *in response to TGF*β

During TGFβ signaling, R-Smads are phosphorylated by the activated receptor and form complexes with the co-Smad Smad4, after which the R-Smad/Smad4 complex enters the nucleus and associates with target genes (Massague and Wotton, 2000). To test whether LMO4 affects the phosphorylation of R-Smads, HEK293T cells were transfected with a control vector or LMO4, followed by treatment with vehicle or TGFβ1. We assessed the phosphorylation of endogenous Smad2 by Western blotting with an antibody recognizing phosphorylated Smad2. LMO4 had no effect on TGFβ1-induced Smad2 phosphorylation (Supplemental Figure 1A). To test whether LMO4 affects the R-Smad–Smad4 interaction, a Flag-tagged Smad3 and an HA-tagged Smad4 were cotransfected into HEK293T cell with or without MT-LMO4. After TGFβ1 treatment, the interaction between Flag-Smad3 and HA-Smad4 was analysed with immunoprecipitation and Western blotting. While TGFβ1 markedly enhanced Smad3/Smad4 complex formation, LMO4 had no effect on the complex formation (Supplemental Figure 1B). Together, these results suggest that LMO4 affects TGFβ signaling downstream of R-Smad phosphorylation and R-Smad/Smad4 complex formation. Based on these experiments and the protein–protein interaction results (Figures 3 and 4), we hypothesized that LMO4 might associate with Smad complexes on target genes.

To test whether LMO4 can associate with the PAI-1 promoter *in vivo*, we performed chromatin immunoprecipitation (ChIP) assays. HEK293T cells, untreated or treated with TGFβ1, were transfected with an empty vector or expression vectors encoding MT-Smad4 or MT-LMO4. ChIP assays were performed as previously described using myc(MT) antibodies with binding to the endogenous PAI-1 promoter detected with PCR using specific oligonucleotides (Kurisaki *et al*., 2003). As expected, Smad4 associates with the PAI-1 promoter, with binding greatly increased after TGFβ1 treatment (Figure 5a; lanes 1 and 2). Interestingly, LMO4 also associates with the PAI-1 endogenous promoter in a TGFβ1-dependent manner (Figure 5a; lanes 4 and 5), consistent with its ability to interact with Smad proteins and regulate the PAI-1 promoter. The MT antibody is specific in this assay because the PAI-1 promoter was not precipitated in cells transfected with an empty vector (Figure 5a; lane 3), and nonspecific IgG did not precipitate the PAI-1 promoter (Figure 5b; lanes 1–4) in an experiment where LMO4 associated with the promoter in a TGFβ1-dependent manner (Figure 5b; lanes 5 and 6). The association of LMO4 to the PAI-1 regulator, region is also promoter specific because no binding was detected to the GAPDH promoter (Figure 5c), which is regulated neither by TGFβ nor LMO4. Taken together with the results from transient transfection assays and protein–protein interaction studies, these data suggest that LMO4 can bind the PAI-1 promoter in a TGFβ-dependent fashion. This may occur via direct association with Smad proteins, resulting in modulation of promoter activity.

*LMO4 potentiates TGF*β*-mediated inhibition of cell proliferation*

Among the many different effects of TGFβ, inhibition of epithelial cell growth, either by suppression of cell proliferation or enhanced apoptosis, is one of the best-characterized (Derynck *et al*., 2001). Therefore, to test

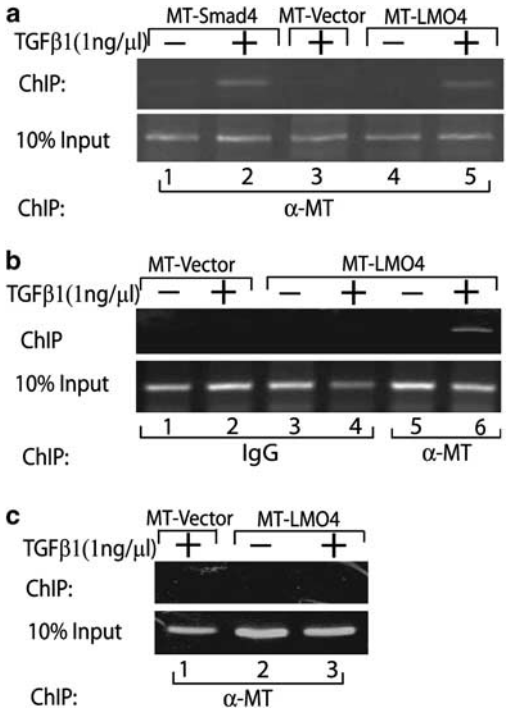

Figure 5 LMO4 associates with the endogenous PAI-1 promoter in a TGFβ-dependent fashion. (**a–c**) HEK293T cells grown in 100 mm dishes were transfected with 2 μg of empty expression vector or the same amount of expression vectors encoding MT-LMO4 or MT-Smad4, using Lipofectamine 2000. On the third day after transfection, cells were treated with vehicle or TGFβ1 (1 ng/ml) for 2 h. LMO4-associated DNA was isolated by ChIP with anti-MT or normal mouse IgG as a negative control, followed by PCR with primers specific for the PAI-1 promoter (**a** and **b**) or the GAPDH promoter (**c**). As a control, 10% of the input DNA was also PCR-amplified (lower panels in **a**, **b**, and **c**).

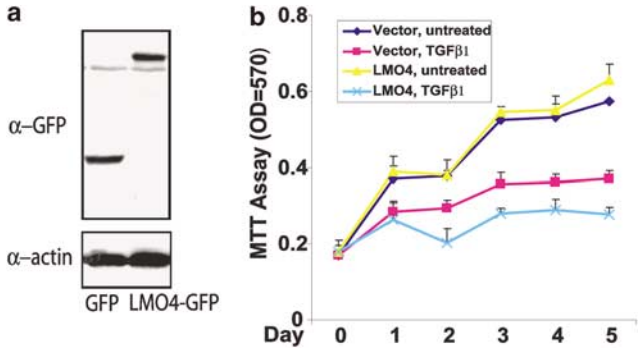

Figure 6 LMO4 enhances the inhibitory effect of TGFβ on human mammary epithelial cell growth. (**a**) HME cells were infected with equivalent pfu of retroviruses encoding GFP alone or LMO4-GFP. After 2–3 rounds of infections, about 80% of HME cells were expressing the target proteins as assessed by immunomicroscopy (not shown). At that time, whole-cell lysates were isolated and analysed by Western blotting with GFP antibody (top panel). As a control, the same blot was also bound to actin antibody (bottom panel). (**b**) HME cells expressing either LMO4-GFP or the control protein GFP were plated onto 96-well plates (5000 cells/well). After treatment with TGFβ1 (1 ng/ml) for 24 h, cells were grown in fresh grow medium for another 4 days; cell growth was monitored, using the MTT assay. MTT assays were performed in 10-replicate determination and results are expressed as the mean $\pm$ s.d. at OD = 570 nm. Three independent experiments were performed; the data from a representative experiment are shown.

whether LMO4 can modulate the *in vivo* function of TGFβ signaling, we introduced viral vectors expressing either green fluorescent protein (GFP) or LMO4-GFP fusion proteins into normal HMEC. Expression from the GFP and LMO4-GFP vectors was equivalent in these experiments (Figure 6a) and for both vectors about 80% of cells expressed the proteins as determined by the GFP signal (data not shown). Cells were treated either with vehicle or TGFβ1 for 24 h and their growth was monitored over the course of 5 days, using the 3-[4,5-dimethylthiazol-2-yl]-2,5-diphenyltetrazolium bromide (MTT) assay. As expected, TGFβ1 inhibited the growth of HMEC in a time-dependent manner (Figure 6b). Interestingly, LMO4 significantly potentiated the cytostatic effect of TGFβ1 (Figure 6b). In contrast, LMO4 had no significant effect on the growth of untreated HMEC (Figure 6b).

To test whether the effect of LMO4 on the growth of HMEC was due to inhibition of proliferation or increased apoptosis, we first examined the effect of LMO4 on proliferation of HMEC, using the 5-(and 6-) carboxy fluoroscein diacetate succimidyl ester (CFSE) assay. As expected, TGFβ1 inhibited the proliferation of HMEC in a time-dependent fashion (Figure 7a; top panels). The introduction of LMO4 by retroviral transduction inhibited proliferation of HMEC (Figure 7a; middle panels). Expression from the control vector (TAP) and the vector expressing LMO4-TAP was similar (Figure 7b). To test whether cell death was modulated by LMO4, we monitored apoptosis after introduction of LMO4 in the presence and absence of TGFβ1 in HMEC, using Annexin V staining in combination with FACS analysis. TGFβ1 treatment increased the fraction of apoptotic HMEC from 6.43 to 11.21% and this effect was not significantly modulated by LMO4 (Figure 7c), suggesting that LMO4 does not alter the growth of HMEC by affecting apoptosis. Together, these experiments suggest that LMO4 affects cell growth by potentiating the inhibitory effect of TGFβ on cell proliferation.

In summary, our results suggest a novel function for LMO4 in TGFβ signaling. Based on our findings, we propose a model in which LMO4 interacts with Smad proteins on target genes, thereby modulating the cytostatic response of TGFβ.

Discussion

In this manuscript, we provide new information that the transcriptional coactivator LMO4 can modulate the cytostatic effects of TGFβ in epithelial cells. Using ChIP and transient transfection transcription assays, we demonstrate that LMO4 can associate with and regulate a prototype Smad target promoter.

One of the striking features of TGFβ signaling is the pleiotropic nature of its biological effect (Massague and

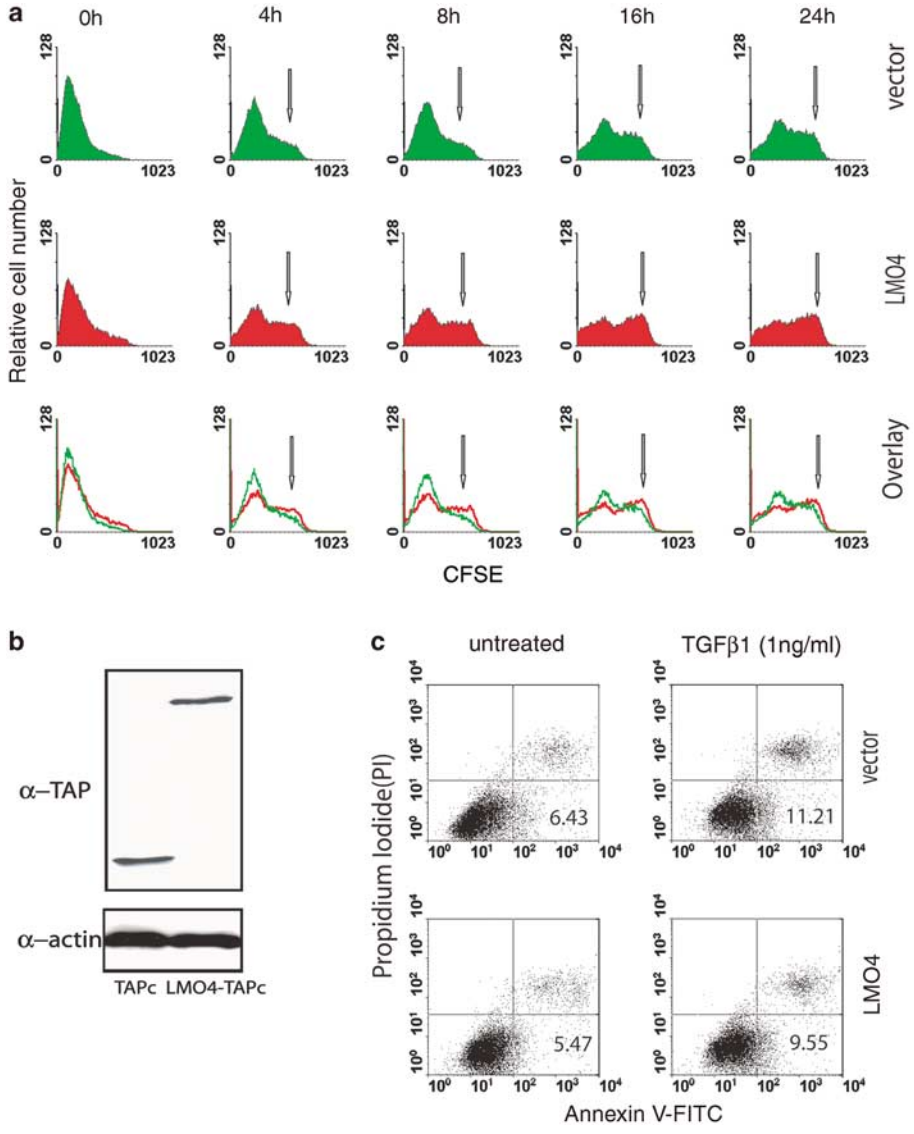

Figure 7 LMO4 enhances the inhibitory effect of TGFβ on HME cell proliferation, but has no effect on TGFβ-induced apoptosis. (**a**) HME cells were infected with retroviruses encoding LMO4-TAPc fusion protein or TAP alone as described for the experiment in Figure 6. HME cells expressing either control protein TAP (top panel) or LMO4-TAPc (middle panel) were stained with CFSE and then plated onto six-well plates (10 000 cells/well). On the second day, cells were treated with TGFβ1 (1 ng/ml) for the indicated time, and then grown in fresh medium for another 3 days. Cell proliferation was assessed with a FACS based on CFSE quantity. The CFSE amount in a single cell will decrease by 50% with each cell division. The arrows point to cells that contain large amount of CSFE, indicating slow proliferation. The third panel contains overlay of the TAPc (vector) and LMO4-TAPc (LMO4) panels and shows the relative abundance of slow-growing cells in the LMO4-infected panel. The data from a single representative experiment (out of three) are shown. (**b**) Expression of TAP and LMO4-TAPc in HME cell lysates was assessed by immunoblotting with TAP antibody (top panel). As a control, the same blot was also analysed by an Actin antibody (bottom panel). (**c**) HME cells expressing either TAP control protein or LMO4-TAPc were seeded onto 60-mm dishes (1×10^5 cells/dish). The next day, cells were treated with either vehicle (untreated) or TGFβ1 (1 ng/ml) for 24 h. Cell apoptosis was analysed with combined propidium iodide/annexin-V-FITC staining. The number in right-bottom half in each panel indicates the percentage of apoptotic cells. Similar results were obtained from three different experiments.

Wotton, 2000; Derynck and Zhang, 2003). Depending on context, TGFβ can selectively regulate proliferation, apoptosis, migration, epithelial–mesenchymal transition, as well as other cellular features. In addition, the effects of TGFβ are highly dependent on the responding cell type. Our data add to the growing literature suggesting that interactions of Smad proteins with other transcription factors may, at least in part, underlie the specificity of the multitude of TGFβ actions. Thus, our data suggest that LMO4 has selective effects on TGFβ actions because it modulates cell proliferation (Figures 6 and 7), but has no effect on apoptosis (Figure 7) and epithelial–mesenchymal transition (data not shown). Also, since LMO4 expression is restricted to epithelial cells, our findings suggest one mechanism whereby TGFβ effects are selectively modulated in distinct cell types.

Interestingly, our data predict that within the same cell type, changes in LMO4 levels may either increase or decrease TGFβ signaling, depending on the levels of LMO4 under the basal condition and the magnitude of LMO4 change (Figure 2c). For example, under conditions of very low LMO4 levels, moderate increases in LMO4 may lead to decreased TGFβ effect. However, under conditions of higher basal levels of LMO4, a further increase may enhance TGFβ effect. Smad proteins participate in multiprotein complexes that include transcriptional coactivators and corepressors, as well as DNA-binding proteins (Massague and Wotton, 2000; Derynck and Zhang, 2003). Since both upregulation and downregulation of LMO4 can lead to potentiation of TGFβ activation of the PAI-1 promoter, it is tempting to speculate that LMO4 helps to coordinate complexes on the PAI-1 gene, and that the stoichiometry of the components of these complexes is important. In such a case, both removal and excess of LMO4 is predicted to disrupt multiprotein complexes (Ramain *et al*., 2000; Thaler *et al*., 2002; Lee and Pfaff, 2003). Our findings are consistent with data in *Drosophila* showing that either upregulation or downregulation of the Clim homologue Chip leads to similar developmental phenotypes (Ramain *et al*., 2000).

Our data, which suggest that TGFβ regulation of at least some genes may be sensitive to LMO4 levels, are likely to have implications for understanding LMO4-mediated gene regulation because LMO4 is highly regulated under a variety of conditions that include normal and cancer development, as well as in response to physiological stimuli (Hinks *et al*., 1997; Wang *et al*., 2004). Owing to the cell- and developmental-specific regulation of LMO4, our findings may provide a mechanistic basis for aspects of cell-type- and context-specific gene regulation by TGFβ. Our results, showing that LMO4 overexpression enhances TGFβ-mediated cytostasis, may seem to contradict recent studies, which indicate that LMO4 overexpression promotes tumorigenic properties of mammary epithelial cells (Visvader *et al*., 2001; Sum *et al*., 2005b). However, there are at least two potential explanations for this apparent contradiction. First, because of the U-shaped TGFβ response curve to LMO4 (Figure 2c), the starting point will determine whether LMO4 potentiates or decreases TGFβ signaling; LMO4 overexpression in tumors may inhibit TGFβ signaling. Second, in addition to a direct cytostatic effect, TGFβ has direct and indirect protumorigenic effects; it is possible that LMO4 potentiates the protumorigenic effects of TGFβ *in vivo*.

A striking feature of LMO4 gene expression is its prominent expression in epithelial cells at locations of active reciprocal mesenchymal–epithelial interactions (Sugihara *et al*., 1998; Hermanson *et al*., 1999; Wang *et al*., 2004; Sum *et al*., 2005a). In such organs, including the developing hair follicles, teeth, mammary gland, lungs, and kidneys, BMP signaling has been shown to be very important (Arias, 2001; Waite and Eng, 2003). While our study has focused on the role of TGFβ signaling, it is quite possible that LMO4 could also modulate BMP signaling because we found that it interacts with Smad1, Smad5, and Smad8, which are primarily responsible for mediating BMP signals (Derynck and Zhang, 2003). In this respect, a recent study that used the yeast two-hybrid assay to screen for Smad8-interacting proteins identified LMO4 as a Smad8 partner (Colland *et al*., 2004). This is consistent with our findings that of all Smads tested, the strongest interaction was found between LMO4 and Smad8. This study also showed that LMO4 siRNA could inhibit BMP-7-stimulated transcription of a BMP-responsive reporter gene and the alkaline phosphatase gene in HepG2 cells (Colland *et al*., 2004). Yet, another potential link between LMO4 and BMP signaling comes from studies in *Xenopus* where it was shown that xLMO4 transcripts in ventral mesoderm and the neural plate are upregulated by BMP-4 (de la Calle-Mustienes *et al*., 2003). Functional studies indicate that xLMO4 plays roles in ventral mesoderm identity and neural plate regionalization. Thus, depending on the context, LMO4 may be both induced by BMP signaling and a modulator of the transcriptional effects of BMPs.

Many of the experiments in our study, including the ChIP experiments, were performed with exogenously expressed LMO4. However, it is important to note that we provide strong support for the potential role of endogenous LMO4 in TGFβ signaling. First, we demonstrated an interaction between endogenous LMO4 and Smad2 proteins, suggesting that LMO4 and Smad2 can interact *in vivo* at normal cellular concentrations (Figure 3b). Second, we showed that RNAi-mediated knockdown of LMO4 affected TGFβ signaling, supporting an *in vivo* role for endogenous LMO4 in TGFβ signaling (Figure 2).

For unknown reasons, LMO4 knockout mice die during later stages of embryogenesis or perinatally (Hahm *et al*., 2004; Tse *et al*., 2004; Lee *et al*., 2005). While a significant portion of these mice show exencephaly, even mice without this abnormality die perinatally. In addition, LMO4 knockout mice have skeletal patterning defects involving the basal skull, vertebrae, and ribs. Other homeotic transformations such as fusions of cranial nerves IX and X and defects in cranial nerve V were also observed (Hahm *et al*., 2004). No mice deleted for genes encoding TGFβ superfamily ligands phenocopy all aspects of the LMO4 knockout mice. However, strikingly, mice deleted for the TGFβ2 gene show defects in the sphenoid bone highly similar to those found in LMO4 mutant mice, including a missing presphenoid body; TGFβ2 knockout mice also exhibit rib cage abnormalities similar to the LMO4 knockout mice (Sanford *et al*., 1997). As in the LMO4 knockout mice, skeletal defects of the basal skull, vertebrae, and ribs are prevalent in BMP7 gene-deleted mice (Luo *et al*., 1995). These skeletal abnormalities include rib cage abnormalities that are common to the two, such as misalignment of the ribs on the sternum. Deletion of the BMP antagonist Noggin leads to altered patterning of somites and the neural tube in the mouse, including neural tube closure defects in the cranial region, similar to those found in the LMO4 knockout mice (McMahon *et al*., 1998). Similarly, Smad5 knockout mice exhibit

failure of cranial neural tube closure and exencephaly (Chang *et al*., 1999). Furthermore, mice deleted for the c-ski gene, which encodes a transcriptional repressor involved in TGFβ/BMP signaling, show both exencephaly and defects in the basal skull bones similar to those found in LMO4 knockout mice (Berk *et al*., 1997). Thus, it is possible that altered signaling by TGFβ superfamily ligands plays roles in some of the abnormalities in LMO4 knockout mice.

In addition to a developmental role, there are several lines of evidence suggesting that LMO4, like other members of this gene family, may play roles in oncogenesis. LMO4 was originally identified as an autoantigen in human breast cancer (Racevskis *et al*., 1999) and subsequently shown to be upregulated in over 50% of breast cancer cases (Visvader *et al*., 2001). Additionally, it was found that LMO4 could interact with the BRCA1 tumor suppressor gene (Sum *et al*., 2002). Consistent with a role in mammary epithelial cells, we have shown that overexpression of a dominant-negative LMO4 inhibits ductular and lobuloalveolar development in the mammary glands of transgenic mice (Wang *et al*., 2004), and others have demonstrated that mammary gland-specific deletion of the LMO4 gene leads to impaired lobuloalveolar development during pregnancy (Sum *et al*., 2005c). LMO4 has also been shown to be upregulated at the invasive fronts of oral cancers, suggesting a role in cancer cell invasion (Mizunuma *et al*., 2003). In the prostate, LMO4 was downregulated during tumor progression and lowered in hormone refractory tumors (Mousses *et al*., 2002). In breast cancers and in breast cancer cell lines, LMO4 levels appear to be disproportionately upregulated as compared to the levels of Clim factors (Visvader *et al*., 1997; Wang *et al*., 2004). Therefore, the effects we have observed may have particular relevance for such situations where LMO4 and Clim levels are not coordinately regulated.

Materials and methods

Cell culture, retroviruses, and transfection assays

Normal HMEC were purchased and cultured according to protocols from Cambrex. The murine mammary epithelial (NMuMG) cells, human embryonic kidney (HEK293T) cells, and human breast cancer cell line T47D were cultured according to the ATCC protocol.

Retroviruses expressing LMO4 gene and control protein were based on the Retro-X™ System from BD Biosciences. Construction of the LMO4 retroviruses and the infection of virus into cells were performed according to the manufacturer's protocol. LMO4 was fused in frame at the C-terminus to the tandem affinity purification (TAPc) tag, which contains two IgG-binding domains of *Staphylococcus aureus* protein A and a calmodulin-binding peptide separated by a TEV protease cleavage site (Puig *et al*., 2001). Another vector was created in which LMO4 was fused in frame at the C-terminal site to GFP. Retrovirus was harvested from the stably transfected packaging cell line GP2-293, and the titer of virus was determined using NIH3T3 cell. In experiments, cells were infected with equivalent virus titer for each construct and for the same length of time. Protein expression was determined by Western blotting to ensure similar expression from the control and experimental viruses.

Transient transfections and luciferase reporter assays were performed as previously described, using calcium precipitation for HEK293 cells, and Lipofectamine™ 2000 (Invitrogen) for HME and NMuMg cells (Sugihara *et al*., 2001). Luciferase activity was normalized for differences in transfection efficiency, using the Renilla luciferase vector (Promega). The plasmids used in these studies have been previously described: 9xGAGA-Luciferase (Dennler *et al*., 1998), pCS2-MT-LMO4 (Sugihara *et al*., 1998), and pCMV5-TβR1-AAD (Chen *et al*., 1997).

The LMO4-specific siRNAs, which were designed based on the human LMO4 mRNA sequence (accession number, NM_006769), were obtained from Ambion. The target sequences of the LMO4 duplex siRNAs are: GGCAATGTGT ATCATCTTA (LMO4#1), GGTCTGCTAAAAGGTCAGA (LMO4#2), and GGAAACGTGTTTCAATCAA (LMO4#3). The control siRNA was unrelated to the LMO4 sequence and not known to affect any endogenous genes (Ambion). The siRNAs were introduced into T47D cells using RNAiFect transfection reagent (Qiagen). For transcriptional assays, LMO4 shRNAs and the control shRNA were synthesized and cloned into RNAi-Ready PSIREN-RetroQ-ZsGreen vector (BD Biosciences). The duplex sequences of the LMO4 shRNAs are: 5′-gatccggcaatgtgtatcatcttattcaagagataagatgatac acattgccttttg-3′ (shRNA #1), 5′-gatccggaaacgtgtttcaatcaattcaa gagattgattgaaacacgtttccttttg-3′ (shRNA #3), and 5′-gatccgtgcg ttgctagtaccaacttcaagagatttttttacgcgtg-3′ (shRNA control).

Recombinant mature human TGFβ1 (R&D Systems) was used according to the manufacturer's recommendations. Unless otherwise indicated, all other chemicals were from Fisher/ICN.

Real-time PCR

Total RNA was extracted from cells using TRIzol reagent (Invitrogen), and complementary DNA was synthesized using 5 μg of total RNA with the High-Capacity cDNA archive kit (Applied Biosystems) (Lin *et al*., 2004). Real-time PCR was performed using SYBR Green PCR Master Mix (Applied Biosystems) and the ABI Prism 7900HT platform (384-well plates; Applied Biosystems), following standard protocols from the supplier to detect threshold cycle (C_t). ΔC_t values were calculated by comparing the C_t measurements of experimental wells to the untreated (basal) wells that were infected with the control virus. All values were then normalized to 18S rRNA to obtain $\Delta\Delta C_t$ values.

Co-immunoprecipitations, Western blots, and GST pull-down assays

Co-immunoprecipitations of extracts from transfected HEK293T cells were performed as previously described (Sugihara *et al*., 2001), using MT (myc) antibody (Invitrogen; R950-25) recognizing tagged LMO4, and HA antibody (Covance; MMS-101R) detecting tagged Smads. The following vectors, pCMV5/Smad1-HA, pCMV5/Smad2-HA, pCMV5/Smad4-HA, and pGCN/HA-Smad5, were described previously (Chen *et al*., 1997; Hata *et al*., 1997). For co-immunoprecipitation of endogenous LMO4 and Smad2 proteins in HEK293T cells, we used antibodies directed against LMO4 (Santa Cruz; SC-11122) and Smad2 (Zymed; 51-1300). For GST pull-down assays, Smad mutant genes were generated by PCR-based deletion, followed by cloning into vectors allowing *in vitro* transcription/translation; the sequences were confirmed by DNA sequencing. Western blot analysis was performed as described previously (Wang *et al*., 2004), using antibodies to

phosphor-Smad2 (Cell Signaling; 3101), LMO4 (Sum *et al*., 2002), MT (Invitrogen; R950-25), HA (Covance; MMS-101R), GFP (Upstate Cell Signaling Solution; 06–896), TAPc (Peroxidase-anti-peroxidase (PAP) antibody, Sigma-Aldrich; P-2026), GAPDH (Ambion; 4300), and β-actin (Santa Cruz; SC-8432).

The GST pull-down assays were performed as previously described (de la Calle-Mustienes *et al*., 2003). Briefly, GST protein or GST-LMO4 fusion protein were incubated with ^{35}S-labeled *in vitro* translated Smad proteins at room temperature for 30 min. After washing three times, the glutathione–agarose beads were resuspended in SDS sample buffer, boiled, and analysed on 10% SDS–polyacrylamide gels.

ChIP

ChIP assays were performed according to the protocol from Upstate Cell Solution. Chromatinized DNA was crosslinked in 1% formaldehyde for 10 min at 37°C. Cells were then washed twice using ice-cold phosphate-buffered saline containing protease inhibitors (Roche Applied Science; 10752800) and then harvested in PBS with protease inhibitors. Thereafter, cells (1×10^6) were resuspended in 0.2-ml SDS lysis buffer (1% SDS, 10 mM EDTA, and 50 mM Tris-HCl, pH 8.1), incubated on ice for 10 min, and sonicated to reduce the chromatin DNA length to 1 kb. The lysates were diluted 10-fold in ChIP dilution buffer (0.01% SDS, 1.1% Triton X-100, 1.2 mM EDTA, 16.7 mM Tris-HCl, pH 8.1, and 167 mM NaCl) and precleared with sperm DNA-protein A-agarose beads (Upstate Cell Signaling Solutions) at 4°C for 1 h. Following overnight incubation with 2 μg of anti-MT or IgG, immune complexes were immobilized by salmon sperm DNA protein A agarose beads. After extensive washing and elution with 1% SDS and 0.1 M $NaHCO_3$, crosslinks were reversed by incubation at 65°C for 4 h in the presence of 0.2 M NaCl. The released DNA was phenol–chloroform-purified, and the PAI-1 and GAPDH promoter sequences were detected by PCR followed by agarose gel visualization. The ChIP primers for PAI-1 are 5′-CCT CCAACCTCAGCCAGACAAG-3′ (forward) and 5′-CCCAG CCCAACAGCCACAG-3′ (reverse) (Kurisaki *et al*., 2003). The primers for GAPDH are 5′-CGGCTACTAGCGGTTTT ACG-3′ (forward) and 5′-AAGAAGATGCGGCTGACTGT-3′ (reverse).

Cell growth assays

Cells were incubated overnight at a density of 5000 cells/well in 96-well plates, and treated with TGFβ1 (1 ng/ml) for 24 h. Then, cells were grown in a fresh growth medium for up to 5 days. Cell growth was assessed daily using the conversion of MTT to formazan production (Matsuda *et al*., 2002). Briefly, cells from 10 wells were incubated with MTT (62.5 μg/well) for 4 h. Cellular MTT was solubilized with acidic isopropanol, and absorbance was measured at 570 nm with an ELISA plate reader (Molecular Devices, Menlo Park, CA, USA). Results were plotted as the mean ± s.d. of 10 determinations for each time point. Four independent experiments were performed; the data from a representative experiment are shown.

Cell proliferation assays

To determine cell proliferation, cells were labeled with 5-(and 6-) carboxy fluoroscein diacetate succimidyl ester (CFSE; Molecular probes, Eugene, USA) to quantify cell division (Lee *et al*., 2004). Briefly, cells were resuspended in PBS at 2×10^7 cells/ml and labeled by incubation in 5 μM CFSE for 8 min at RT. Cells were then quenched with Fetal Bovine Serum, washed three times with PBS and plated onto six-well plates (10 000 cells/well). On the second day, cells were treated with TGFβ1 (1 ng/ml) for 4, 8, 16, 24 h, and then grown in fresh medium for another 3 days. Cells were detached by 0.05% trypsin (Invitrogen), suspended in 1 ml PBS, and analysed by a FACSCaliber flow meter (Becton Dickinson, Mountain View, CA, USA) using CellQuest software.

Apoptosis assays

For annexin V staining, cells were seeded at a density of 1×10^5 cells/60-mm dish on day 0. On day 1, cells were treated with TGFβ1 (1 ng/ml) for 24 h. Then, cells and supernatant were collected and stained with annexin-V-FITC and propidium iodide (PI), using the Annexin V-FLUOS Staining Kit (Roche Applied Science; 1858777). Duplicate samples were analysed on a FACSCaliber flow meter (Becton Dickinson, Mountain View, CA, USA) using CellQuest software.

Acknowledgements

We thank Yeguang Chen for the 9xCAGA-Luciferase construct; Jane Visvader for LMO4 antibody; Murray Korc for advice and reagents; and Steve Lipkin, Ping Wang, and Kevin Lin for reading the manuscript. This work was supported by National Institutes of Health Grant AR44882 (to BA), the Irving F Weinstein Foundation, the Breast Cancer Research Program of the United States Army Medical Research and Material Command (to BA, NW, and ZL), and the California Breast Cancer Research Program (to XX).

References

Agulnick AD, Taira M, Breen JJ, Tanaka T, Dawid IB, Westphal H. (1996). *Nature* **384**: 270–272.
Aoyama M, Ozaki T, Inuzuka H, Tomotsune D, Hirato J, Okamoto Y *et al*. (2005). *Cancer Res* **65**: 4587–4597.
Arias AM. (2001). *Cell* **105**: 425–431.
Bach I. (2000). *Mech Dev* **91**: 5–17.
Bach I, Carriere C, Ostendorff HP, Andersen B, Rosenfeld MG. (1997). *Genes Dev* **11**: 1370–1380.
Bach I, Rodriguez-Esteban C, Carriere C, Bhushan A, Krones A, Rose DW *et al*. (1999). *Nat Genet* **22**: 394–399.
Berk M, Desai SY, Heyman HC, Colmenares C. (1997). *Genes Dev* **11**: 2029–2039.
Chang H, Huylebroeck D, Verschueren K, Guo Q, Matzuk MM, Zwijsen A. (1999). *Development* **126**: 1631–1642.
Chen YG, Liu F, Massague J. (1997). *EMBO J* **16**: 3866–3876.
Colland F, Jacq X, Trouplin V, Mougin C, Groizeleau C, Hamburger A *et al*. (2004). *Genome Res* **14**: 1324–1332.
de la Calle-Mustienes E, Lu Z, Cortes M, Andersen B, Modolell J, Gomez-Skarmeta JL. (2003). *Dev Biol* **264**: 564–581.
Dennler S, Itoh S, Vivien D, ten Dijke P, Huet S, Gauthier JM. (1998). *EMBO J* **17**: 3091–3100.
Derynck R, Akhurst RJ, Balmain A. (2001). *Nat Genet* **29**: 117–129.
Derynck R, Zhang YE. (2003). *Nature* **425**: 577–584.
Dong-Le Bourhis X, Lambrecht V, Boilly B. (1998). *Br J Cancer* **77**: 396–403.
Grutz G, Forster A, Rabbitts TH. (1998). *Oncogene* **17**: 2799–2803.
Hahm K, Sum EY, Fujiwara Y, Lindeman GJ, Visvader JE, Orkin SH. (2004). *Mol Cell Biol* **24**: 2074–2082.

Hata A, Lo RS, Wotton D, Lagna G, Massague J. (1997). *Nature* **388**: 82–87.
Hermanson O, Sugihara TM, Andersen B. (1999). *Cell Mol Biol (Noisy-le-grand)* **45**: 677–686.
Hinks GL, Shah B, French SJ, Campos LS, Staley K, Hughes J *et al*. (1997). *J Neurosci* **17**: 5549–5559.
Jurata LW, Kenny DA, Gill GN. (1996). *Proc Natl Acad Sci USA* **93**: 11693–11698.
Kenny DA, Jurata LW, Saga Y, Gill GN. (1998). *Proc Natl Acad Sci USA* **95**: 11257–11262.
Kudryavtseva EI, Sugihara TM, Wang N, Lasso RJ, Gudnason JF, Lipkin SM *et al*. (2003). *Dev Dyn* **226**: 604–617.
Kurisaki K, Kurisaki A, Valcourt U, Terentiev AA, Pardali K, Ten Dijke P *et al*. (2003). *Mol Cell Biol* **23**: 4494–4510.
Lee MKt, Moore DJ, Jarrett BP, Lian MM, Deng S, Huang X *et al*. (2004). *J Immunol* **172**: 6539–6544.
Lee SK, Jurata LW, Nowak R, Lettieri K, Kenny DA, Pfaff SL *et al*. (2005). *Mol Cell Neurosci* **28**: 205–214.
Lee SK, Pfaff SL. (2003). *Neuron* **38**: 731–745.
Lin KK, Chudova D, Hatfield GW, Smyth P, Andersen B. (2004). *Proc Natl Acad Sci USA* **101**: 15955–15960.
Luo G, Hofmann C, Bronckers AL, Sohocki M, Bradley A, Karsenty G. (1995). *Genes Dev* **9**: 2808–2820.
Manetopoulos C, Hansson A, Karlsson J, Jonsson JI, Axelson H. (2003). *Biochem Biophys Res Commun* **307**: 891–899.
Massague J, Wotton D. (2000). *EMBO J* **19**: 1745–1754.
Matsuda K, Idezawa T, You XJ, Kothari NH, Fan H, Korc M. (2002). *Cancer Res* **62**: 5611–5617.
Matthews JM, Visvader JE. (2003). *EMBO Rep* **4**: 1132–1137.
McMahon JA, Takada S, Zimmerman LB, Fan CM, Harland RM, McMahon AP. (1998). *Genes Dev* **12**: 1438–1452.
Milan M, Cohen SM. (1999). *Mol Cell* **4**: 267–273.
Milan M, Cohen SM. (2000). *Development* **127**: 3069–3078.
Milan M, Diaz-Benjumea FJ, Cohen SM. (1998). *Genes Dev* **12**: 2912–2920.
Mizunuma H, Miyazawa J, Sanada K, Imai K. (2003). *Br J Cancer* **88**: 1543–1548. (2: van Meyel DJ, *et al*. Ssdp proteins bind to LIM-int.[PMID:12642495]Related Articles, Links).
Mousses S, Bubendorf L, Wagner U, Hostetter G, Kononen J, Cornelison R *et al*. (2002). *Cancer Res* **62**: 1256–1260.
Puig O, Caspary F, Rigaut G, Rutz B, Bouveret E, Bragado-Nilsson E *et al*. (2001). *Methods* **24**: 218–229.
Rabbitts TH. (1998). *Genes Dev* **12**: 2651–2657.
Racevskis J, Dill A, Sparano JA, Ruan H. (1999). *Biochim Biophys Acta* **1445**: 148–153.
Ramain P, Khechumian R, Khechumian K, Arbogast N, Ackermann C, Heitzler P. (2000). *Mol Cell* **6**: 781–790.
Sanford LP, Ormsby I, Gittenberger-de Groot AC, Sariola H, Friedman R, Boivin GP *et al*. (1997). *Development* **124**: 2659–2670.
Sugihara TM, Bach I, Kioussi C, Rosenfeld MG, Andersen B. (1998). *Proc Natl Acad Sci USA* **95**: 15418–15423.
Sugihara TM, Kudryavtseva EI, Kumar V, Horridge JJ, Andersen B. (2001). *J Biol Chem* **276**: 33036–33044.
Sum EY, O'Reilly LA, Jonas N, Lindeman GJ, Visvader JE. (2005a). *J Histochem Cytochem* **53**: 475–486.
Sum EY, Peng B, Yu X, Chen J, Byrne J, Lindeman GJ *et al*. (2002). *J Biol Chem* **277**: 7849–7856.
Sum EY, Segara D, Duscio B, Bath ML, Field AS, Sutherland RL *et al*. (2005b). *Proc Natl Acad Sci USA* **102**: 7659–7664.
Sum EY, Shackleton M, Hahm K, Thomas RM, O'Reilly LA, Wagner KU *et al*. (2005c). *Oncogene* **24**: 4820–4828.
Thaler JP, Lee SK, Jurata LW, Gill GN, Pfaff SL. (2002). *Cell* **110**: 237–249.
Torigoi E, Bennani-Baiti IM, Rosen C, Gonzalez K, Morcillo P, Ptashne M *et al*. (2000). *Proc Natl Acad Sci USA* **97**: 2686–2691.
Tse E, Smith AJ, Hunt S, Lavenir I, Forster A, Warren AJ *et al*. (2004). *Mol Cell Biol* **24**: 2063–2073.
van Meyel DJ, O'Keefe DD, Jurata LW, Thor S, Gill GN, Thomas JB. (1999). *Mol Cell* **4**: 259–265.
Visvader JE, Mao X, Fujiwara Y, Hahm K, Orkin SH. (1997). *Proc Natl Acad Sci USA* **94**: 13707–13712.
Visvader JE, Venter D, Hahm K, Santamaria M, Sum EY, O'Reilly L *et al*. (2001). *Proc Natl Acad Sci USA* **98**: 14452–14457.
Wadman I, Li J, Bash RO, Forster A, Osada H, Rabbitts TH *et al*. (1994). *EMBO J* **13**: 4831–4839.
Wadman IA, Osada H, Grutz GG, Agulnick AD, Westphal H, Forster A *et al*. (1997). *EMBO J* **16**: 3145–3157.
Waite KA, Eng C. (2003). *Nat Rev Genet* **4**: 763–773.
Wang N, Kudryavtseva E, Ch'en IL, McCormick J, Sugihara TM, Ruiz R *et al*. (2004). *Oncogene* **23**: 1507–1513.
Wieser R, Wrana JL, Massague J. (1995). *EMBO J* **14**: 2199–2208.
Yamada Y, Warren AJ, Dobson C, Forster A, Pannell R, Rabbitts TH. (1998). *Proc Natl Acad Sci USA* **95**: 3890–3895.
Zeng C, Justice NJ, Abdelilah S, Chan YM, Jan LY, Jan YN. (1998). *Proc Natl Acad Sci USA* **95**: 10637–10642.

Supplementary Information accompanies the paper on Oncogene website (http://www.nature.com/onc).

The LIM only factor LMO4 regulates expression of the BMP7 gene through an HDAC2-dependent mechanism, and controls cell proliferation and apoptosis of mammary epithelial cells

Ning Wang*, Zhongxian Lu*, Kervin Lin*, Kaye Starr Lam*, Xiaoman Xu*, Gordon N. Grill[&], Bogi Andersen*.

*Departments of Medicine and Biological Chemistry, University of California, Irvine, California 92697. [&]Department of Medicine, University of California, San Diego, La Jolla, California 92093.

Corresponding author:
Bogi Andersen
University of California, Irvine
Sprague Hall, Room 206
Irvine, CA 92697-4030
Phone: 949-824-9093
Fax: 949-824-2200
Email: bogi@uci.edu

Abstract

The LIM-only factor LMO4 is implicated in regulation of mammary gland development and breast cancer. Knockout of *LMO4* in mammary glands of mice leads to decreased proliferation and increased apoptosis of mammary epithelial cells, starting in early pregnancy. We identified *BMP7* as an LMO4-responsive gene in breast cancer cells and normal mouse mammary glands; both increases and decreases in LMO4 levels can increase BMP7 transcripts. In addition, we found a significant correlation between LMO4 and BMP7 transcript levels in a large dataset of human breast cancers, providing additional support that *BMP7* is a *bona fide* target gene of LMO4. BMP7 and LMO4 have similar effects on proliferation and survival of mammary epithelial cells, and interference with BMP7 partially blocks the effects of LMO4 on apoptosis, indicating that BMP7 mediates some of the functions of LMO4. We further demonstrate that LMO4 and its co-factor Clim2 are recruited to the BMP7 promoter and that association of HDAC2 with the promoter is sensitive to LMO4 levels. Our studies suggest a novel mechanism for LMOs; LMO4, Clim2 and HDAC2 are part of a transcriptional complex, and alterations in LMO4 levels can disrupt the complex, leading to decreased HDAC2 recruitment and increased promoter activity.

Introduction

Lim-only factor 4 (LMO4) belongs to a family of four mammalian LMO proteins characterized by the presence of two tandem LIM domains and no other functional domains [1]. Since the only known function of LIM domains is to mediate protein-protein interactions, it is proposed that LMOs function as adapters in larger protein complexes and as sequesters of distinct proteins. All LMOs interact with high affinity to two transcriptional co-factors referred to as Co-factors of LIM domains (Clims)/LIM domain binding proteins (Ldbs)/Nuclear LIM interactors (Nli), which enhance transactivation by LIM homeodomain factors [2-7]. LMOs are proposed to function as transcriptional activators by recruiting Clims to DNA binding proteins such as GATA, certain HLH transcription factors [8-10], and possibly others such as DEAF1 [11, 12], Get-1/Grhl3 [13] and Smads [14]. Another model of LMO function comes from studies in the fly wing showing that LMOs can repress target genes of LIM homeodomain factors by sequestering Clims [15-17]. Recently, chromatin-modifying transcriptional co-factors have been identified as LMO4-interactors, suggesting that LMOs use additional mechanisms to regulate gene transcription [14, 18, 19], including recruitment of HDAC to repress transcription [14, 18].

LMOs play critical roles in distinct pathways of mammalian development, and deregulation of their expression has been implicated in oncogenesis. Deletion of the *LMO2* gene causes early embryonic lethality and complete disruption of hematopoiesis at an early stage [20, 21], and combined deletion of the *LMO1* and *LMO3* genes leads to perinatal lethality with no obvious anatomical abnormalities [22]. Deletion of the *LMO4* gene causes perinatal lethality, impaired neural tube closure, homeotic transformations involving the sphenoid bone and ribs, and cranial nerve defects [12, 22, 23]. The *LMO1* and *LMO2* genes act as oncogenes in acute lymphoblastic leukemia [24-27], and the *LMO4* gene has been implicated in the cause or progression of breast cancers [28, 29], squamous cell carcinomas of oral cavity [30] and in primary prostate cancer[31].

The *LMO4* gene is most highly expressed in mammary epithelial cells during midpregnancy [32, 33], a stage of active proliferation and invasion, and interference with the protein [32] or deletion of the gene [33] leads to impaired lobuloalveolar development of the mammary gland. LMO4 is also overexpressed in over half of primary breast tumors and its expression is associated with worse prognosis [28, 29]. In addition, the *LMO4* gene is activated by heregulin [32] and overexpressed in Her2-mediated tumors [34]. Furthermore, overexpression of LMO4 in the mammary gland of mice leads to hyperplasia and intraepithelial neoplasia [29]. Together, these observations provide strong support that LMO4 plays critical functions in mammary epithelial cells.

While recent studies suggest that the *LMO4* gene promotes both normal development and tumor formation in the mammary gland, the molecular mechanisms underlying these effects remain unknown. In the present study, we demonstrate that LMO4 not only regulates mammary epithelial cell proliferation, but also apoptosis. We also identify Bone Morphogenic Protein 7 (BMP7) as a target gene of LMO4, capable of carrying out many

of the functions of LMO4. Our studies show that LMO4 associates with the BMP7 promoter and that alterations in the levels of LMO4 can regulate the recruitment of histone deacetylase HDAC2 to this promoter. Our studies have identified a novel transcriptional mechanism for LMO4 in which it activates transcription by decreasing recruitment of HDAC2 to the BMP7 promoter.

Materials and Methods

Generation of mammary gland *LMO4* knockout mice. B6129-Tg(Wap-cre)11738Mam/J and B6129-Tg(MMTV-cre)4Mam/J mice [35] were purchased from the Jackson Laboratory. *LMO4*$^{fl/fl}$ mice on the C57/BL6 background were previously described [23]. We generated mice carrying mammary gland *LMO4* knockouts by mating the Wap-Cre or MMTV-Cre mice with *LMO4*$^{fl/fl}$ mice. Genotypes were determined by PCR. We used published PCR primer sequences for identifying MMTV-Cre and Wap-Cre mice according to instructions from the Jackson Laboratory. PCR primers for detecting wild type, floxed and deleted *LMO4* alleles are previously published [23].

Real-time quantitative PCR analysis of mRNA expression. Total RNA was extracted from mouse mammary glands and cell lines with TRIzol® Reagent (Invitrogen). cDNAs were generated with the High-Capacity cDNA archive kit (Applied Biosystems) according to the manufacture's protocol. Real-time PCR was performed on the ABI Prism 7900HT platform, using SYBR Green PCR Master Mix and TaqMan Universal Master Kit, or commercially available TaqMan Gene Expression Assays (Applied Biosystems). For mouse LMO4, mRNA primers were TCACTTGCAGGAATCGACTG (forward) and GGACCGCTTTCTGCTCTATG (reverse); for mouse BMP7, primers were GGTGGCGTTCATGTAGGAGT (forward) and GAAAACAGCAGCAGTGACCA (reverse); and for mouse 18S primers, primers were ATGGCCGTTCTTAGTTGGTG (forward) and GAACGCCACTTGTCCCTCTA (reverse). Expression of the following genes was analyzed by TaqMan Gene Expression Assays (Applied Biosystems): Human 18S, human AGR2, human BMP7, human FGFR4, human IGFBP2, human IGFBP5, human IL8, human LMO4, human MBD1, human NDRG1, human PLAG1, human RET, mouse casein, mouse Cdkn1a (p21), mouse Cdkn1b (p27), mouse Cdkn2b (p15), mouse Cyclin D1, mouse Myc, and mouse Wap. Real-time PCR results were analyzed as previously described [36].

Whole mount mammary gland preparation, histology and immunostaining. The inguinal mammary glands were processed for whole mount analysis as previously described [32]. For histology, the inguinal mammary glands were fixed in 10% neutral formalin overnight, paraffin embedded, and 6 μm sections were stained with hematoxylin and eosin. To evaluate mammary gland cell proliferation, sections were stained with Ki67 antibody (Novocastra) at 1:1000 dilution. To detect apoptosis in the mammary gland, formalin-fixed and paraffin-embedded sections were analyzed with the ApopTag® Plus Peroxidase *In Situ* Apoptosis Detection Kit (Chemicon International). We quantified cell proliferation by counting around 500 cells in random fields from each mouse, determining the fraction of cells stained with Ki67 antibody. We quantified apoptosis by counting around 2000 epithelial cells in random fields from each mouse, determining the fraction of cells that were stained.

Cell proliferation and apoptosis assays. Cell numbers were evaluated with the CellTiter 96® AQueous Non-Radioactive Cell Proliferation Assay (Promega). For cell proliferation, cells were labeled with 5-(and 6-) carboxy fluorescein diacetate succimidyl ester (CFSE; Molecular Probes) and analysed by FACS as previously described [14]. Apoptosis was

quantified with the Cell Death Detection ELISA^{PLUS} kit (Roche), and by Annexin V staining (Roche; 1858777) and FACS analysis as previously described [14].

Construction of viral vectors and plasmids. The pLNCX2 retroviral vectors were previously described [14]. We generated the tetracycline repressible LMO4 and DN-Clim expression plasmids by cloning -tagged LMO4 [11] and dominant negative (DN)-Clim [4, 32] into the pTRE2hyg vector. The pGL3-1.9BMP7 reporter construct containing 1.9 kb of 5' flanking region of the BMP7 gene was generated by cloning a PCR fragment corresponding to nucleotides 1478 to 3338 (accession # AF289090) upstream of firefly luciferase gene in the pGL3 basic vector (Promega). The deletion mutations of pGL3-1.9BMP7, pGL3-1.2BMP7 and pGL3-0.6BMP7, were prepared by cutting the promoter with restriction enzymes Kpn I and Pvu II, respectively. The GAL-TKLuciferase [32], pCS2MT-LMO4 [11, 32], pCS2MT-DN-Clim [5], and pME18FLAG-HDAC2 [37] plasmids are previously described. Previously described LMO4-specific shRNA, LMO4#3 [14], and a negative control shRNA (BD Biosciences) were cloned into the RNAi-Ready pSIREN RetroQ Vector (BD Biosciences). The pKD-HDAC2-V4 HDAC2 siRNA expression plasmid was from Upstate USA, Inc.

Cell culture and generation of stable cell lines. Un-modified HEK293T, MCF-7 and T47D cells were maintained in DMEM/F12 medium containing 10% fetal calf serum with 100 units/ml penicillin and 100ng/ml streptomycin. The MCF7 Tet-Off Cell Line was obtained from Clontech (cat#630907) and maintained according to the vendor's recommendations. The tetracycline repressible LMO4 and DN-Clim expression plasmids, and the empty pTRE2hyg vector, were transfected into the MCF7 Tet-Off Cell Line with DOTAP Liposomal Transfection Reagent (Roche). Hygromycin-resistant colonies were isolated by growing the cells in MEM/F12 selection medium (GIBCO) containing 10% Tet System approved fetal bovine serum (FBS) (BD Biosciences), 100 units/ml penicillin, 100 ng/ml streptomycin, 100 ng/ml G418, 100 μg/ml Hygromcin and 1 μg/ml doxocycline. The selected colonies were screened for the induction of LMO4 and DN-Clim expressions by Western blotting with Myc tag antibody. For each construct, several positive clones with low background expression and robust induction were expanded and maintained in the selection medium. All clones were periodically examined to ensure stable low background and induction upon doxycycline withdrawal. We generated stable T47D-LMO4-RNAi and T47D-control-RNAi cell lines by transfecting the LMO4 and control shRNA pSIREN RetroQ plasmids into T47D cells, using DOTAP Liposomal Transfection Reagent (Roche). Puromycin resistant colonies were isolated by culturing the transfected cells in DMEM/F12 medium containing 10% FBS, antibiotics, and 1 μg/ml puromycin for 2 to 3 weeks. Three different control- and LMO4-shRNA clones were used for analyses. Normal human mammary epithelial cells (HMEC) were purchased from Cambrex, and grown according to the manufacturer's instructions.

Western blots and reagents. Western blots were performed as previously described [14], using Myc antibody (Invitrogen; R950-25) to detect Myc-tagged LMO4 and DN-Clim, and caspase-7 (Cell Signaling; No. 9492) and cleaved caspase-7 (Cell Signaling; No 9491) antibodies to detect full-length and cleaved caspase 7. HA, TAPc and β-actin antibodies were as previously described [14]. Human recombinant BMP2 was from R & D Systems

(355-BM-010), human BMP7 from R & D Systems (354-BP-010) and Alpha Diagnostic International (BMP75-R), human recombinant IGFBP5 from Sigma (I 8529), Follistatin from Sigma (F1175) and Estradiol from Sigma (E-8875). Z-VAD-FMK was purchased from Enzyme System Products (Livermore CA; FK009). Donkey anti-mouse antibody was from Jackson ImmunoResearch (715-001-003) and goat anti-rabbit antibody was from Cell Signaling (7074).

Microarray analysis. Total RNA was isolated with TRIzol® Reagent from three distinct MCF7-LMO4-TetOff cells and three distinct MCF7-DN-Clim-TetOff cells lines in presence and absence of DOX after 6 days. The RNA was further purified with RNeasy® Mini Kit (Qiagen) according to manufacturer's instructions. To decrease false positives, we pooled RNAs from three experiments for each of the three cell lines. RNA was labeled and hybridized to Affymetrix DNA chips as previously described [36]. For MCF7-LMO4-TetOff cells, we used the HG-U133A and B arrays and for the MCF7-DN-Clim-TetOff cells we used U133 plus 2.0 arrays. For both LMO4 and DN-Clim microarrays, we implemented the following filtering criteria to exclude absent genes from subsequent analysis: all three replicate samples of either + or – DOX have "present" or "marginally present" calls, as determined by MAS 5.0. A Bayesian statistical program, Cyber-T, was used to identify statistically differentially expressed genes [38]. Overrepresented Gene Ontology biological process categories were discovered using the DAVID (Database for Annotation, Visualization and Integrated Discovery) 2.1 program [39].

Transient transfection reporter assays. HEK293T Cells were seeded into 6 well-plates one day before transfection. Luciferase reporter (1 μg) and effector plasmids (0.5 μg) were co-transfected with the calcium phosphate method, and luciferase activity was measured 2 days after transfection as described [14]. All experiments were carried out at least three times, each time in triplicate.

Co-immunoprecipition (Co-IP) and Chromatin Immunoprecipitations (ChIP) assays. Co-IPs were performed with extracts from MCF7-LMO4-TetOff cells as previoulsy described [14]. The HDAC2 antibody was from Abcam (ab7029). ChIP assays were performed according to the protocol from Upstate Cell Signaling Solutions. HDAC1 antibody was from Upstate Cell Signaling Solutions (05-614). The following antibodies were from Abcam: HDAC2 (ab7029), HDAC3 (ab7030) and HDAC4 (ab1437). The following antibodies were from Santa Cruz: Clim2 (sc-11198), LMO4 (sc-22833) and normal mouse IgG (sc-2025). The double ChIP assay was performed as described by Sinkkonen et al [40]. Sequences of PCR primers are: TCTGAGTGGTCTGGGGACTC (BMP7 forward), GTTCTTCCCACCTCCTCCTC (BMP7 reverse), GGCCTATTTCCCATGATTCC (U6 forward), and ATTTGCGTGTCATCCTTGC (U6 reverse).

Results

Mammary gland-specific deletion of the LMO4 gene impairs lobuloalveolar development during pregnancy.

LMO4 knockout mice die during embryogenesis or at birth [12, 22, 23], precluding their use for studying the role of LMO4 in postnatal mammary gland development. We interbred floxed *LMO4* mice [23] with either Whey Acidic Protein (WAP)-Cre [35] or Mouse Mammary Tumor Virus (MMTV)-Cre [35] transgenic mice to achieve two types of Cre recombinase-mediated deletion of the *LMO4* gene within mammary glands of mice. Although both the WAP and the MMTV promoters are active in mammary gland epithelial cells, these two promoters have distinct features. The MMTV-Cre transgene is expressed in all major epithelial subtypes (luminal and myoepithelial cells), while expression of the WAP-Cre transgene is limited to the secretory epithelium [41, 42]. Also, the MMTV-Cre transgene is active at a low constitutive level during ductular growth in virgin mice, whereas the WAP promoter is only active during midpregnacy and later; the WAP promoter is not active in the mammary gland of virgin mice [35, 42]. Therefore, we investigated mammary gland development of mice with MMTV-Cre-mediated deletion of *LMO4* (MMTV-Cre-*LMO4*$^{fl/fl}$) during virgin development, as well as in pregnancy and lactation of the first pregnancy. Mice with WAP-Cre-mediated deletion of *LMO4* (Wap-Cre-*LMO4*$^{fl/fl}$) were studied during pregnancy and lactation of the second pregnancy.

To assess whether LMO4 levels are effectively lowered in both knockout models, total RNA was isolated from the inguinal mammary glands of knockout mice and heterozygous littermates as controls. By means of quantitative real-time PCR, we found that LMO4 mRNA levels were dramatically decreased in both MMTV-Cre-*LMO4*$^{fl/fl}$ and Wap-Cre-*LMO4*$^{fl/fl}$ mice (Fig. 1A and B). To test whether deletion of the *LMO4* gene interfered with the function of the mammary gland, we studied the growth of pups nursed by MMTV-Cre-*LMO4*$^{fl/fl}$ female mice, and compared to pups nursed by control females (MMTV-Cre-*LMO4*$^{fl/+}$). Pups nursed by *LMO4* knockout mothers show significantly decreased weight gain (Fig. 1C). The quantitative real-time PCR showed that LMO4 Knockout mice have low mRNA expression level of milk protein (whey and casein) compared to their control(data not shown). Whole mount and histological analyses of Wap-Cre-*LMO4*$^{fl/fl}$ mammary glands showed impaired lobuloalveolar development at days 13.5 and 17.5 of pregnancy, and at the first day of lactation (Fig. 1D). A similar phenotype was observed in the mammary glands of MMTV-Cre-*LMO4*$^{fl/fl}$ mice (Fig. 1E), and in this model, striking impairment of lobuloalveolar development was observed as early as day 5.5 of pregnancy (Fig. 1E; top panels). A decrease in ductular growth was also observed in 3-week old MMTV-Cre-*LMO4*$^{fl/fl}$ virgin mice (Supplemental file 1A). The similar pregnancy phenotypes of both types of *LMO4* knockout mice provide strong support for an important role of *LMO4* in lobuloalveolar development of the mammary gland. These data, in combination with previous studies [32, 33], demonstrate that the *LMO4* gene is important for lobuloalveolar development during pregnancy, and that deletion of the *LMO4* gene results in decreased lobuloalveolar structures.

Deletion of the LMO4 gene leads to decreased proliferation and increased apoptosis of mammary epithelial cells.

To determine the cause of decreased lobuloalveolar development in *LMO4* knockout mice, we investigated proliferation and apoptosis of mammary epithelial cells with Ki67 immunostaining and terminal deoxynucleotidyltransferase-mediated dUTP end-labeling (TUNEL) assays, respectively (Fig. 2A-F). In the normal mammary gland, expression of the proliferation marker Ki 67 peaks in midpregnancy and by lactation day 1 there are few positive cells. Mammary epithelial cell proliferation was reduced by about 50% at pregnancy days 13.5 and 17.5 in both MMTV-Cre-*LMO4*$^{fl/fl}$ and Wap-Cre-*LMO4*$^{fl/fl}$ mice (Fig. 2A-D). In Wap-Cre-*LMO4*$^{fl/fl}$, apoptosis of mammary epithelial cells was significantly increased in midpregnancy at day 13.5, and a similar, but non-significant trend was also observed in late pregnancy at day 17.5 (Fig. 2E and F). Consistent with this finding, we noticed large spaces with loss of epithelial structures in about half of Wap-Cre-*LMO4*$^{fl/fl}$ mice at lactation day 1 (Supplemental file 1B). Increased apoptosis was not observed in MMTV-Cre-*LMO4*$^{fl/fl}$ mammary glands (data not shown), perhaps related to the different kinetics of deletion in the two types of *LMO4* knockout mice.

To gain insights into the molecular event underlying the cellular phenotype of *LMO4* knockout mice, we investigated the expression of cell cycle regulators known to be important for mammary gland development. Increased expression of p15 was found in the mammary glands of *LMO4* knockout mice both during midpregnancy and at day one of lactation (Fig. 2G). Since p15 is a cell cycle inhibitor [43, 44], increased p15 expression may lead to decreased proliferation and increased apoptosis in *LMO4* knockout mice. These effects are specific because we found no alterations in the expression of p21, p27, cyclin D and Myc (data not shown) – all cell cycle regulators implicated in mammary gland development [45-48]. Together, our results indicate that the *LMO4* gene plays a role in maintaining proliferation and survival of mammary epithelial cells during lobuloalveolar development. Decreased cellular proliferation during early and midpregnancy appears to be the main mechanism underlying decreased lobuloalveolar development in *LMO4* knockout mice, but increased apoptosis also contributes to the phenotype.

Engrailed-LMO4 fusion protein decreases proliferation and increases apoptosis of normal human mammary epithelial cells.

To investigate the effect of LMO4 at a cellular level, we transduced normal human mammary epithelial cells (HMEC) with equivalent titres of retroviruses expressing LMO4, Engrailed-LMO4 fusion protein, Engrailed domain alone, and TAPc as a control. The fusion of the Engrailed repression domain to LMO4 creates a strong dominant-negative molecule or factor predicted to actively repress LMO4 target genes [32]. The Engrailed-LMO4 fusion protein clearly inhibited cell growth (Fig. 3 A and B) and this effect was specific because Engrailed alone had no effect (Fig. 3A, third column). In this experiment, LMO4 caused a slight inhibition of cell growth (Fig. 3B) but in most experiments, LMO4 did not change overall growth of HMEC. The infection efficiency was comparable for the different vectors (not shown) and expression of the different proteins was similar as assessed by western blotting (Fig. 3C). To test whether the effect

of Engrailed-LMO4 was due to inhibition of proliferation or increased apoptosis, we used a FACS-based CSFE assay [49] (Fig. 3D). In vector-infected (TAPc) cells, two peaks were observed with the left peak representing cells having undergone one cell division (Fig. 3D, black). In LMO4-infected cells, the left peak is higher, indicating somewhat increased rate of proliferation (Fig. 3D, green). In Engrailed-infected cells, only the right peak is observed (Fig. 3D, red), indicating a striking decrease in proliferation. In the Engrailed-LMO4-infected cells, the overall number of cells is decreased probably due to increased cell death (see later). To test whether there was increased cell death, we used a FACS-based Annexin V assay [50]. Whereas LMO4 had small effect on apoptosis, Engrailed-LMO4 nearly doubled live Annexin V staining cells, and caused increased number of dead cells (Fig. 3E). In summary, expression of a dominant negative LMO4 leads to a decrease in proliferation and an increase in apoptosis in normal mammary epithelial cells. LMO4 alone has mild proliferation-promoting effects in these same cells, but little effect on overall growth. Together these data suggest that LMO4 plays roles in the regulation of cell proliferation and apoptosis of mammary epithelial cells.

LMO4 induces apoptosis in MCF-7 breast cancer cells.

To gain insight into mechanisms of action for LMO4 in mammary gland development and breast cancer, we identified LMO4 target genes. Because of the complexity of the mouse mammary gland, and the inability to tightly control the onset of LMO4 deletion, we selected the MCF-7 breast cancer cell line for establishing an inducible LMO4 expression system; MCF-7 cells have low levels of endogenous LMO4 expression [28, 32]. We took advantage of the Tet-off system [51], and established several distinct MCF-7 cell clones, referred to as MCF7-LMO4-TetOff cells, in which the expression of LMO4 was repressed by the presence of doxycycline in the medium, and removal of doxycycline resulted in the increased expression of LMO4 (Fig. 4A).

To investigate whether expression of LMO4 affected apoptosis in MCF-7 cells, we measured apoptosis in the presence (low LMO4) and absence (increased LMO4) of doxycycline, using a Cell Death Detection ELISA^{PLUS} kit [52], which is based on quantitative detection of histone-associated DNA fragments in mono- and oligonucleosomes. Removal of doxycycline significantly increased apoptosis in the MCF7-LMO4-TetOff cell, whereas no effect was observed in vector-transfected cells (Fig. 4B); LMO4 increased apoptosis in a time-dependent manner (Fig. 4C). Consistent with results from the cell death detection ELISA assay, FACS analysis detected a moderate increase in annexin V staining, as well as more annexin V positive dead cells, in the absence of doxycycline (increased LMO4) than in the presence of doxycycline (low LMO4) (Fig. 4D). In addition, elevated expression of LMO4 clearly increased the amount of cleaved caspase 7 as detected by western blotting with antibodies against both uncleaved and cleaved caspase 7 (Fig. 4E). When MCF7-LMO4-TetOff cells were treated with the general caspase inhibitor Z-VAD-FMZ, LMO4 was incapable of inducing apoptosis, indicating that the process was caspase dependent (Fig. 4F). Together, these results show that LMO4 upregulation can induce caspase-dependent apoptosis in breast cancer cells.

In contrast to the *in vivo* mouse results, we did not observe striking LMO4 effects on proliferation in MCF-7 cells (data not shown) by LMO4 overexpression, but knockdown LMO4 in MCF7 cells decrease cell proliferation(ref), all these data indicating that the effects of LMO4 in mammary epithelial cells may be context dependent and dose dependent. Since we did observe increased apoptosis in the Wap-Cre-*LMO4*$^{fl/fl}$ mice, it is interesting that increased levels of LMO4 can also promote apoptosis. These findings are consistent with previous results with LMOs and other components of Clim-containing transcription complexes, showing that both increases and decreases in the levels of components of the complex can result in similar effects [14] and phenotypes [53-55]. Together, the *in vivo* mouse and the *in vitro* breast cancer results indicate that in mammary epithelial cells, LMO4 is involved in control of cell proliferation and apoptosis.

Identification of LMO4-responsive genes.

To identify LMO4-responsive genes we profiled gene expression in three distinct MCF7-LMO4-TetOff cell clones, L1-3, in the presence (low LMO4) and absence (increased LMO4) of doxycycline (Fig. 4A). After labeling and hybridization to Affymetrix HG-

U133 A and B gene arrays [36], we used the Cyber-T program to identify statistically significant differentially expressed genes [38] (Fig. 5A). Using a cutoff *P*-value of < 0.01, we found that out of nearly 18,000 expressed probe sets only 111 and 98 were upregulated and downregulated, respectively. A list of the top 20 upregulated and downregulated genes by LMO4 is provided in Supplemental File 2. We then used DAVID 2.1 to determine which biological processes were overrepresented in the significantly differentially expressed genes [39]. Of all Gene Ontology biological processes, only apoptosis was significantly (*P*=0.006) enriched (Fig. 5B), which is consistent with and supports the biological data presented in Fig. 4.

LMO proteins lack DNA-binding domains and are thought to regulate gene expression by at least two different mechanisms. First, LMOs can recruit LIM-domain transcriptional co-factors Clim/Ldb/Nli to DNA-binding proteins in gene regulatory regions thereby activating transcription [8, 9, 56]. Second, LMOs may act as dominant negative molecules and repress transcription by sequestering Clim co-factors away from DNA-binding proteins [15-17]. Since both models of LMO action are based on interactions with Clims, we reasoned that interfering with Clim function in MCF-7 cells would help identify *bone fide* LMO4-responsive genes. We therefore also created MCF7-DN-Clim-TetOff cell lines where expression of a dominant-negative (DN) Clim protein [5] is induced upon doxycycline removal (Supplemental File 3A). Using the same methodology as with the MCF7-LMO4-TetOff cell lines, we performed microarray analysis in these cells, comparing expression profiles under control conditions with cells expressing the DN-Clim (Fig. 5A). A list of the top 20 upregulated and downregulated genes by DN-Clim is provided in Supplemental File 3B. Using DAVID 2.1, we also found an enrichment of the apoptosis category (*P*=0.049) in the differentially expressed genes. The enrichment is not as significant as that found in LMO4 microarrays, consistent with milder effect of DN-Clim on apoptosis in MCF-7 cells (data not shown). Interestingly, we identified three genes that were significantly differentially expressed (*P*<0.01) by both LMO4 and DN-Clim: BMP7, GAS5, and LIN7A. All three genes were altered in the same direction in both cell lines, suggesting that in MCF-7 cells, LMO4 functions as a dominant negative protein or molecule. We noticed that nearly all of significant LMO4-responsive genes were regulated in the same direction by DN-Clim, suggesting that if sufficiently powered, our study would have detected many more common genes. We used quantitative real-time PCR to validate the microarray results for several LMO4-responsive genes, including BMP7 (Fig. 5C).

To investigate whether there was a correlation between LMO4 and BMP7 levels in human breast cancer, we analysed a recent study on 49 primary breast cancers that also used Affymetrix microarrays to profile expression [57]. Consistent with a previous report, showing association between high LMO4 expression and ER-negative status of tumors [58], the average LMO4 expression level is significantly higher (2.21 fold; *P*<0.0001) in basal than luminal tumor samples (Fig. 5D). In addition, there is a strong correlation (r=0.69) between LMO4 and BMP7 expression levels in all subtypes of tumors (Fig. 5E). When we examined the distribution of correlation coefficients between the expression of LMO4 and each probe set on the Affymetrix U133A array across all breast tumors, we found that BMP7 has one of the highest correlation coefficients and is

significantly (P<0.0001) correlated (Fig. 5F). As expected, the top correlation coefficient is another probe set for LMO4 (Fig. 5F).

Since our studies in MCF-7 cells focused on the consequences of increased LMO4 levels, we investigated the effect of LMO4 knockdowns on BMP7 expression. The T47D breast cancer cell line expresses high levels of LMO4 [28] and is therefore suitable for testing the effect of lowering LMO4. The T47D cells were stably transfected either with a vector encoding a shRNA against antisense luciferase gene as a control, or a vector encoding a shRNA against LMO4 [14]. As expected, introduction of the LMO4 shRNA led to dramatic lowering of LMO4 transcript levels. In contrast, BMP7 expression was robustly upregulated, indicating that lower LMO4 levels enhance BMP7 expression (Fig. 5G) in T47D cells. Together with results from the conditional expression of LMO4, these data indicate that both up-regulation and down-regulation of LMO4 can lead to increased expression of the *BMP7* gene. To test whether LMO4 downregulation also affected BMP7 expression *in vivo*, we measured BMP7 transcripts in the mammary glands of MMTV-Cre-*LMO4*$^{fl/fl}$ mice and found significant upregulation of BMP7 mRNA (Fig. 5H). These experiments indicate that LMO4 can regulate BMP7 expression both *in vivo* in the normal mammary gland and in breast cancer, and *in vitro* in breast cancer cell lines.

BMP7 can mediate LMO4 functions.

We selected BMP7 for further study because perturbations of LMO4 levels lead to alterations in cellular proliferation and survival, and previous studies have linked BMP7 to control of cell apoptosis and cell proliferation in many different organ systems, including the limbs, eyes, uterus, and kidneys [59-61]. To start investigating whether BMP7 could mediate the actions of LMO4, we assessed the effects of BMP7 on cell proliferation and apoptosis in MCF-7 breast cancer cells and normal human mammary epithelial cells (HMEC). We treated MCF7 cells with increasing concentrations of human recombinant BMP7 and monitored cell proliferation with the Celltiter 96 Aqueous Non-radioactive cell proliferation assay (Promega). BMP7 inhibited proliferation and increased apoptosis of MCF-7 cells in a dose-dependent manner (Fig. 6A and B). Similar effects on apoptosis were observed with the related BMP2, but not with another LMO4-responsive gene, IGFBP5 (Fig. 6B). BMP7 had similar dose-dependent effects on cell proliferation and apoptosis of HMEC (Fig. 6C and D). Together, these experiments indicate that BMP7 can decrease proliferation and increase apoptosis of normal and cancerous mammary epithelial cells, making it a plausible candidate molecule for mediating biological effects of LMO4.

We then investigated more directly whether BMP7 contributes to LMO4-induced apoptosis. Under conditions where MCF7-LMO4-TetOff cells were maintained without doxycycline, the BMP inhibitor follistatin decreased apoptosis by approximately 50% as monitored by Cell Death Detection ELISA assay (Fig. 6E), indicating that LMO4-stimulated apoptosis is at least in part mediated by BMPs. Estradiol has been shown to downregulate BMP7 and its receptor actRIIB in a variety of hormone responsive epithelial cells [59, 62]. In fact, it has been proposed that estradiol inhibits apoptosis in epithelial cells of the endometrium by suppressing BMP7 signaling, and Esntrogen

opposes the apoptotic effects of BMP7 on tissue remodeling [59, 62]. Interestingly, estradiol completely inhibited LMO4-mediated apoptosis in MCF7 cells (Fig. 6E). Together, these results suggest that BMP7 is a mediator of LMO4 effects on mammary epithelial cell proliferation and apoptosis.

The BMP7 gene is a direct target of LMO4.

To start investigating whether LMO4 directly regulates the *BMP7* gene, we cloned 1.9kb of the proximal 5' flanking region of the *BMP7* gene [63, 64] upstream of the luciferase reporter gene in the pGL3 vector (pGL3-1.9BMP7). When transfected into HEK293T cells, LMO4 was able to upregulate luciferase activity by as much as 8-fold (Fig. 7A). Consistent with the previously established relationship between LMO4 and BMP7 mRNA levels in the mammary glands of mice and in breast cancer cells, LMO4 RNAi also caused significant upregulation of the BMP7 promoter (Fig. 7A; left panel). In addition, consistent with up-regulation of BMP7 expression in MCF7-DN-Clim-TetOff cells, DN-Clim also up-regulated the promoter (Fig. 7A). These effects were specific because a negative control RNAi had no effect on the BMP7 promoter (Fig. 7A), and LMO4, DN-Clim and LMO4 siRNA had no effect on expression of the unrelated GAL-TK-Luciferase plasmid (Fig. 7A; right panel). Further specificity was demonstrated in experiments where we tested the effect of LMO4 on 5' deletion mutants of the pGL3-1.9BMP7 plasmid (Fig. 7B). LMO4 was incapable of activating the expression of BMP7 reporter plasmids containing 1.2 kb and 0.6 kb of proximal 5' flanking sequence (Fig. 7B). Together, these results suggest that BMP7 may be a direct target of LMO4 and that the promoter region from –1.2 to –1.9 kb is critical for LMO4 activation of the BMP7 promoter. Interestingly, this region of the promoter has been proposed to contain a repressor element [64].

To test whether LMO4 binds to BMP7 promoter, we performed chromatin immunoprecipitation assays in MCF7-LMO4-TetOff cells in the presence and absence of doxycycline. A Myc antibody precipitated the BMP7 promoter in the absence of doxycycline (high LMO4) (Fig. 7C; lane 6), indicating that LMO4 associates with the BMP7 promoter. These results are specific because the BMP7 promoter was not precipitated by normal serum IgG (Fig. 7C; lane 5), and the Myc antibody did not precipitate the U6 promoter, which is not regulated by LMO4 (Fig. 7C, lanes 3-6). Since BMP7 is also upregulated by DN-Clim in MCF-7 cells, we performed similar experiments in the MCF7-DN-Clim-TetOff cells. Also in these cells, Myc antibody specifically precipitated the BMP7 promoter under conditions of high DN-Clim expression (Fig. 7D, lane 6), indicating that the DN-Clim associates with the BMP7 promoter. Together, these studies suggest that Clim and LMO4 can form a complex on the BMP7 promoter. To test this idea, we performed double chromatin immunoprecipitation assays in the MCF7-LMO4-TetOff cells, first precipitating LMO4 with a Myc antibody and then with a Clim2 antibody against the endogenous Clim2 protein. Under conditions of high LMO4 expression, Clim antibody could precipitate the LMO4 complex on the BMP7 promoter (Fig. 7E; lane 6), indicating that both LMO4 and Clim2 bind to the BMP7 promoter, most likely in a complex given the high-affinity interaction between these proteins. These results are specific because the Clim2 antibody

was not able to precipitate IgG precipitated BMP7 promoter (Fig. 7E; lane 5). We next tested whether endogenous LMO4 and Clim2 can simultaneously bind to the BMP7 promoter in T47D breast cancer cells. In these experiments, where we first precipitated with an LMO4 antibody and then with a Clim2 antibody, both LMO4 and Clim2 associate with the BMP7 promoter (Fig. 7F; lane 3). Together, the transcription and ChIP results suggest that a transcriptional complex containing LMO4 and Clim2 directly regulates the promoter activity of the *BMP7* gene.

The histone deacetylase HDAC2 is involved in regulation of BMP7 by LMO4.

To understand the mechanisms whereby modulation of LMO4 levels can regulate transcription of the *BMP7* gene, we investigated the recruitment of histone deacetylases to the BMP7 promoter. First, we performed *BMP7* chromatin immunoprecipitation assays in the MCF7-LMO4-TetOff cells, using specific antibodies against HDAC1, HDAC2, HDAC3 and HDAC4. Under condition of low LMO4 expression, we could clearly detect HDAC2 and HDAC3 association with the BMP7 promoter (Fig. 8A; lanes 2 and 3). While HADC3 binding was unchanged, HDAC2 binding to BMP7 promoter was moderately decreased under conditions of high LMO4 expression, (Fig. 8A; lanes 6 and 7). Since HDAC2 is a well-known inhibitor of transcription [65, 66], these findings suggested that LMO4 might upregulate the BMP7 gene by decreasing recruitment of HDAC2 to the promoter. To test this hypothesis, we performed double chromatin immunoprecipitation studies, first precipitating LMO4 and then HDAC2 in the MCF7-LMO4-TetOff cells (Fig. 8B). Consistent with the model of LMO4 regulation of HDAC2 recruitment, we found that HDAC2 was primarily recruited to the BMP7 promoter under low LMO4 levels (Fig. 8B, lanes 3 and 6). As expected, high LMO4 levels increased the recruitment of Clim2 to the promoter (Fig. 8B; lanes 2 and 5). Further support for LMO4 involvement in HDAC2 regulation are from immunoprecipitation experiments where HDAC2 antibody could pull down LMO4 (Fig. 8C), consistent with a recent report also showing that LMO4 can interact with HDAC2 [18]. In transfection assays, an HDAC2shRNA and HDAC2 expression vector increased and decreased, respectively, expression of the BMP7 promoter (Fig. 8D), indicating that HDAC2 suppresses the promoter under basal conditions. When the HDAC2 expression vector was co-transfected with LMO4, it blocked the LMO4-mediated stimulation of the BMP7 promoter (Fig. 8D), consistent with the idea that decreased recruitment of HDAC2 could account for LMO4-regulation of the promoter.

Together, this work has identified the BMP7 gene as a direct target of LMO4. Our findings suggest a novel mechanism for LMO-mediated stimulation of gene expression. According to this model, a transcription complex containing LMO4, Clim2 and HDAC2 is sensitive to stoichiometry of components such that either overexpression or lowering of LMO4 leads to decreased recruitment of HDAC2 and increased promoter activity (Fig. 6E).

Discussion

Previous work with transgenic mice expressing a dominant-negative Engrailed-LMO4 fusion protein indicated a role for LMO4 in ductular and lobuloalveolar development of the mammary gland [32]. Also, a study with Wap-Cre-mediated deletion of the LMO4 gene showed decreased proliferation and impaired lobuloalvolar structures at the end of pregnancy [33]. The present study extends previous work by showing in two distinct types of Cre-mediated mammary gland knockouts of LMO4 that there is decreased proliferation of mammary epithelial cells starting in early pregnancy, ultimately resulting in impaired lobuloalveolar development and mammary gland function at the end of pregnancy. Therefore, one of the roles of LMO4 is to maintain proliferation of mammary epithelial cells during early pregnancy.

In addition, we observed increased apoptosis in Wap-Cre-mediated LMO4 knockouts during midpregnancy, indicating a role for LMO4 in suppressing apoptosis during this phase of mammary gland development. However, we did not observe this effect with MMTV-Cre-mediated deletion of LMO4. A possible reason for the difference between the two types of knockouts is that the Wap promoter is not activated until midpregnancy [35], whereas MMTV promoter becomes active earlier and adaptive changes may have prevented the apoptosis phenotype. Mice expressing the Engrailed-LMO4 fusion protein had a more striking impairment in ductular development than the MMTV-Cre-*LMO4*$^{fl/fl}$ mice [32]. This difference may be due to differences in the strength and spatial extent of transgene expression. Alternativly, other LMOs may compensate for LMO4 in the MMTV-Cre-*LMO4*$^{fl/fl}$ mice whereas the Engrailed-LMO4 protein is predicted to interfere with all LMOs.

How LMO4 mediates its proliferative and apoptotic effects in the normal mammary gland remains unknown. No changes in phosphorylation of Stat5 and Erk1/Erk2 were found in mammary glands with Wap-Cre-mediated LMO4 deletion [33]. We investigated the expression of cell cycle regulators p15, p21, p27, cyclin D1, and Myc, and found selective increase in expression of cell cycle inhibitor p15 in mammary glands of LMO4 knockout mice. Upregulation of p15, which has been linked to TGFβ and activin activation [45, 67-69], could mediate proliferative and apopototic effects in the *LMO4* knockout mice.

Since knockout and dominant-negative experiments suggested a role for LMO4 in suppressing apoptosis (Fig. 2E and 3E), we were surprised to observe a clear caspase-dependent pro-apoptotic effect in response to LMO4 upregulation in normal mammary epithelial cells and in breast cancer cells. This data suggests that either increase or decrease in LMO4 levels may enhance apoptosis, which is similar to findings with several other effectors of apoptosis, including c- and ras [70-73]. Interestingly, *in vivo*, upregulation of LMO4 leads to mammary gland epithelial hyperplasia [29]. In contrast, upregulation of LMO4 in normal mammary epithelial cells, and in breast cancer cells, has minimal effects on cell proliferation, and a dominant apoptosis-promoting effect. These findings highlight that LMO4 effects are context-dependent and suggest the possibility

that LMO4-mediated signaling to stroma and/or other neighboring cells may be important for the pro-proliferative and proposed pro-tumorigenic effects of LMO4 upregulation.

We used a highly stringent expression profiling strategy in MCF-7 breast cancer cells to identify candidate genes that might mediate LMO4 actions in the mammary gland. A top differentially expressed gene in response to LMO4 expression is BMP7, a member of the bone morphogenetic proteins (BMP) family, which has more than 15 mammalian members [74]. The regulation of BMP7 by LMO4 was validated by independent methods, both in mouse mammary gland during normal development and in two different human breast cancer cell lines. In addition, analysis of expression profiles of human breast cancer cases [57] showed a highly significant correlation between LMO4 and BMP7 expression levels, indicating that BMP7 could be LMO4 responsive in human breast cancer. The link between LMO4 and BMP7 is especially intriguing because BMPs are secreted cytokines that can control multiple cellular processes, including proliferation, differentiation and apoptosis [75-77]. By regulating BMP7, LMO4 can have pleiotrophic effects both in cancer and in development. In addition, LMO4 can modulate BMP7 signaling downstream by interacting with Smad8 [14, 78], one of the effector Smads that mediates BMP7 signaling. Together, these studies suggest that LMO4 can enhance BMP7 signaling at two different levels.

Like LMO4, BMP7 is highly expressed in the ductular end buds of the developing mammary gland [33, 79, 80], the site of active proliferation and stromal invasion of the mammary epithelium. Also, the levels for both transcripts are highest during pregnancy (Supplemental file 5). LMO4 and BMP7 are also highly expressed in primary breast cancer [28, 81] and as demonstrated here, their expression is significantly correlated in human breast cancer cases. The fact that BMP7 regulates cell proliferation and apoptosis in mammary epithelial cells in the same way as LMO4 is consistent with the idea that it mediates LMO4 actions. Interestingly, LMO4 and BMP7 knockout mice share common phenotypes, including early postnatal death, malformed sphenoid bones, and fusion of some ribs [60, 61, 82]. The strongest evidence that BMP7 acts downstream from LMO4 comes from studies showing that follistatin, a BMP blocker[83-85], can partially block the pro-apoptotic effect of LMO4.

Traditionally, two major models have been advanced to explain how LMO proteins regulate gene transcription. In the first model, derived from studies in the hematopoietic system, LMO2 activates transcription by recruiting Clims to transcriptional complexes containing DNA-binding proteins of the GATA and HLH classes in association with specific DNA sites [8, 9, 56]. In the second model, derived from studies on the *Drosophila* wing [15-17], LMO acts by sequestering the Clim homolog Chip from the LIM homeodomain protein Apterous, thereby controlling the transcriptional activity of Apterous-regulated promoters. More recent studies have suggested, by analogy with the hematopoietic system, that LMOs may activate transcription by recruiting Clims to several different types of transcription factors, including DEAF-1 [11, 12], Get-1/Grhl3 [86], and Smads [14]. In addition, a recent study proposed that LMO4 could repress transcription by recruiting histone deacetylase HDAC2 to ER-responsive promoters [18]. These studies and others that have discovered interactions between LMO4 and additional

transcriptional co-factors [19] suggest that LMOs may regulate transcription by multiple mechanisms.

In the current study on BMP7 regulation, we have identified a novel mechanism for how LMO4 can activate transcription. The histone deacetyl transferase HDAC2 associates with the BMP7 promoter and suppresses its acitivity as demonstrated by both overexpression and loss-of-function experiments for HDAC2 (Fig. 8). Our experiments suggest that on the BMP7 promoter, HDAC2 associates with a complex containing LMO4 and Clim2 as well as possibly other proteins that remain to be defined. Either increasing or lowering the levels of LMO4 decreases the association of HDAC2 to the BMP7 promoter leading to activation of transcription. This aspect of the model is consistent with previous studies in *Drosophila* showing that the stoichiometry of different components in LMO/Clim-containing complexes is critical for activation; in these studies, either up- or down-regulation of Clim resulted in a similar phenotype [87]. We propose that changes in the levels of LMO4 disrupt transcription complexes containing LMO4, Clims and HDAC2, and that with the release of HDAC2 the promoter is activated.

In summary, we have identified BMP7 as an LMO4-responsive gene, both during normal mammary gland development and in human breast cancer. Our biochemical experiments indicate that BMP7 is a direct target gene, with LMO4 associating with its promoter and controlling transcription by regulating the recruitment of the histone deacetylase HDAC2. LMO4 and BMP7 have similar effects on proliferation and apoptosis of mammary epithelial cells, and follistatin partially blocks the effect of LMO4, suggesting that BMP7 may at least partially mediate the effects of LMO4 in mammary epithelial cells. Our studies also suggest the possibility that BMP7 may play roles in mammary gland development, and in breast cancer where LMO4 is frequently overexpressed [28], especially in ER negative cases, and is associated with a poor outcome [29, 58].

Acknowledgements:

We thank Hung Lin for PCR, Julie Fernandez for cell culture, UCI microarry core facility for microarray experiments, Steve Lipkin for reading the manuscript. This work was supported by NIH Grant AR44882 and the Irving Weinstein Foundation (BA); the California Breast Cancer Research Program (ZY and XX); and the Breast Cancer Research Program of the United States Army Medical Research and Material Command (NW and ZL).

Figure legends

FIG. 1. Deletion of the LMO4 gene in mammary glands of mice leads to impaired lobuloalveolar development.

(**A**) LMO4 mRNA levels relative to 18S rRNA in Wap-Cre-*LMO4*$^{fl/+}$ (control) and Wap-Cre-*LMO4*$^{fl/fl}$ (KO) mice from indicated stages of mammary gland development. (**B**) LMO4 mRNA levels relative to 18S rRNA in MMTV-Cre-*LMO4*$^{fl/+}$ (control) and MMTV-Cre-*LMO4*$^{fl/fl}$ (KO) mice from the indicated stages of mammary gland development. Transcripts in A and B were measured with quantitative real-time PCR from at least three samples for each condition. (**C**) Growth curves of offsprings of MMTV-Cre-*LMO4*$^{fl/+}$ (control) and MMTV-Cre-*LMO4*$^{fl/fl}$ (KO) female mice during the first 19 days of lactation. Thirty mice from four control litters and 23 mice from three knockout litters were weighed every other day. There was significant difference (P<0.01) in weight at each time point except day 1. (**D and E**) Whole mount (first two colums) and histological analyses (last two columns, 100X magnification) of the fourth inguinal mammary gland from MMTV-Cre-*LMO4*$^{fl/fl}$ and Wap-Cre-*LMO4*$^{fl/fl}$ mice and their controls (the genotypes of controls for MMTV-Cre-*LMO4*$^{fl/fl}$ and Wap-Cre-*LMO4*$^{fl/fl}$ are MMTV-Cre-*LMO4*$^{fl/+,}$ and Wap-Cre-*LMO4*$^{fl/+}$, respectively). Data in panels A, B and C represents mean and SEM. KO, knockout; L, lactation; Preg, Pregnancy; CTL, Control.

FIG. 2. Decreased lobuloalveolar development in LMO4 knockout mice is due to decreased proliferation and increased apoptosis of mammary epithelial cells.

(**A**) Ki67 antibody staining of paraffin-embedded sections of mammary glands from control and Wap-Cre-*LMO4*$^{fl/fl}$ mice from the indicated stages. (**B**) Quantification of Ki67 positive cells in control and Wap-Cre-*LMO4*$^{fl/fl}$ mice from the indicated stages. (**C**) Ki67 antibody staining of paraffin-embedded sections of mammary glands from MMTV-Cre-*LMO4*$^{fl/fl}$ and their control mice from the indicated stages. (**D**) Quantification of Ki67 positive cells in MMTV-Cre-*LMO4*$^{fl/fl}$ mice and their control mice from the indicated stages. For the quantification in B and D, 500 cells were counted in at least 3 wild type and knockout mice. Arrows and arrowheads in A and C point to exemplary positive and negative cells, respectively. (**E**) TUNEL staining of paraffin-embedded sections of mammary glands from Wap-Cre-*LMO4*$^{fl/fl}$ mice and their control mice from the indicated stage. (**F**) Quantification of TUNEL positive cells in Wap-Cre-*LMO4*$^{fl/fl}$ mice and their control mice from the indicated stages. For these studies, 2000 cells were counted in at least 4 wild type and knockout mice. (**G**) p15 mRNA levels normalized to 18S rRNA expression were quantified with real-time PCR in MMTV-Cre-*LMO4*$^{fl/fl}$ mice. The results are from at least three mice for each condition. The data in all panels represents mean and SEM; *P*-values were calculated using t-test.

FIG. 3. Engrailed- LMO4 inhibits normal human mammary epithelial cell growth.

(**A**) HMEC were infected with pLNCX2 retroviral vectors encoding the indicated proteins. After infection, cells were plated and cell number was estimated after 7 days using crystal violet staining. (**B**) Growth curves of HMEC after retroviral infection with the indicated vectors using Celltiter 96 Aqueous Non-radioactive cell proliferation assay (Promega). (**C**) Western blots showing the expression of the indicated proteins from the viral vectors in the experiment described in A and B. (**D**) HMEC were infected with the

retroviruses encoding the indicated proteins and then labeled with CFSE. CFSE intensity was measured by FACS after 4 days. (**E**) HMEC infected with retroviruses encoding the indicated proteins was stained with PI and annexin V-FITC, and then analyzed by FACS.

FIG. 4. LMO4 expression increases apoptosis in MCF-7 cells.
(**A**) Western blot analysis of LMO4 expression in three distinct MCF7-LMO4-TetOff cell clones, L1-3. Equal amount of protein extracts from cells treated with (+) and without (-) doxycycline were fractionated by SDS-PAGE and probed with a antibody to detect the Myc-tagged LMO4. (**B**) MCF7-LMO4-TetOff cells and MCF-7 cells transfected with vector alone were treated with and without doxycycline for 6 days. Apoptosis was evaluated with Cell Death Detection ELISA^{PLUS} kit. (**C**) MCF7-LMO4-TetOff cells and MCF-7 cells transfected with an empty vector were treated with doxycycline for the indicated times. Apoptosis was measured with Cell Death Detection ELISA^{PLUS} kit as described in panel B. The enrichment factor is the ratio of apoptosis in cells grown in the absence of DOX to apoptosis in the corresponding control cells grown in the presence of DOX. (**D**) MCF7-LMO4-TetOff cells were grown in the presence and absence of doxycycline for 6 days and analyzed with combined propidum iodide/annexin-V-FITC staining. The numbers in the right bottom and top halfs in each panel indicate the percentage of early and late apoptotic cells, respecitvely. (**E**) MCF7-LMO4-TetOff cells were treated with (+) and without (-) doxycycline for 6 days. Cell lysates were fractionated and analyzed by caspase 7 and cleaved caspase 7 antibodies. (**F**) MCF7-LMO4-TetOff cells were treated with (+) and without (-) doxycycline for 4 days in the presence of vehicle or the caspase inhibitor Z-VAD-FMK. Apoptosis was assessed with the Cell Death Detection ELISA^{PLUS} kit. The data in B, C and F represents mean and SEM from at least three different experiments.

FIG. 5. Identification of LMO4 target genes.
(**A**) Overview of data processing for microarray gene expression profiling experiments in MCF-7 cells with inducible LMO4 and DN-Clim expression. (**B**) Genes belonging to the only significantly enriched Gene Ontology biological process category, apoptosis, as identified by DAVID 2.1. Added to the table was data for BMP7 (marked with *), an extensively characterized apoptosis gene that was not identified by DAVID 2.1. (**C**) Quantitative real-time PCR validation of selective genes from the LMO4 microarray data. Doxycycline had no effect on the expression of these genes in cell clones transfected with vector alone (not shown). (**D**) LMO4 transcript levels, shown as log base 2 transformed RMA (Robust Multichip Average) normalized expression levels, in a previous microarray study of 49 individual breast cancer samples [57]. Broken vertical lines separate the three tumor subtypes defined in this study: apocrine, A; basal, B; and luminal, L. (**E**) Correlation between LMO4 and BMP7 expression levels in breast tumors. Pearson product moment correlation coefficient, r, for the unlogged RMA values is 0.69. (**F**) Distribution of correlation coefficients between the expression of LMO4 and each probe set on the Affymetrix HG-U133A array across all breast tumors. Red arrow, probe set for BMP7. Black arrow, another probe set for LMO4. (**G**) Expression of LMO4 and BMP7 mRNAs relative to 18S rRNA by quantitative real-time PCR. The RNA was isolated from T47D cells that were stably transfected with either empty vector (vector) or a vector encoding LMO4 shRNA (LMO4). The results represent mean and SEM from 3

independent experiments. (**H**) Expression of LMO4 and BMP7 mRNAs relative to 18S rRNA by quantitative PCR. The RNA was isolated from mammary glands of wild type and MMTV-Cre-*LMO4*$^{fl/fl}$ mice at laction day 1. Results represent the mean and SEM from 3 wild type and 4 knockout mice.

FIG. 6. BMP7 inhibits cell proliferation and induces cell apoptosis

(**A**) Cell proliferation of MCF7 cells in response to the indicated concentrations of BMP7. Cells were harvested after 48 hours and cell numbers assessed with non-radioactive cell proliferation assay (Promega). (B) Apoptosis of MCF7 cells in response to BMP7, IGFBP5 and BMP2 in the indicated concentrations. Cells were harvested after 48-hour treatment and apoptosis assessed with Cell Death Detection ELISA^{PLUS} kit (Roche). (**C**) Cell proliferation of HMEC in response to the indicated concentrations of BMP7. Cells were harvested after 48 hours and cell numbers assessed with the Non-radioactive cell proliferation assay (Promega). (D) Apoptosis of HMEC in response to the indicated concentrations of BMP7. Cells were harvested after 48-hour treatment and apoptosis assessed with ELISA Cell Death Detection ELISA^{PLUS} kit (Roche). (E) Inhibition of apoptosis in MCF7-LMO4-TetOff cells by follistatin and estradiol. Doxycycline was removed from MCF7-LMO4-TetOff cell cultures and 3 days later follistatin (250ng/ml) or estradiol (20nM) was added for 3 days. Apoptosis was assessed with the Cell Death Detection ELISA^{PLUS} kit. Results represent the mean and SEM from 3 independent experiments.

FIG. 7. LMO4 and Clim2 associate with and regulate the BMP7 promoter.

(**A**) The pGL3-1.9BMP7 and the GAL-TK-Luciferase reporter plasmids were cotransfected with indicated expression plasmids and siRNAs into HEK293T cells. (**B**) The indicated deletion constructs of pGL3-1.9BMP7 were cotransfected with an LMO4 expression plasmid into HEK293T cells. In A and B, luciferase activity represents the mean and SEM from at least 3 independent transfections. (**C**) Chromatin immunoprecipitation assays in MCF7-LMO4-TetOff cells in the presence (DOX+) and absence (DOX-) of doxycycline. Antibodies were against Myc to precipitate the Myc-tagged LMO4 and non-specific IgG as a negative control. Primers were located at 1733-2008 (AF289090) and 141158-141488 (AC022254) on the BMP7 and U6 promoter regions, respectively. (**D**) Chromatin immunoprecipitation assays in MCF7-LMO4-TetOff cells in the presence (DOX+) and absence (DOX-) of doxycycline. Antibodies were against Myc to precipitate the Myc-tagged DN-Clim and non-specific IgG as a negative control. Primers were the same as in C. (**E**) Double chromatin immunoprecipitation assays in the MCF7-LMO4-TetOff cells under the indicated conditions. The first antibody was against Myc to precipitate the Myc-tagged LMO4.The second antibody recognized the endogenous Clim2 protein. (**F**) Double chromatin immunoprecipitation assays in T47D cells. The first antibody recognized the endogenous LMO4 protein and the second antibody recognized the endogenous Clim2 protein.

FIG. 8. Interactions between LMO4 and HDAC2 on the BMP7 promoter.

(**A**) Chromatin immunoprecipitation assays in MCF7-LMO4-TetOff cells in the presence (DOX+) and absence (DOX-) of doxycycline. Antibodies were against HDAC1, HDAC2, HDAC3 and HDAC4, and primers were the same as in FIG. 5C. (**B**) Double chromatin

immunoprecipitation assays in MCF7-LMO4-TetOff cells under the indicated conditions. The first antibody was against Myc to precipitate the Myc-tagged LMO4. The second antibody recognized HDAC2 and Clim2, respectively, Ig G as a negative control. (**C**) Immunoprecipitation of MCF7-LMO4-TetOff cell lysates with IgG and HDAC2 antibodies. The western blot was probed with antibody against Myc to detect the Myc-tagged LMO4. (**D**) The PGL3-1.9 BMP7 reporter plasmid was co-transfected with the indicated expression plasmids into HEK293T cells. Luciferase activity represents the mean and SEM from at least 3 independent transfections.

References

1. Bach, I., *The LIM domain: regulation by association.* Mech Dev, 2000. **91**(1-2): p. 5-17.
2. Agulnick, A.D., et al., *Interactions of the LIM-domain-binding factor Ldb1 with LIM homeodomain proteins.* Nature, 1996. **384**(6606): p. 270-2.
3. Jurata, L.W., D.A. Kenny, and G.N. Gill, *Nuclear LIM interactor, a rhombotin and LIM homeodomain interacting protein, is expressed early in neuronal development.* Proc Natl Acad Sci U S A, 1996. **93**(21): p. 11693-8.
4. Bach, I., et al., *A family of LIM domain-associated cofactors confer transcriptional synergism between LIM and Otx homeodomain proteins.* Genes Dev, 1997. **11**(11): p. 1370-80.
5. Bach, I., et al., *RLIM inhibits functional activity of LIM homeodomain transcription factors via recruitment of the histone deacetylase complex.* Nat Genet, 1999. **22**(4): p. 394-9.
6. Visvader, J.E., et al., *The LIM-domain binding protein Ldb1 and its partner LMO2 act as negative regulators of erythroid differentiation.* Proc Natl Acad Sci U S A, 1997. **94**(25): p. 13707-12.
7. Matthews, J.M. and J.E. Visvader, *LIM-domain-binding protein 1: a multifunctional cofactor that interacts with diverse proteins.* EMBO Rep, 2003. **4**(12): p. 1132-7.
8. Wadman, I.A., et al., *The LIM-only protein Lmo2 is a bridging molecule assembling an erythroid, DNA-binding complex which includes the TAL1, E47, GATA-1 and Ldb1/NLI proteins.* Embo J, 1997. **16**(11): p. 3145-57.
9. Wadman, I., et al., *Specific in vivo association between the bHLH and LIM proteins implicated in human T cell leukemia.* Embo J, 1994. **13**(20): p. 4831-9.
10. de la Calle-Mustienes, E., et al., *Xenopus Xlmo4 is a GATA cofactor during ventral mesoderm formation and regulates Ldb1 availability at the dorsal mesoderm and the neural plate.* Dev Biol, 2003. **264**(2): p. 564-81.
11. Sugihara, T.M., et al., *Mouse deformed epidermal autoregulatory factor 1 recruits a LIM domain factor, LMO-4, and CLIM coregulators.* Proc Natl Acad Sci U S A, 1998. **95**(26): p. 15418-23.
12. Hahm, K., et al., *Defective neural tube closure and anteroposterior patterning in mice lacking the LIM protein LMO4 or its interacting partner Deaf-1.* Mol Cell Biol, 2004. **24**(5): p. 2074-82.
13. Kudryavtseva, E.I., et al., *Identification and characterization of Grainyhead-like epithelial transactivator (GET-1), a novel mammalian Grainyhead-like factor.* Dev Dyn, 2003. **226**(4): p. 604-17.
14. Lu, Z., et al., *LMO4 can interact with Smad proteins and modulate transforming growth factor-beta signaling in epithelial cells.* Oncogene, 2006.
15. Milan, M., F.J. Diaz-Benjumea, and S.M. Cohen, *Beadex encodes an LMO protein that regulates Apterous LIM-homeodomain activity in Drosophila wing development: a model for LMO oncogene function.* Genes Dev, 1998. **12**(18): p. 2912-20.

16. Zeng, C., et al., *The Drosophila LIM-only gene, dLMO, is mutated in Beadex alleles and might represent an evolutionarily conserved function in appendage development.* Proc Natl Acad Sci U S A, 1998. **95**(18): p. 10637-42.
17. Milan, M. and S.M. Cohen, *Temporal regulation of apterous activity during development of the Drosophila wing.* Development, 2000. **127**(14): p. 3069-78.
18. Singh, R.R., et al., *Negative regulation of estrogen receptor alpha transactivation functions by LIM domain only 4 protein.* Cancer Res, 2005. **65**(22): p. 10594-601.
19. Sum, E.Y., et al., *The LIM domain protein LMO4 interacts with the cofactor CtIP and the tumor suppressor BRCA1 and inhibits BRCA1 activity.* J Biol Chem, 2002. **277**(10): p. 7849-56.
20. Warren, A.J., et al., *The oncogenic cysteine-rich LIM domain protein rbtn2 is essential for erythroid development.* Cell, 1994. **78**(1): p. 45-57.
21. Yamada, Y., et al., *The T cell leukemia LIM protein Lmo2 is necessary for adult mouse hematopoiesis.* Proc Natl Acad Sci U S A, 1998. **95**(7): p. 3890-5.
22. Tse, E., et al., *Null mutation of the Lmo4 gene or a combined null mutation of the Lmo1/Lmo3 genes causes perinatal lethality, and Lmo4 controls neural tube development in mice.* Mol Cell Biol, 2004. **24**(5): p. 2063-73.
23. Lee, S.K., et al., *The LIM domain-only protein LMO4 is required for neural tube closure.* Mol Cell Neurosci, 2005. **28**(2): p. 205-14.
24. Kenny, D.A., et al., *Identification and characterization of LMO4, an LMO gene with a novel pattern of expression during embryogenesis [In Process Citation].* Proc Natl Acad Sci U S A, 1998. **95**(19): p. 11257-62.
25. Racevskis, J., et al., *Molecular cloning of LMO41, a new human LIM domain gene.* Biochim Biophys Acta, 1999. **1445**(1): p. 148-53.
26. Rabbitts, T.H., *LMO T-cell translocation oncogenes typify genes activated by chromosomal translocations that alter transcription and developmental processes.* Genes Dev, 1998. **12**(17): p. 2651-7.
27. Grutz, G., A. Forster, and T.H. Rabbitts, *Identification of the LMO4 gene encoding an interaction partner of the LIM-binding protein LDB1/NLI1: a candidate for displacement by LMO proteins in T cell acute leukaemia.* Oncogene, 1998. **17**(21): p. 2799-803.
28. Visvader, J.E., et al., *The LIM domain gene LMO4 inhibits differentiation of mammary epithelial cells in vitro and is overexpressed in breast cancer.* Proc Natl Acad Sci U S A, 2001. **98**(25): p. 14452-7.
29. Sum, E.Y., et al., *Overexpression of LMO4 induces mammary hyperplasia, promotes cell invasion, and is a predictor of poor outcome in breast cancer.* Proc Natl Acad Sci U S A, 2005. **102**(21): p. 7659-64.
30. Mizunuma, H., et al., *The LIM-only protein, LMO4, and the LIM domain-binding protein, LDB1, expression in squamous cell carcinomas of the oral cavity.* Br J Cancer, 2003. **88**(10): p. 1543-1548. 2: van Meyel DJ, et al. Ssdp proteins bind to LIM-int.[PMID:12642495]Related Articles, Links.
31. Mousses, S., et al., *Clinical validation of candidate genes associated with prostate cancer progression in the CWR22 model system using tissue microarrays.* Cancer Res, 2002. **62**(5): p. 1256-60.

32. Wang, N., et al., *Expression of an engrailed-LMO4 fusion protein in mammary epithelial cells inhibits mammary gland development in mice.* Oncogene, 2004. **23**(8): p. 1507-13.
33. Sum, E.Y., et al., *Loss of the LIM domain protein Lmo4 in the mammary gland during pregnancy impedes lobuloalveolar development.* Oncogene, 2005. **24**(30): p. 4820-8.
34. Landis, M.D., et al., *Gene expression profiling of cancer progression reveals intrinsic regulation of transforming growth factor-beta signaling in ErbB2/Neu-induced tumors from transgenic mice.* Oncogene, 2005. **24**(33): p. 5173-90.
35. Wagner, K.U., et al., *Cre-mediated gene deletion in the mammary gland.* Nucleic Acids Res, 1997. **25**(21): p. 4323-30.
36. Lin, K.K., et al., *Identification of hair cycle-associated genes from time-course gene expression profile data by using replicate variance.* Proc Natl Acad Sci U S A, 2004. **101**(45): p. 15955-60.
37. Davis, C.A., et al., *PRISM/PRDM6, a transcriptional repressor that promotes the proliferative gene program in smooth muscle cells.* Mol Cell Biol, 2006. **26**(7): p. 2626-36.
38. Baldi, P. and A.D. Long, *A Bayesian framework for the analysis of microarray expression data: regularized t -test and statistical inferences of gene changes.* Bioinformatics, 2001. **17**(6): p. 509-19.
39. Dennis, G., Jr., et al., *DAVID: Database for Annotation, Visualization, and Integrated Discovery.* Genome Biol, 2003. **4**(5): p. P3.
40. Sinkkonen, L., et al., *Regulation of the human cyclin C gene via multiple vitamin D3-responsive regions in its promoter.* Nucleic Acids Res, 2005. **33**(8): p. 2440-51.
41. Wagner, K.U., et al., *Spatial and temporal expression of the Cre gene under the control of the MMTV-LTR in different lines of transgenic mice.* Transgenic Res, 2001. **10**(6): p. 545-53.
42. Wagner, K.U., et al., *Impaired alveologenesis and maintenance of secretory mammary epithelial cells in Jak2 conditional knockout mice.* Mol Cell Biol, 2004. **24**(12): p. 5510-20.
43. Hartwell, L.H. and M.B. Kastan, *Cell cycle control and cancer.* Science, 1994. **266**(5192): p. 1821-8.
44. Morgan, D.O., *Principles of CDK regulation.* Nature, 1995. **374**(6518): p. 131-4.
45. Sandhu, C., et al., *Transforming growth factor beta stabilizes p15INK4B protein, increases p15INK4B-cdk4 complexes, and inhibits cyclin D1-cdk4 association in human mammary epithelial cells.* Mol Cell Biol, 1997. **17**(5): p. 2458-67.
46. Massague, J. and D. Wotton, *Transcriptional control by the TGF-beta/Smad signaling system.* Embo J, 2000. **19**(8): p. 1745-54.
47. Muraoka, R.S., et al., *Cyclin-dependent kinase inhibitor p27(Kip1) is required for mouse mammary gland morphogenesis and function.* J Cell Biol, 2001. **153**(5): p. 917-32.
48. Blakely, C.M., et al., *Developmental stage determines the effects of MYC in the mammary epithelium.* Development, 2005. **132**(5): p. 1147-60.

49. McKarns, S.C., R.H. Schwartz, and N.E. Kaminski, *Smad3 is essential for TGF-beta1 to suppress IL-2 production and TCR-induced proliferation, but not IL-2-induced proliferation.* J Immunol, 2004. **172**(7): p. 4275-84.
50. Lei, X., et al., *Autocrine TGFbeta supports growth and survival of human breast cancer MDA-MB-231 cells.* Oncogene, 2002. **21**(49): p. 7514-23.
51. Gossen, M. and H. Bujard, *Tight control of gene expression in mammalian cells by tetracycline-responsive promoters.* Proc Natl Acad Sci U S A, 1992. **89**(12): p. 5547-51.
52. Catalano, A., et al., *Induction of stem cell factor/c-Kit/slug signal transduction in multidrug-resistant malignant mesothelioma cells.* J Biol Chem, 2004. **279**(45): p. 46706-14.
53. Ramain, P., et al., *Interactions between chip and the achaete/scute-daughterless heterodimers are required for pannier-driven proneural patterning.* Mol Cell, 2000. **6**(4): p. 781-90.
54. Thaler, J.P., et al., *LIM factor Lhx3 contributes to the specification of motor neuron and interneuron identity through cell-type-specific protein-protein interactions.* Cell, 2002. **110**(2): p. 237-49.
55. Lee, S.K. and S.L. Pfaff, *Synchronization of neurogenesis and motor neuron specification by direct coupling of bHLH and homeodomain transcription factors.* Neuron, 2003. **38**(5): p. 731-45.
56. Grutz, G.G., et al., *The oncogenic T cell LIM-protein Lmo2 forms part of a DNA-binding complex specifically in immature T cells.* Embo J, 1998. **17**(16): p. 4594-605.
57. Farmer, P., et al., *Identification of molecular apocrine breast tumours by microarray analysis.* Oncogene, 2005. **24**(29): p. 4660-71.
58. Gruvberger, S., et al., *Estrogen receptor status in breast cancer is associated with remarkably distinct gene expression patterns.* Cancer Res, 2001. **61**(16): p. 5979-84.
59. Monroe, D.G., D.F. Jin, and M.M. Sanders, *Estrogen opposes the apoptotic effects of bone morphogenetic protein 7 on tissue remodeling.* Mol Cell Biol, 2000. **20**(13): p. 4626-34.
60. Jena, N., et al., *BMP7 null mutation in mice: developmental defects in skeleton, kidney, and eye.* Exp Cell Res, 1997. **230**(1): p. 28-37.
61. Luo, G., et al., *BMP-7 is an inducer of nephrogenesis, and is also required for eye development and skeletal patterning.* Genes Dev, 1995. **9**(22): p. 2808-20.
62. Kusumegi, T., et al., *BMP7/ActRIIB regulates estrogen-dependent apoptosis: new biomarkers for environmental estrogens.* J Biochem Mol Toxicol, 2004. **18**(1): p. 1-11.
63. Dorai, H., et al., *The 5' flanking region of the human bone morphogenetic protein-7 gene.* Biochem Biophys Res Commun, 2001. **282**(3): p. 823-31.
64. Kawai, S. and T. Sugiura, *Characterization of human bone morphogenetic protein (BMP)-4 and -7 gene promoters: activation of BMP promoters by Gli, a sonic hedgehog mediator.* Bone, 2001. **29**(1): p. 54-61.
65. Rountree, M.R., K.E. Bachman, and S.B. Baylin, *DNMT1 binds HDAC2 and a new co-repressor, DMAP1, to form a complex at replication foci.* Nat Genet, 2000. **25**(3): p. 269-77.

66. Glass, C.K. and M.G. Rosenfeld, *The coregulator exchange in transcriptional functions of nuclear receptors.* Genes Dev, 2000. **14**(2): p. 121-41.
67. Hannon, G.J. and D. Beach, *p15INK4B is a potential effector of TGF-beta-induced cell cycle arrest.* Nature, 1994. **371**(6494): p. 257-61.
68. Burdette, J.E., et al., *Activin A mediates growth inhibition and cell cycle arrest through Smads in human breast cancer cells.* Cancer Res, 2005. **65**(17): p. 7968-75.
69. Ho, J., et al., *Activin induces hepatocyte cell growth arrest through induction of the cyclin-dependent kinase inhibitor p15INK4B and Sp1.* Cell Signal, 2004. **16**(6): p. 693-701.
70. Pelengaris, S., M. Khan, and G. Evan, *c-MYC: more than just a matter of life and death.* Nat Rev Cancer, 2002. **2**(10): p. 764-76.
71. Wang, Y.H., et al., *Knockdown of c-Myc expression by RNAi inhibits MCF-7 breast tumor cells growth in vitro and in vivo.* Breast Cancer Res, 2005. **7**(2): p. R220-8.
72. Chi, S., et al., *Oncogenic Ras triggers cell suicide through the activation of a caspase-independent cell death program in human cancer cells.* Oncogene, 1999. **18**(13): p. 2281-90.
73. Hendry, B.M., et al., *Distinct functions for Ras GTPases in the control of proliferation and apoptosis in mouse and human mesangial cells.* Kidney Int, 2006. **69**(1): p. 99-104.
74. Massague, J., *TGF-beta signal transduction.* Annu Rev Biochem, 1998. **67**: p. 753-91.
75. Hogan, B.L., *Bone morphogenetic proteins: multifunctional regulators of vertebrate development.* Genes Dev, 1996. **10**(13): p. 1580-94.
76. Yokouchi, Y., et al., *BMP-2/-4 mediate programmed cell death in chicken limb buds.* Development, 1996. **122**(12): p. 3725-34.
77. Bhatia, M., et al., *Bone morphogenetic proteins regulate the developmental program of human hematopoietic stem cells.* J Exp Med, 1999. **189**(7): p. 1139-48.
78. Colland, F., et al., *Functional proteomics mapping of a human signaling pathway.* Genome Res, 2004. **14**(7): p. 1324-32.
79. Schwalbe, M., et al., *Differential expression and regulation of bone morphogenetic protein 7 in breast cancer.* Int J Oncol, 2003. **23**(1): p. 89-95.
80. Sum, E.Y., et al., *The LIM domain protein Lmo4 is highly expressed in proliferating mouse epithelial tissues.* J Histochem Cytochem, 2005. **53**(4): p. 475-86.
81. Alarmo, E.L., et al., *Bone morphogenetic protein 7 is widely overexpressed in primary breast cancer.* Genes Chromosomes Cancer, 2006. **45**(4): p. 411-9.
82. Dudley, A.T. and E.J. Robertson, *Overlapping expression domains of bone morphogenetic protein family members potentially account for limited tissue defects in BMP7 deficient embryos.* Dev Dyn, 1997. **208**(3): p. 349-62.
83. Yamashita, H., et al., *Osteogenic protein-1 binds to activin type II receptors and induces certain activin-like effects.* J Cell Biol, 1995. **130**(1): p. 217-26.
84. Liem, K.F., Jr., G. Tremml, and T.M. Jessell, *A role for the roof plate and its resident TGFbeta-related proteins in neuronal patterning in the dorsal spinal cord.* Cell, 1997. **91**(1): p. 127-38.

85. Augsburger, A., et al., *BMPs as mediators of roof plate repulsion of commissural neurons.* Neuron, 1999. **24**(1): p. 127-41.
86. Kudryavtseva, E.I., et al., *Identification and characterization of Grainyhead-like epithelial transactivator (GET-1), a novel mammalian Grainyhead-like factor.* Dev Dyn, 2003. **226**(4): p. 604-17.
87. Ramain, P., et al., *Interactions between chip and the achaete/scute-daughterless heterodimers are required for pannier-driven proneural patterning.* Mol Cell, 2000. **6**(4): p. 781-90.

Fig. 1

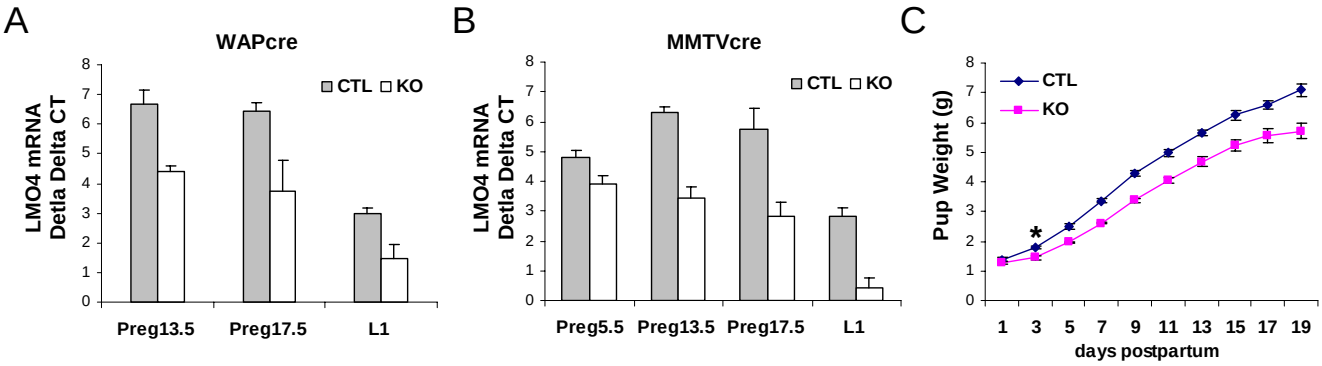
A
WAPcre
LMO4 mRNA
Detla Delta CT
CTL
KO
Preg13.5
Preg17.5
L1
B
MMTVcre
LMO4 mRNA
Detla Delta CT
CTL
KO
Preg5.5
Preg13.5
Preg17.5
L1
C
Pup Weight (g)
CTL
KO
*
days postpartum

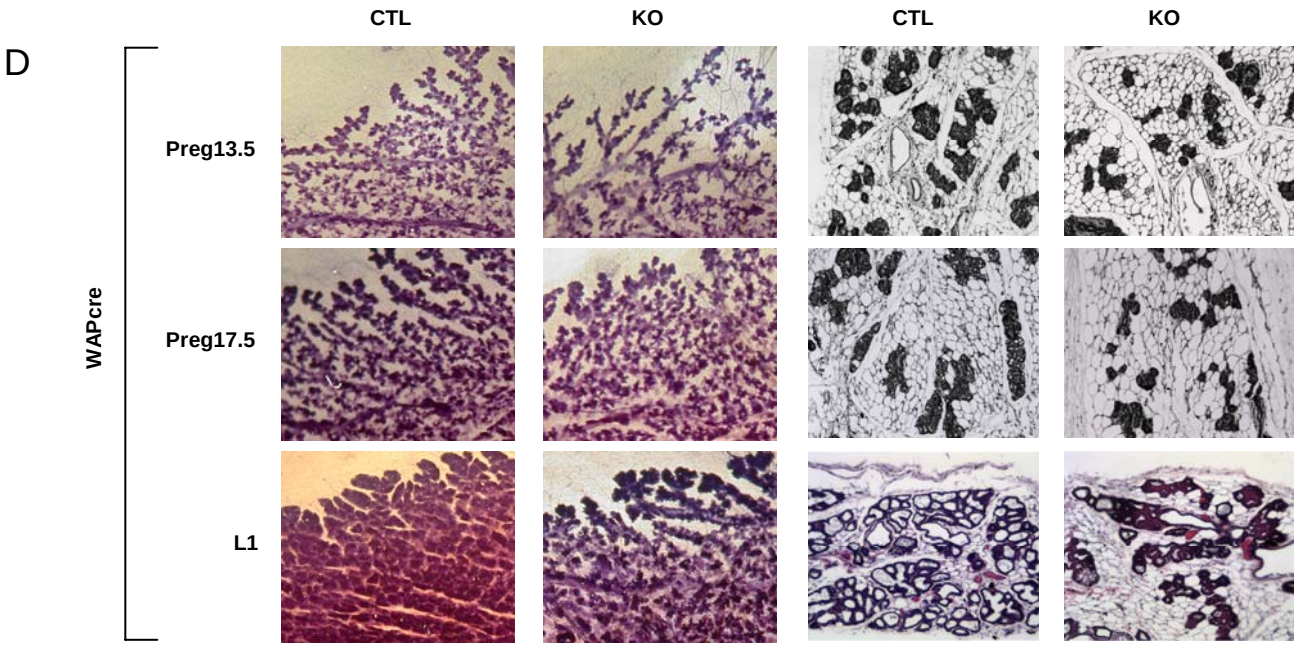
D
CTL
KO
CTL
KO
WAPcre
Preg13.5
Preg17.5
L1

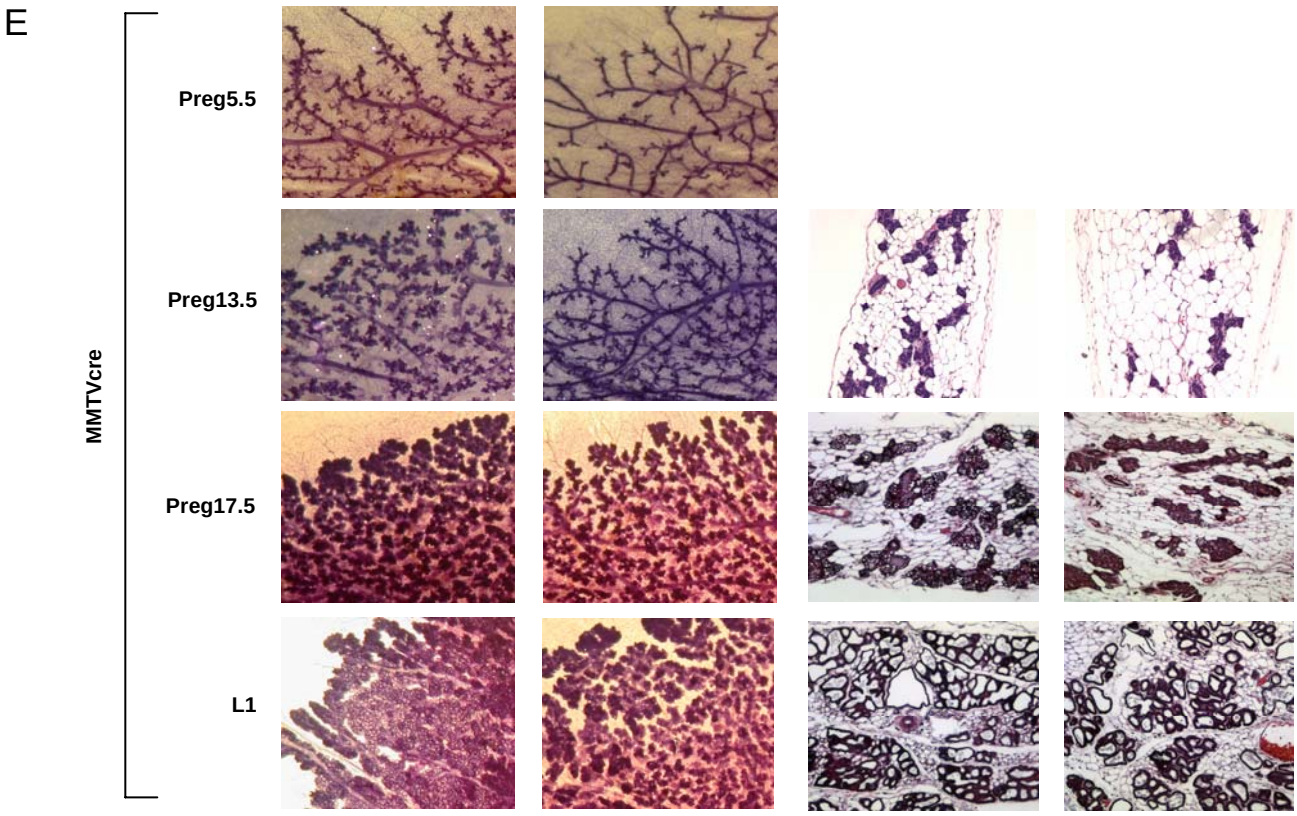
E
MMTVcre
Preg5.5
Preg13.5
Preg17.5
L1

Fig. 2

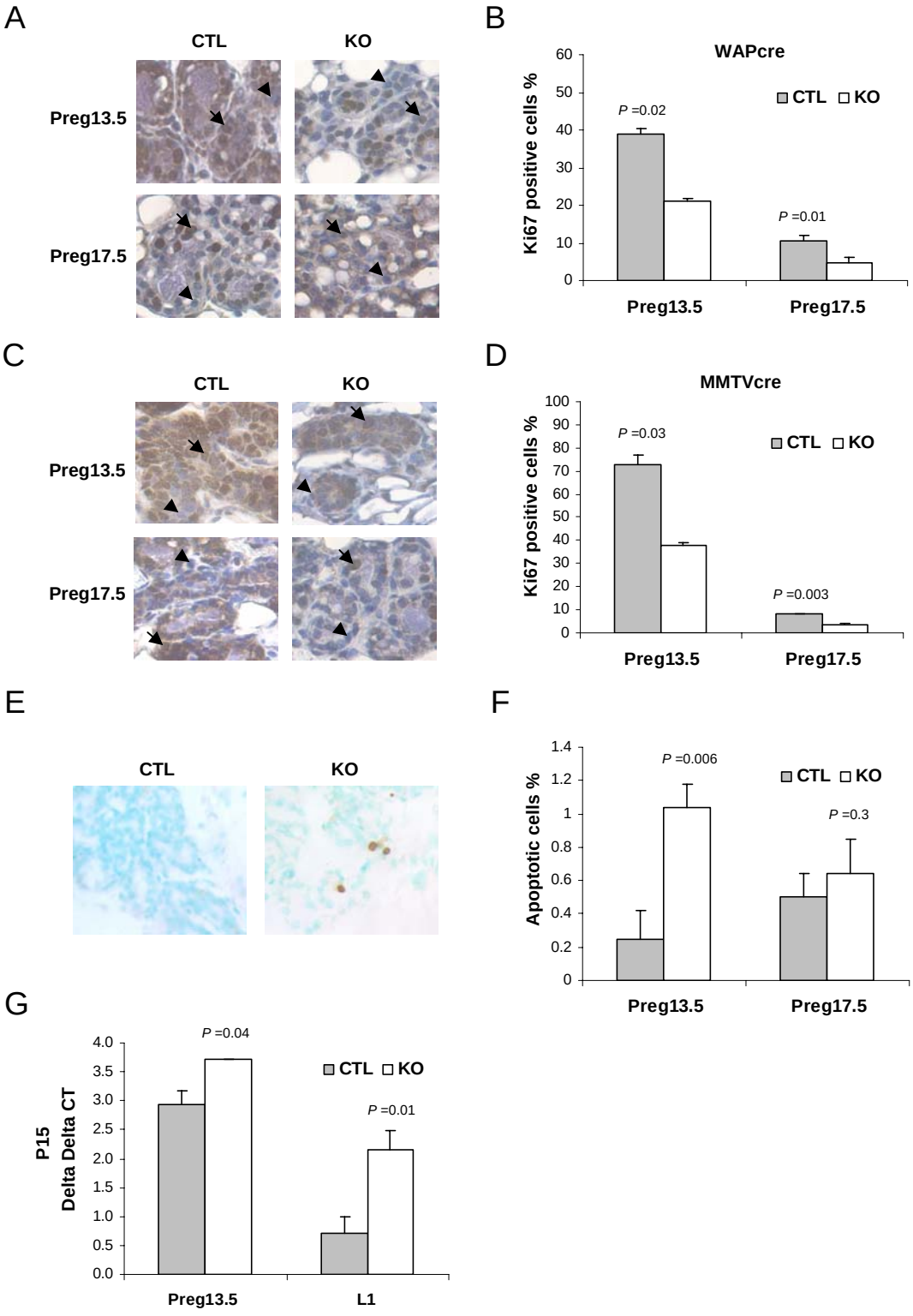
A
CTL
KO
Preg13.5
Preg17.5
B
WAPcre
CTL KO
Ki67 positive cells %
P =0.02
P =0.01
Preg13.5
Preg17.5
C
CTL
KO
Preg13.5
Preg17.5
D
MMTVcre
CTL KO
Ki67 positive cells %
P =0.03
P =0.003
Preg13.5
Preg17.5
E
CTL
KO
F
CTL KO
Apoptotic cells %
P =0.006
P =0.3
Preg13.5
Preg17.5
G
P15
Delta Delta CT
P =0.04
CTL KO
P =0.01
Preg13.5
L1

Fig. 3

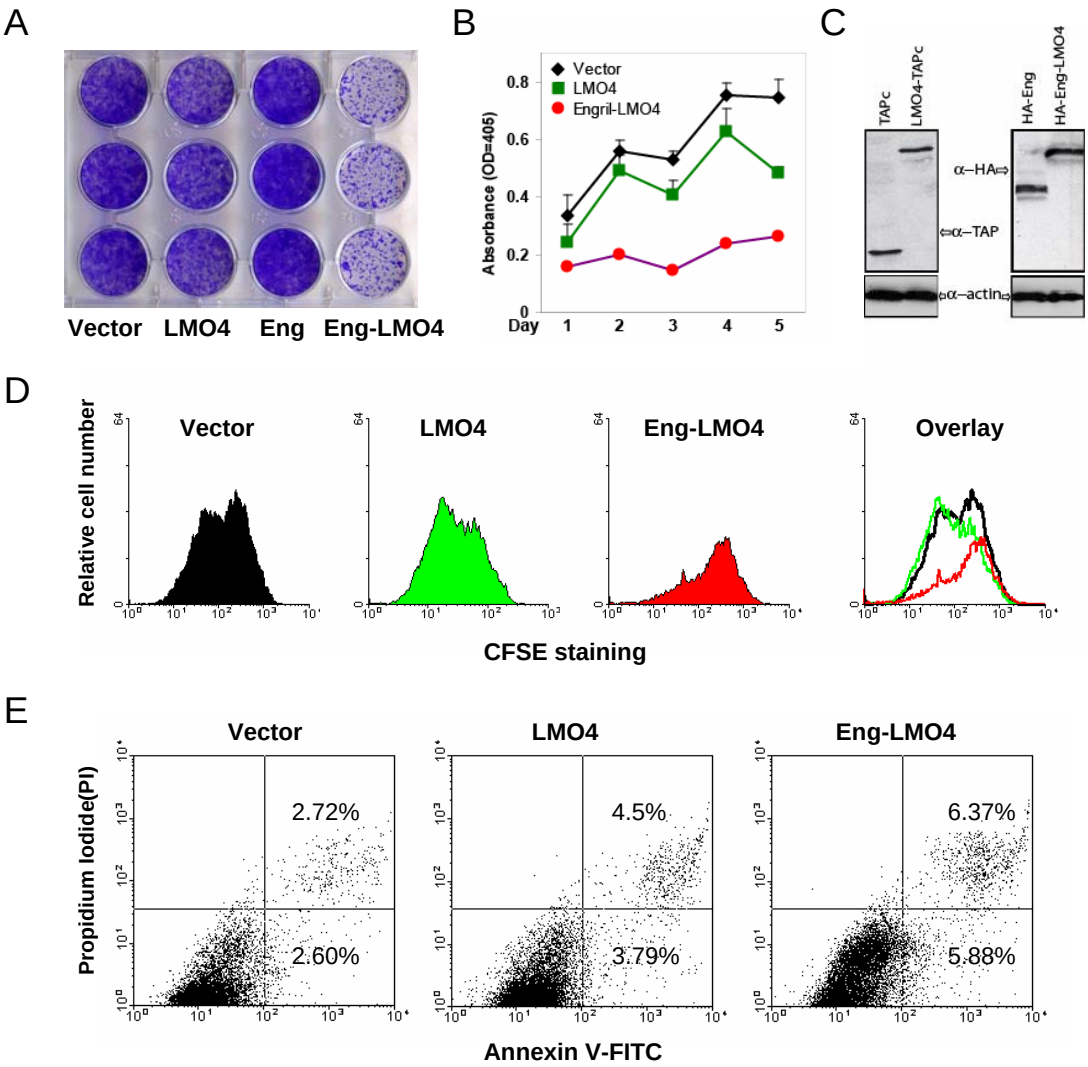
A
Vector
LMO4
Eng
Eng-LMO4
B
Vector
LMO4
Engril-LMO4
Absorbance (OD=405)
Day
C
TAPc
LMO4-TAPc
HA-Eng
HA-Eng-LMO4
α–HA
α–TAP
α–actin
D
Vector
LMO4
Eng-LMO4
Overlay
Relative cell number
CFSE staining
E
Vector
LMO4
Eng-LMO4
2.72%
2.60%
4.5%
3.79%
6.37%
5.88%
Propidium Iodide(PI)
Annexin V-FITC

Fig. 4

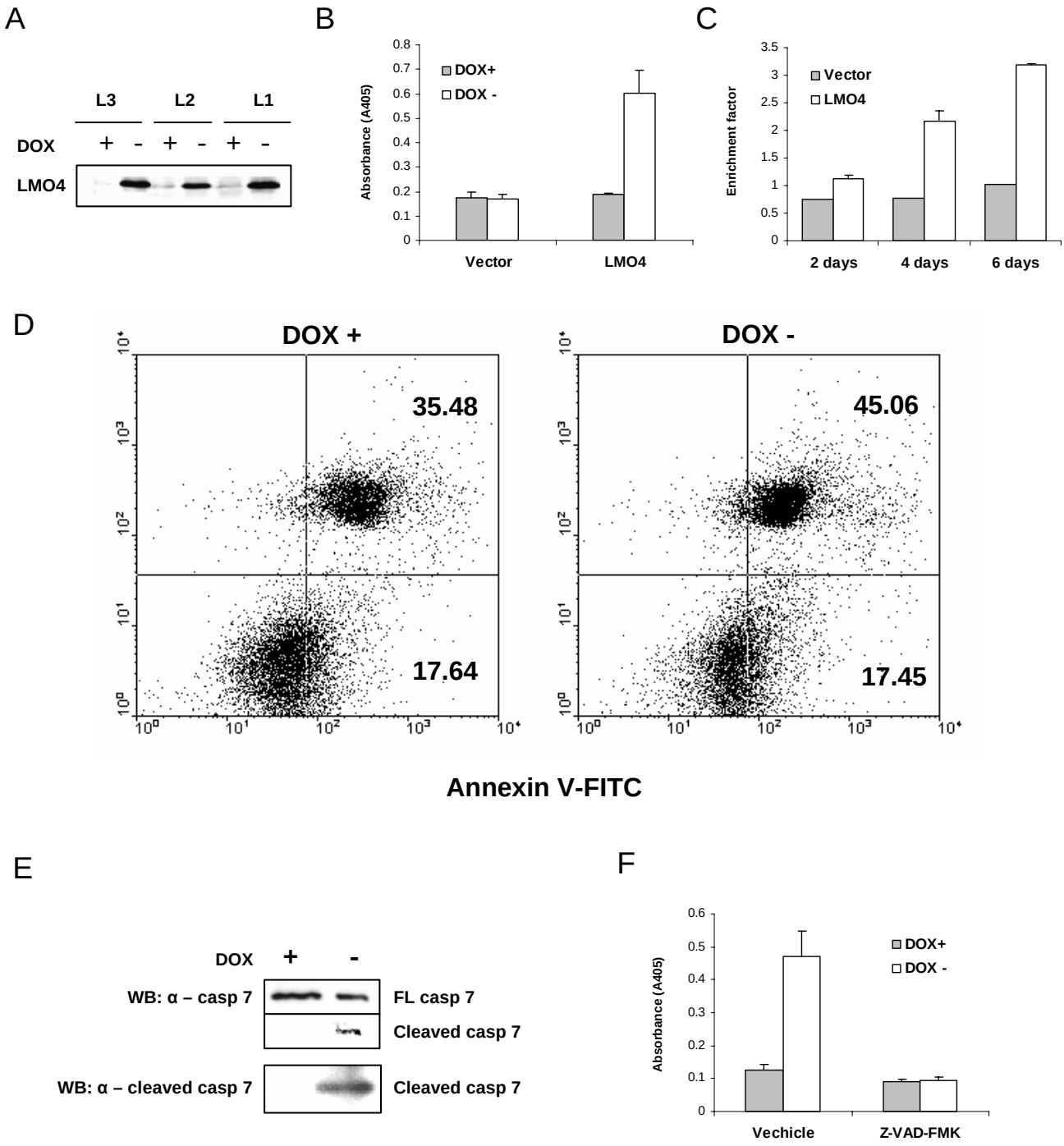
A
L3
L2
L1
DOX
+ - + - + -
LMO4
B
Absorbance (A405)
DOX+
DOX -
Vector
LMO4
C
Enrichment factor
Vector
LMO4
2 days
4 days
6 days
D
DOX +
35.48
17.64
DOX -
45.06
17.45
Annexin V-FITC
E
DOX + -
WB: α – casp 7
FL casp 7
Cleaved casp 7
WB: α – cleaved casp 7
Cleaved casp 7
F
Absorbance (A405)
DOX+
DOX -
Vechicle
Z-VAD-FMK

Fig. 5

A

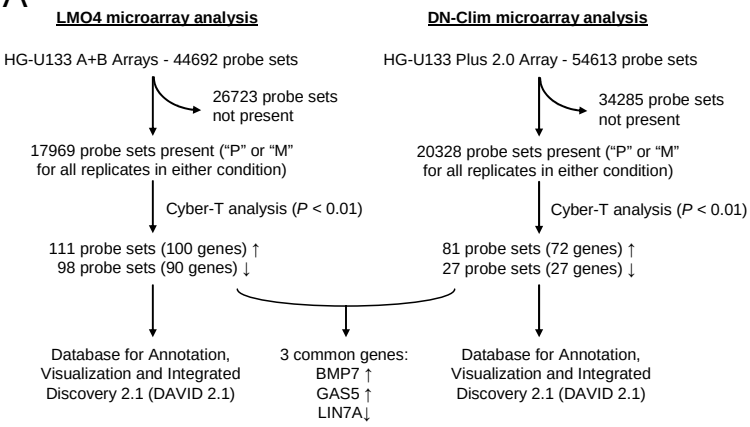

B

Enriched Gene Ontology category - apoptosis

UniGene ID	Gene Symbol	*P*-value	Fold
Hs.390736	CFLAR	0.0079	2.02
Hs.232543	PDCD4	0.0001	2.00
Hs.421986	CXCR4	0.0092	1.67
Hs.293753	BOK	0.0044	1.42
Hs.525622	AKT1	0.0044	1.41
Hs.502876	RHOB	0.0055	1.39
Hs.476018	CTNNB1	0.0080	1.38
Hs.397465	HIPK2	0.0061	1.37
Hs.80409	GADD45A	0.0066	-1.73
Hs.470887	GULP1	0.0045	-1.75
Hs.473163	BMP7*	0.0002	2.21

C

Q-PCR validation of genes from LMO4 microarray

	Gene	Fold change Microarray	Double ΔCt Q-PCR
Upregulated	BMP7	2.21	-1
	RET	1.66	-1
	NDRG1	1.63	-0.5
	IGFBP2	1.39	-0.5
	IGFBP5	2.01	-0.5
Downregulated	MBD1	-1.58	1
	PLAG1	-6.90	1
	IL8	-1.60	1.8
	FGFR4	-1.57	1
	AGR2	-1.82	0.6

D

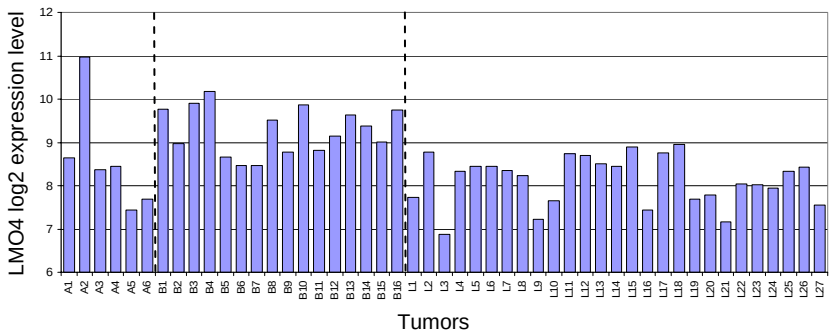

E

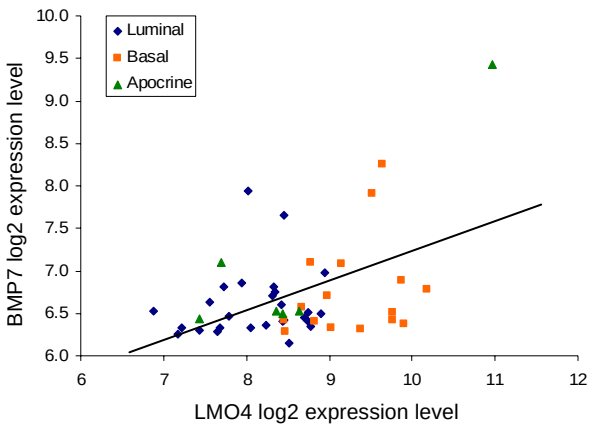

F

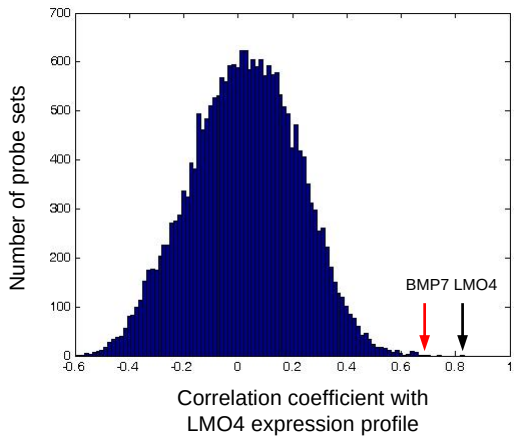

G

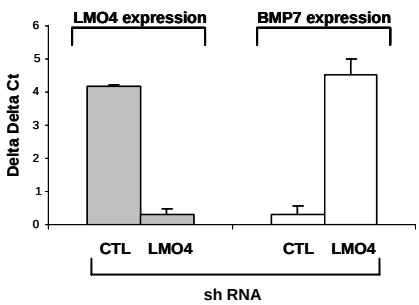

H

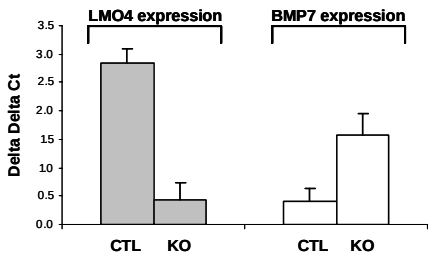

Fig. 6

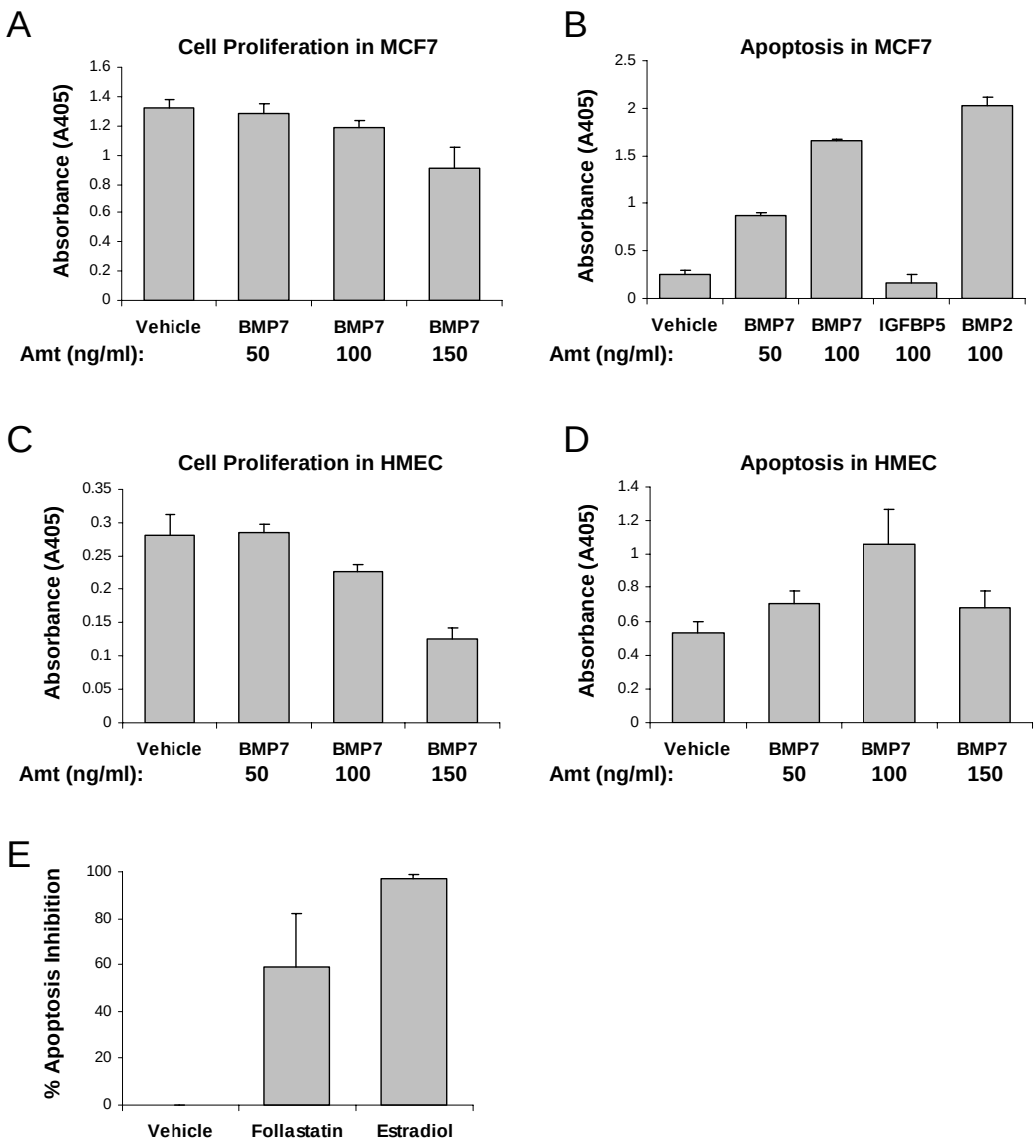
A
Cell Proliferation in MCF7
Absorbance (A405)
1.6
1.4
1.2
1
0.8
0.6
0.4
0.2
0
Vehicle
BMP7
BMP7
BMP7
Amt (ng/ml):
50
100
150
B
Apoptosis in MCF7
Absorbance (A405)
2.5
2
1.5
1
0.5
0
Vehicle
BMP7
BMP7
IGFBP5
BMP2
Amt (ng/ml):
50
100
100
100
C
Cell Proliferation in HMEC
Absorbance (A405)
0.35
0.3
0.25
0.2
0.15
0.1
0.05
0
Vehicle
BMP7
BMP7
BMP7
Amt (ng/ml):
50
100
150
D
Apoptosis in HMEC
Absorbance (A405)
1.4
1.2
1
0.8
0.6
0.4
0.2
0
Vehicle
BMP7
BMP7
BMP7
Amt (ng/ml):
50
100
150
E
% Apoptosis Inhibition
100
80
60
40
20
0
Vehicle
Follastatin
Estradiol

Fig. 7

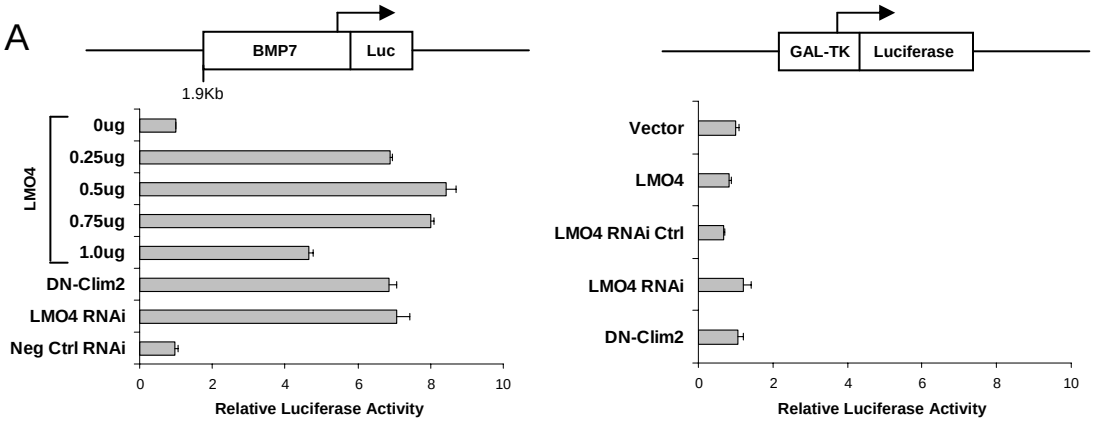
A
BMP7
Luc
1.9Kb
LMO4
0ug
0.25ug
0.5ug
0.75ug
1.0ug
DN-Clim2
LMO4 RNAi
Neg Ctrl RNAi
0
2
4
6
8
10
Relative Luciferase Activity
GAL-TK
Luciferase
Vector
LMO4
LMO4 RNAi Ctrl
LMO4 RNAi
DN-Clim2
0
2
4
6
8
10
Relative Luciferase Activity

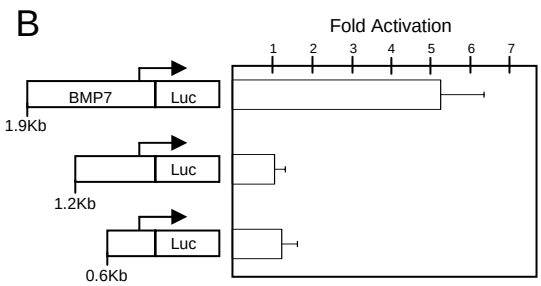
B
Fold Activation
1
2
3
4
5
6
7
BMP7
Luc
1.9Kb
Luc
1.2Kb
Luc
0.6Kb

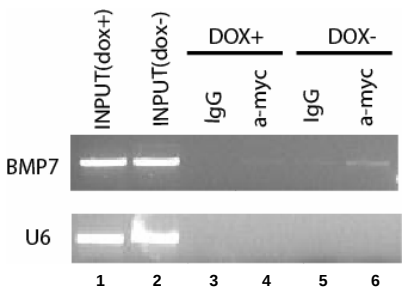
C
INPUT(dox+)
INPUT(dox-)
DOX+
DOX-
IgG
a-myc
IgG
a-myc
BMP7
U6
1
2
3
4
5
6

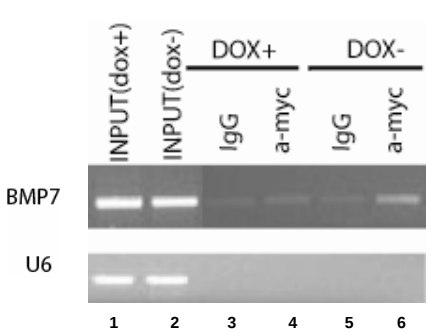
D
INPUT(dox+)
INPUT(dox-)
DOX+
DOX-
IgG
a-myc
IgG
a-myc
BMP7
U6
1
2
3
4
5
6

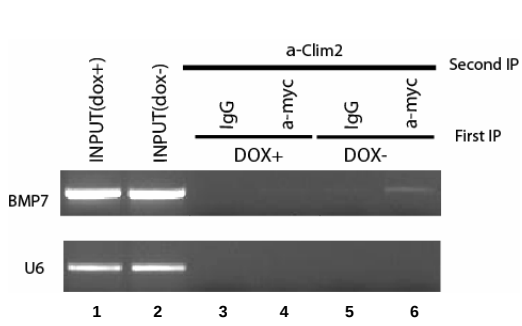
E
a-Clim2
Second IP
INPUT(dox+)
INPUT(dox-)
IgG
a-myc
IgG
a-myc
First IP
DOX+
DOX-
BMP7
U6
1
2
3
4
5
6

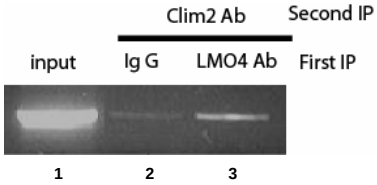
F
Clim2 Ab
Second IP
input
Ig G
LMO4 Ab
First IP
1
2
3

Fig. 8

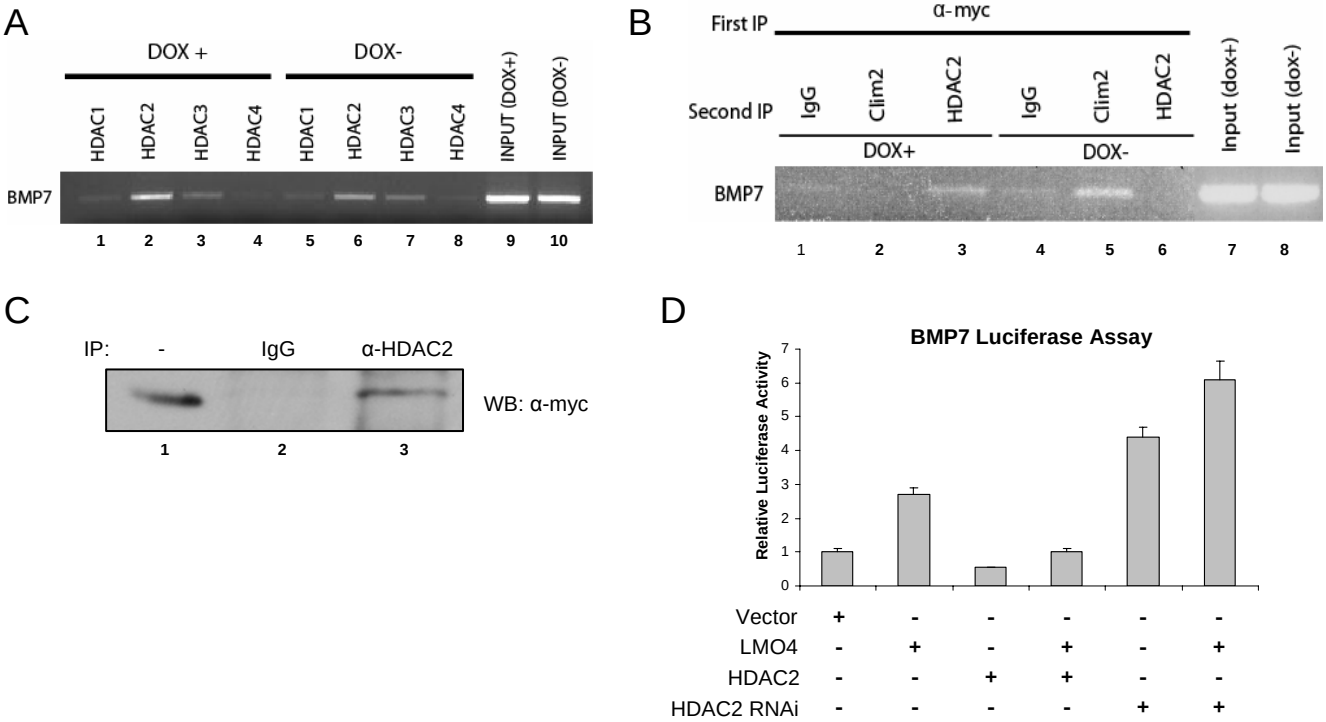
A
DOX +
DOX-
HDAC1
HDAC2
HDAC3
HDAC4
HDAC1
HDAC2
HDAC3
HDAC4
INPUT (DOX+)
INPUT (DOX-)
BMP7
1 2 3 4 5 6 7 8 9 10
B
First IP
α-myc
Second IP
IgG
Clim2
HDAC2
IgG
Clim2
HDAC2
Input (dox+)
Input (dox-)
DOX+
DOX-
BMP7
1 2 3 4 5 6 7 8
C
IP: - IgG α-HDAC2
WB: α-myc
1 2 3
D
BMP7 Luciferase Assay
Relative Luciferase Activity
0 1 2 3 4 5 6 7
Vector + - - - - -
LMO4 - + - + - +
HDAC2 - - + + - -
HDAC2 RNAi - - - - + +

Supplemental File 1

A

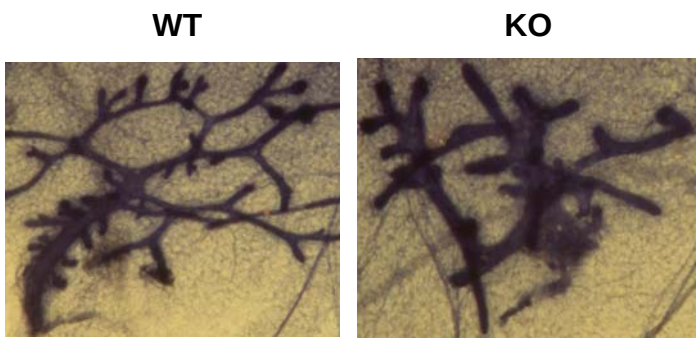

B

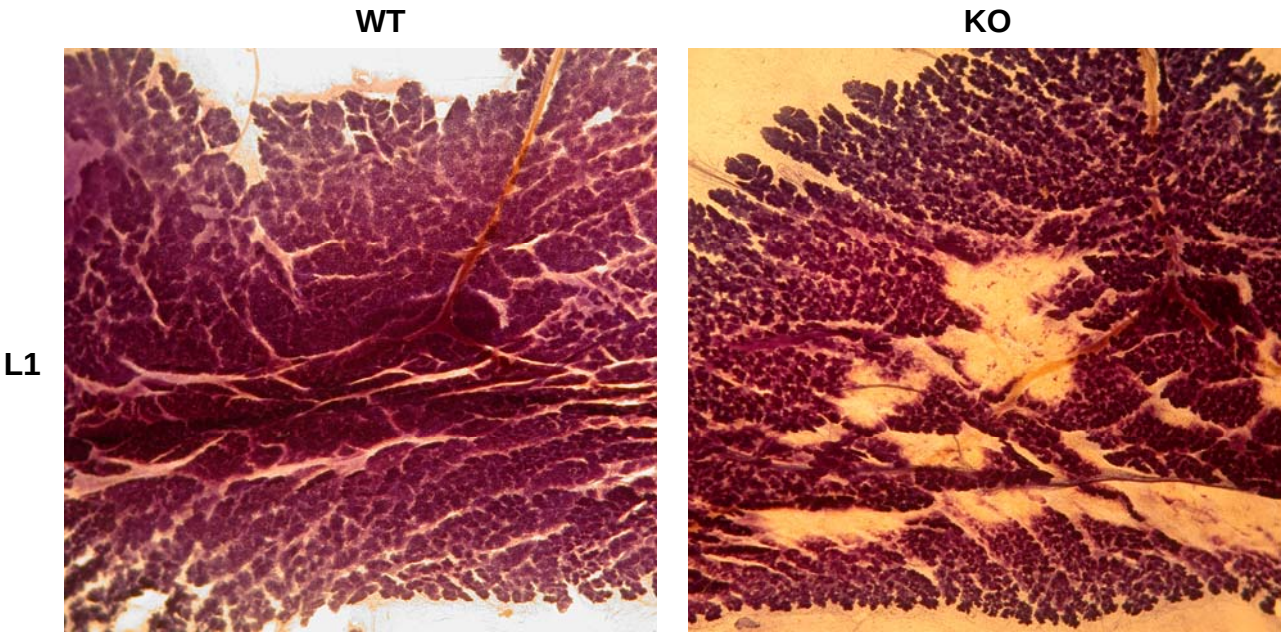

Supplemental File 2

Top 20 genes upregulated by LMO4

Probe Set ID	UniGene ID	Gene Name	Gene Symbol	*P*-value	Fold
227964_at	Hs.362974	FKSG44 gene	FKSG44	3.85E-06	1.98
228238_at	Hs.531856	growth arrest-specific 5	GAS5	2.17E-05	1.91
201369_s_at	Hs.503093	zinc finger protein 36, C3H type-like 2	ZFP36L2	2.86E-05	1.82
212593_s_at	Hs.232543	programmed cell death 4	PDCD4	1.14E-04	2.00
215771_x_at	Hs.350321	ret proto-oncogene	RET	1.23E-04	1.91
202428_x_at	Hs.78888	diazepam binding inhibitor	DBI	1.62E-04	1.57
204326_x_at	Hs.374950	metallothionein 1X	MT1X	2.06E-04	1.73
211259_s_at	Hs.473163	bone morphogenetic protein 7	BMP7	2.50E-04	2.21
201334_s_at	Hs.24598	Rho guanine nucleotide exchange factor (GEF) 12	ARHGEF12	2.58E-04	1.76
224671_at	Hs.347535	mitochondrial ribosomal protein L10	MRPL10	1.01E-03	1.58
230964_at	Hs.253994	FRAS1 related extracellular matrix protein 2	FREM2	1.04E-03	1.57
202948_at	Hs.557403	interleukin 1 receptor, type I	IL1R1	1.11E-03	1.86
204573_at	Hs.125039	carnitine O-octanoyltransferase	CROT	1.22E-03	1.97
225433_at	Hs.547415	General transcription factor IIA, 1, 19/37kDa	GTF2A1	1.31E-03	1.50
232797_at	Hs.436873	Integrin, alpha V (vitronectin receptor, alpha polypeptide, antigen CD51)	ITGAV	1.42E-03	1.89
40093_at	Hs.155048	Lutheran blood group (Auberger b antigen included)	LU	1.55E-03	1.56
233274_at	Hs.477693	NCK adaptor protein 1	NCK1	1.67E-03	1.67
204112_s_at	Hs.42151	histamine N-methyltransferase	HNMT	1.78E-03	1.66
200028_s_at	Hs.469331	START domain containing 7	STARD7	1.92E-03	1.48
217009_at	Hs.367727	phosphoglycerate kinase 2	PGK2	2.00E-03	2.36

Top 20 genes downregulated by LMO4

Probe Set ID	UniGene ID	Gene Name	Gene Symbol	*P*-value	Fold
233305_at	Hs.302754	EF-hand calcium binding protein 1	EFCBP1	1.92E-06	-2.38
231713_s_at	Hs.8739	signal transducer and activator of transcription 3 interacting protein 1	STATIP1	2.21E-04	-1.47
233208_x_at	Hs.435675	cleavage and polyadenylation specific factor 2, 100kDa	CPSF2	2.36E-04	-1.68
233588_x_at	Hs.446374	HLA class II region expressed gene KE2	HKE2	6.99E-04	-1.91
238346_s_at	Hs.335068	nuclear receptor coactivator 6 interacting protein	NCOA6IP	8.11E-04	-1.82
225415_at	Hs.518201	deltex 3-like (Drosophila)	DTX3L	8.40E-04	-1.42
238496_at	Hs.32099	Wolf-Hirschhorn syndrome candidate 1-like 1	WHSC1L1	1.14E-03	-2.51
212444_at	Hs.194691	G protein-coupled receptor, family C, group 5, member A	GPCR5A	1.16E-03	-1.51
225496_s_at	Hs.369520	synaptotagmin-like 2	SYTL2	1.33E-03	-1.34
218462_at	Hs.481202	brix domain containing 5	BXDC5	1.47E-03	-1.64
207626_s_at	Hs.448520	solute carrier family 7, member 2	SLC7A2	1.52E-03	-1.60
220319_s_at	Hs.484738	myosin regulatory light chain interacting protein	MYLIP	1.71E-03	-1.51
236300_at	Hs.386791	Phosphodiesterase 3A, cGMP-inhibited	PDE3A	1.78E-03	-1.74
225152_at	Hs.60300	zinc finger protein 622	ZNF622	2.45E-03	-1.39
208430_s_at	Hs.58919	dystrobrevin, alpha	DTNA	2.70E-03	-1.60
223211_at	Hs.63290	2-hydroxyphytanoyl-CoA lyase	HPCL2	2.86E-03	-1.42
205774_at	Hs.1321	coagulation factor XII (Hageman factor)	F12	2.92E-03	-1.52
202272_s_at	Hs.64691	F-box protein 28	FBXO28	3.11E-03	-1.48
232337_at	Hs.299329	UDP-GlcNAc:betaGal beta-1,3-N-acetylglucosaminyltransferase 7	B3GNT7	3.16E-03	-1.54
240027_at	Hs.144333	lin-7 homolog A (C. elegans)	LIN7A	3.16E-03	-2.14

Supplemental File 3

A

B

Top 20 genes upregulated by DN-Clim

Probe Set ID	UniGene ID	Gene Name	Gene Symbol	*P*-value	Fold
1560596_at	Hs.468864	Glutamine-fructose-6-phosphate transaminase 1	GFPT1	1.46E-04	2.38
202718_at	Hs.438102	insulin-like growth factor binding protein 2, 36kDa	IGFBP2	3.27E-04	1.85
210076_x_at	Hs.530412	SERPINE1 mRNA binding protein 1	SERBP1	4.40E-04	1.68
242216_at	Hs.499000	DnaJ (Hsp40) homolog, subfamily C, member 1	DNAJC1	6.76E-04	2.75
206511_s_at	Hs.101937	sine oculis homeobox homolog 2 (Drosophila)	SIX2	7.91E-04	2.31
206081_at	Hs.173092	solute carrier family 24 (sodium/potassium/calcium exchanger), member 1	SLC24A1	8.99E-04	1.99
206405_x_at	Hs.448851	ubiquitin specific peptidase 6 (Tre-2 oncogene)	USP6	1.10E-03	1.69
234339_s_at	Hs.421907	glioma tumor suppressor candidate region gene 2	GLTSCR2	1.48E-03	2.24
202887_s_at	Hs.523012	DNA-damage-inducible transcript 4	DDIT4	1.56E-03	1.61
1565906_at	Hs.503137	NAD synthetase 1	NADSYN1	1.86E-03	2.14
227205_at	Hs.558404	TAF1 RNA polymerase II, TATA box binding protein (TBP)-associated factor, 250kDa	TAF1	1.88E-03	1.64
203426_s_at	Hs.369982	insulin-like growth factor binding protein 5	IGFBP5	2.01E-03	1.88
227526_at	Hs.38034	Cdon homolog (mouse)	CDON	2.17E-03	1.77
244310_at	Hs.511626	RAR-related orphan receptor A	RORA	2.51E-03	1.88
222792_s_at	Hs.90527	HSPC128 protein	HSPC128	2.64E-03	1.65
243992_at	Hs.507433	Zinc finger protein 198	ZNF198	2.74E-03	1.77
203425_s_at	Hs.369982	insulin-like growth factor binding protein 5	IGFBP5	2.94E-03	1.88
234984_at	Hs.270084	neural precursor cell expressed, developmentally down-regulated 1	NEDD1	2.98E-03	1.57
213213_at	Hs.551527	death associated transcription factor 1	DATF1	3.70E-03	1.72
209753_s_at	Hs.11355	thymopoietin	TMPO	3.81E-03	1.66

Top 20 genes downregulated by DN-Clim

Probe Set ID	UniGene ID	Gene Name	Gene Symbol	*P*-value	Fold
210293_s_at	Hs.369373	Sec23 homolog B (S. cerevisiae)	SEC23B	3.41E-05	-2.11
217731_s_at	Hs.446450	integral membrane protein 2B	ITM2B	2.22E-04	-1.95
241652_x_at	Hs.144333	Lin-7 homolog A (C. elegans)	LIN7A	7.38E-04	-2.37
216295_s_at	Hs.522114	clathrin, light polypeptide (Lca)	CLTA	1.50E-03	-1.53
222989_s_at	Hs.9589	ubiquilin 1	UBQLN1	2.09E-03	-1.65
212781_at	Hs.188553	retinoblastoma binding protein 6	RBBP6	2.57E-03	-1.64
212209_at	Hs.159799	thyroid hormone receptor associated protein 2	THRAP2	3.72E-03	-1.52
201763_s_at	Hs.336916	death-associated protein 6	DAXX	3.97E-03	-1.70
226616_s_at	Hs.473937	NADH dehydrogenase (ubiquinone) flavoprotein 3, 10kDa	NDUFV3	4.63E-03	-1.45
1565900_at	Hs.243326	Methyltransferase 5 domain containing 1	METT5D1	4.67E-03	-2.15
201237_at	Hs.446123	capping protein (actin filament) muscle Z-line, alpha 2	CAPZA2	5.66E-03	-1.51
201260_s_at	Hs.80919	synaptophysin-like 1	SYPL1	6.31E-03	-1.45
214281_s_at	Hs.48297	ring finger and CHY zinc finger domain containing 1	RCHY1	6.59E-03	-1.53
236128_at	Hs.558418	Zinc finger protein 91 (HPF7, HTF10)	ZNF91	6.67E-03	-1.88
201330_at	Hs.506215	arginyl-tRNA synthetase	RARS	7.14E-03	-1.65
209115_at	Hs.154320	ubiquitin-activating enzyme E1C (UBA3 homolog, yeast)	UBE1C	7.16E-03	-1.55
204496_at	Hs.401843	striatin, calmodulin binding protein 3	STRN3	7.28E-03	-1.55
233078_at	Hs.435771	apoptosis inhibitor 5	API5	7.37E-03	-2.15
209099_x_at	Hs.224012	jagged 1 (Alagille syndrome)	JAG1	7.43E-03	-1.95
218247_s_at	Hs.465144	ring finger and KH domain containing 2	RKHD2	7.84E-03	-1.62

Supplemental File 2

Top 20 genes upregulated by LMO4

Probe Set ID	UniGene ID	Gene Name	Gene Symbol	*P*-value	Fold
227964_at	Hs.362974	FKSG44 gene	FKSG44	3.85E-06	1.98
228238_at	Hs.531856	growth arrest-specific 5	GAS5	2.17E-05	1.91
201369_s_at	Hs.503093	zinc finger protein 36, C3H type-like 2	ZFP36L2	2.86E-05	1.82
212593_s_at	Hs.232543	programmed cell death 4	PDCD4	1.14E-04	2.00
215771_x_at	Hs.350321	ret proto-oncogene	RET	1.23E-04	1.91
202428_x_at	Hs.78888	diazepam binding inhibitor	DBI	1.62E-04	1.57
204326_x_at	Hs.374950	metallothionein 1X	MT1X	2.06E-04	1.73
211259_s_at	Hs.473163	bone morphogenetic protein 7	BMP7	2.50E-04	2.21
201334_s_at	Hs.24598	Rho guanine nucleotide exchange factor (GEF) 12	ARHGEF12	2.58E-04	1.76
224671_at	Hs.347535	mitochondrial ribosomal protein L10	MRPL10	1.01E-03	1.58
230964_at	Hs.253994	FRAS1 related extracellular matrix protein 2	FREM2	1.04E-03	1.57
202948_at	Hs.557403	interleukin 1 receptor, type I	IL1R1	1.11E-03	1.86
204573_at	Hs.125039	carnitine O-octanoyltransferase	CROT	1.22E-03	1.97
225433_at	Hs.547415	General transcription factor IIA, 1, 19/37kDa	GTF2A1	1.31E-03	1.50
232797_at	Hs.436873	Integrin, alpha V (vitronectin receptor, alpha polypeptide, antigen CD51)	ITGAV	1.42E-03	1.89
40093_at	Hs.155048	Lutheran blood group (Auberger b antigen included)	LU	1.55E-03	1.56
233274_at	Hs.477693	NCK adaptor protein 1	NCK1	1.67E-03	1.67
204112_s_at	Hs.42151	histamine N-methyltransferase	HNMT	1.78E-03	1.66
200028_s_at	Hs.469331	START domain containing 7	STARD7	1.92E-03	1.48
217009_at	Hs.367727	phosphoglycerate kinase 2	PGK2	2.00E-03	2.36

Top 20 genes downregulated by LMO4

Probe Set ID	UniGene ID	Gene Name	Gene Symbol	*P*-value	Fold
233305_at	Hs.302754	EF-hand calcium binding protein 1	EFCBP1	1.92E-06	-2.38
231713_s_at	Hs.8739	signal transducer and activator of transcription 3 interacting protein 1	STATIP1	2.21E-04	-1.47
233208_x_at	Hs.435675	cleavage and polyadenylation specific factor 2, 100kDa	CPSF2	2.36E-04	-1.68
233588_x_at	Hs.446374	HLA class II region expressed gene KE2	HKE2	6.99E-04	-1.91
238346_s_at	Hs.335068	nuclear receptor coactivator 6 interacting protein	NCOA6IP	8.11E-04	-1.82
225415_at	Hs.518201	deltex 3-like (Drosophila)	DTX3L	8.40E-04	-1.42
238496_at	Hs.32099	Wolf-Hirschhorn syndrome candidate 1-like 1	WHSC1L1	1.14E-03	-2.51
212444_at	Hs.194691	G protein-coupled receptor, family C, group 5, member A	GPCR5A	1.16E-03	-1.51
225496_s_at	Hs.369520	synaptotagmin-like 2	SYTL2	1.33E-03	-1.34
218462_at	Hs.481202	brix domain containing 5	BXDC5	1.47E-03	-1.64
207626_s_at	Hs.448520	solute carrier family 7, member 2	SLC7A2	1.52E-03	-1.60
220319_s_at	Hs.484738	myosin regulatory light chain interacting protein	MYLIP	1.71E-03	-1.51
236300_at	Hs.386791	Phosphodiesterase 3A, cGMP-inhibited	PDE3A	1.78E-03	-1.74
225152_at	Hs.60300	zinc finger protein 622	ZNF622	2.45E-03	-1.39
208430_s_at	Hs.58919	dystrobrevin, alpha	DTNA	2.70E-03	-1.60
223211_at	Hs.63290	2-hydroxyphytanoyl-CoA lyase	HPCL2	2.86E-03	-1.42
205774_at	Hs.1321	coagulation factor XII (Hageman factor)	F12	2.92E-03	-1.52
202272_s_at	Hs.64691	F-box protein 28	FBXO28	3.11E-03	-1.48
232337_at	Hs.299329	UDP-GlcNAc:betaGal beta-1,3-N-acetylglucosaminyltransferase 7	B3GNT7	3.16E-03	-1.54
240027_at	Hs.144333	lin-7 homolog A (C. elegans)	LIN7A	3.16E-03	-2.14

Supplemental File 3

A

B

Top 20 genes upregulated by DN-Clim

Probe Set ID	UniGene ID	Gene Name	Gene Symbol	*P*-value	Fold
1560596_at	Hs.468864	Glutamine-fructose-6-phosphate transaminase 1	GFPT1	1.46E-04	2.38
202718_at	Hs.438102	insulin-like growth factor binding protein 2, 36kDa	IGFBP2	3.27E-04	1.85
210076_x_at	Hs.530412	SERPINE1 mRNA binding protein 1	SERBP1	4.40E-04	1.68
242216_at	Hs.499000	DnaJ (Hsp40) homolog, subfamily C, member 1	DNAJC1	6.76E-04	2.75
206511_s_at	Hs.101937	sine oculis homeobox homolog 2 (Drosophila)	SIX2	7.91E-04	2.31
206081_at	Hs.173092	solute carrier family 24 (sodium/potassium/calcium exchanger), member 1	SLC24A1	8.99E-04	1.99
206405_x_at	Hs.448851	ubiquitin specific peptidase 6 (Tre-2 oncogene)	USP6	1.10E-03	1.69
234339_s_at	Hs.421907	glioma tumor suppressor candidate region gene 2	GLTSCR2	1.48E-03	2.24
202887_s_at	Hs.523012	DNA-damage-inducible transcript 4	DDIT4	1.56E-03	1.61
1565906_at	Hs.503137	NAD synthetase 1	NADSYN1	1.86E-03	2.14
227205_at	Hs.558404	TAF1 RNA polymerase II, TATA box binding protein (TBP)-associated factor, 250kDa	TAF1	1.88E-03	1.64
203426_s_at	Hs.369982	insulin-like growth factor binding protein 5	IGFBP5	2.01E-03	1.88
227526_at	Hs.38034	Cdon homolog (mouse)	CDON	2.17E-03	1.77
244310_at	Hs.511626	RAR-related orphan receptor A	RORA	2.51E-03	1.88
222792_s_at	Hs.90527	HSPC128 protein	HSPC128	2.64E-03	1.65
243992_at	Hs.507433	Zinc finger protein 198	ZNF198	2.74E-03	1.77
203425_s_at	Hs.369982	insulin-like growth factor binding protein 5	IGFBP5	2.94E-03	1.88
234984_at	Hs.270084	neural precursor cell expressed, developmentally down-regulated 1	NEDD1	2.98E-03	1.57
213213_at	Hs.551527	death associated transcription factor 1	DATF1	3.70E-03	1.72
209753_s_at	Hs.11355	thymopoietin	TMPO	3.81E-03	1.66

Top 20 genes downregulated by DN-Clim

Probe Set ID	UniGene ID	Gene Name	Gene Symbol	*P*-value	Fold
210293_s_at	Hs.369373	Sec23 homolog B (S. cerevisiae)	SEC23B	3.41E-05	-2.11
217731_s_at	Hs.446450	integral membrane protein 2B	ITM2B	2.22E-04	-1.95
241652_x_at	Hs.144333	Lin-7 homolog A (C. elegans)	LIN7A	7.38E-04	-2.37
216295_s_at	Hs.522114	clathrin, light polypeptide (Lca)	CLTA	1.50E-03	-1.53
222989_s_at	Hs.9589	ubiquilin 1	UBQLN1	2.09E-03	-1.65
212781_at	Hs.188553	retinoblastoma binding protein 6	RBBP6	2.57E-03	-1.64
212209_at	Hs.159799	thyroid hormone receptor associated protein 2	THRAP2	3.72E-03	-1.52
201763_s_at	Hs.336916	death-associated protein 6	DAXX	3.97E-03	-1.70
226616_s_at	Hs.473937	NADH dehydrogenase (ubiquinone) flavoprotein 3, 10kDa	NDUFV3	4.63E-03	-1.45
1565900_at	Hs.243326	Methyltransferase 5 domain containing 1	METT5D1	4.67E-03	-2.15
201237_at	Hs.446123	capping protein (actin filament) muscle Z-line, alpha 2	CAPZA2	5.66E-03	-1.51
201260_s_at	Hs.80919	synaptophysin-like 1	SYPL1	6.31E-03	-1.45
214281_s_at	Hs.48297	ring finger and CHY zinc finger domain containing 1	RCHY1	6.59E-03	-1.53
236128_at	Hs.558418	Zinc finger protein 91 (HPF7, HTF10)	ZNF91	6.67E-03	-1.88
201330_at	Hs.506215	arginyl-tRNA synthetase	RARS	7.14E-03	-1.65
209115_at	Hs.154320	ubiquitin-activating enzyme E1C (UBA3 homolog, yeast)	UBE1C	7.16E-03	-1.55
204496_at	Hs.401843	striatin, calmodulin binding protein 3	STRN3	7.28E-03	-1.55
233078_at	Hs.435771	apoptosis inhibitor 5	API5	7.37E-03	-2.15
209099_x_at	Hs.224012	jagged 1 (Alagille syndrome)	JAG1	7.43E-03	-1.95
218247_s_at	Hs.465144	ring finger and KH domain containing 2	RKHD2	7.84E-03	-1.62

Supplemental File 5

A

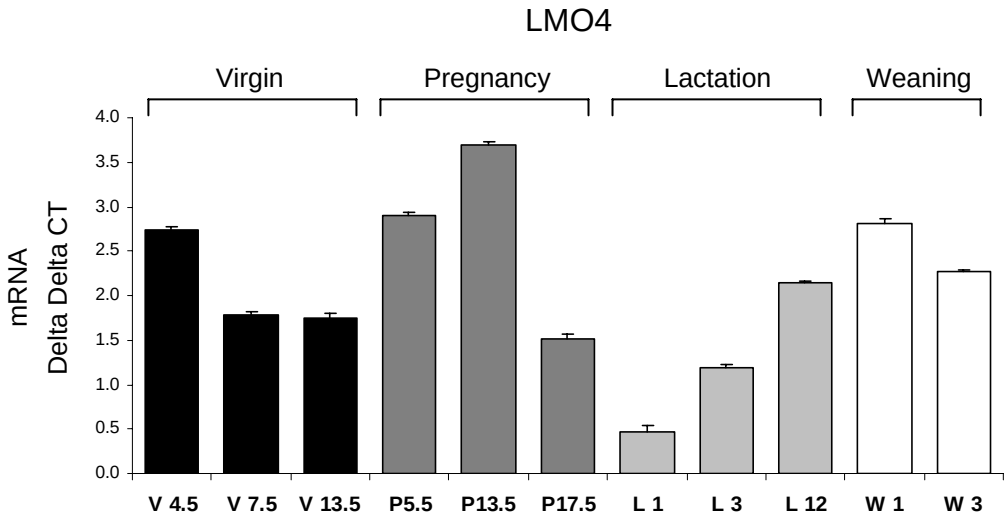

B

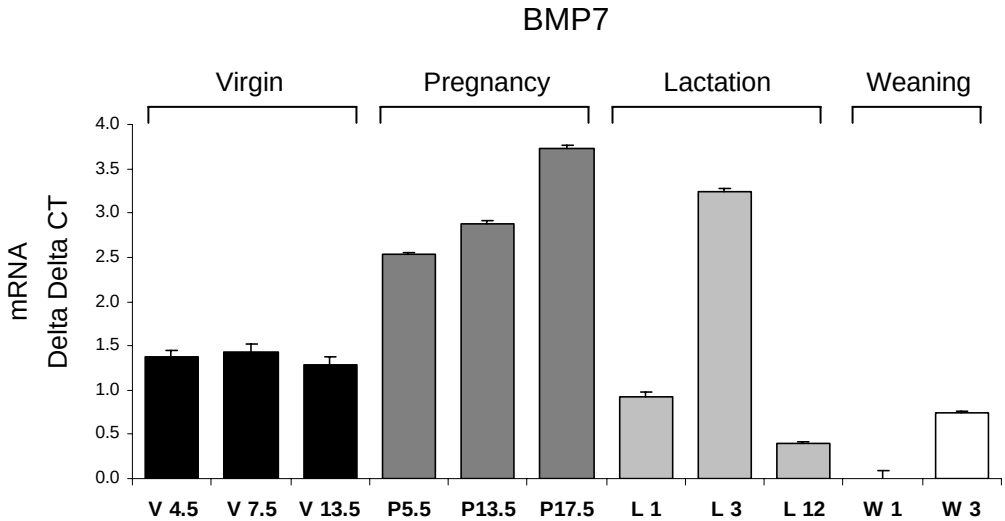

C